NATIONAL UNIVERSITY OF SCIENCE AND TECHNOLOGY
BUCHAREST POLYTECHNIC
DOCTORAL SCHOOL OF AEROSPACE ENGINEERING

THESIS

DGCMG DYNAMICS AND CONTROL WITH APPLICATIONS TO SATELLITE ATTITUDE STABILIZATION

SUMMARY

SCIENTIFIC LEADER:
Prof.Univ.Dr.Ing.Romulus LUNGU

CANDIDATE:
Ing.Nicoleta Claudia EFRIM

2023

Keywords:

CONTENT

INTRODUCTION

For the performance of various satellite missions, an essential problem is the attitude control of satellites, which has been addressed in many specialized works, among which we mention the following: [2], [5], [10], [24], [26] , [28], [29], [35], [36], [38], [49], [59], [62], [64], [68], [69], [71], [74], [77], [79], [80], [81], [90], [92], [98], [100], [101], [102], [103], [104] , [105], [106], [107].

As indispensable subsystems of satellite attitude control systems, CMGs have an essential role as actuators. They can be classified into two categories: classic mechanical bearing gyroscopes and magnetic suspension gyroscopes (MSCMG). MSCMGs, compared to CMGs with mechanical bearings, have the advantage that the friction moments are zero, thus eliminating lubrication, noises and vibrations [40], [89], [70].

In terms of the number of degrees of freedom, CMGs are single-gimbal (SGCMG) or double-gimbal (DGCMG). Compared to SGCMGs, DGCMGs generate two gyroscopic torques thus reducing the occupied volume on the satellite.

Actuators with SGCMGs have different structures, among which we mention pyramidal clusters [26], [36], [39], [40], [49], [59], [64], [67], [73], [100], [102], [103].

DGMSCMG incorporates the advantages of magnetic bearings with those of having two frames. Among the works that address topics related to DGMSCMGs and their use as gyroscopic actuators we mention: [1], [3], [7], [10], [14], [15], [17], [23] , [28], [34], [42], [44], [45], [47], [48], [53], [57], [58], [61], [62], [69], [70], [74], [75], [76], [78], [79], [80], [81], [84], [86], [88], [89] , [90], [91], [94], [99], [105], [106], [107].

The construction of the AMB-Rotor (rotor with magnetic bearings, active magneting bearing) allows decoupling the translational dynamics of the rotor from the dynamics of rotor rotations and gyroscopic frames [14], [34], [99], for which non-linear observations are required [10], [72], [86], [89].

An important problem in the specialized literature is that of vibration control [1], [3], [34], [84].

Another problem addressed in the literature is that of designing servo systems for actuating gyroscopic frames [22], [23].

In order to avoid singularities using the concept of "zero movement", without the control of the stored energy, actuator structures with N=2 DGMSCMGs in parallel configuration [78], [94] or with N=3 DGMSCMGs have been proposed and studied in orthogonal configuration [107]. Also, to avoid singularities using "zero motion", with the control of the stored energy, according to the model of pyramidal clusters with SGCMGs [49], [59], structures for automatic attitude control of satellites by

changing the angular velocities were proposed and studied of the gyroscopic frames of the DGMSCMG, as well as of the self-rotation velocities of the gyroscopes [75], [81].

The laws used to control the dynamic components of DGMSCMG are of the P.I., P.D., P.I.D. type, optimal (based on the criteria H_2, H_∞, H_2/H_∞) or adaptive [70], [84], [89], [99].

In [106], using a P.D.-type attitude controller, the gyroscopic rotor dynamics control of the DGMSCMG-type actuator and sensor is P.-type; dynamic models of magnetically suspended gyro rotors do not take into account the interactions with the gyro frames, and therefore the attitude control of the satellite is not sufficiently accurate.

The first chapter presents the derivation of the nonlinear models of the translational and rotational dynamics of the AMB-Rotor, without taking into account the interactions with the gyroscopic frames, then the derivation of the nonlinear models of the AMB-Rotor rotations and the gyroscopic frames taking into account the rotor-frame interactions gyroscopic. Finally, dynamic models expressed in the form of state equations are obtained, in which the input vectors have as components the currents applied to the correction coils of the magnetic bearings and the currents applied to the motors of the servo systems for driving the gyroscopic frames. The relative degrees of the components of the output vector of the non-linear model of the DGMSCMG are determined, finally resulting in the second-order matrix-vector differential equation of the output vector, having as components the rotation angles of the AMB-Rotor and the gyroscopic frames. Differential geometry theory was used to calculate the matrices of the nonlinear model. Then, by dynamic inversion, the command vector of the DGMSCMG model is obtained as a function of the state vector and the pseudo-command vector.

The model of the rotor translation dynamics is decoupled from its rotation dynamics and from the rotation dynamics of the gyroscopic frames.

The design of a DGMSCMG control system consisting of two subsystems is presented: one for controlling the linear displacements of the AMB-Rotor and one for controlling its angular deviations and the rotation angles of the gyroscopic frames. Using the Simulink model built in the work, the evolution over time of the respective linear and angular variables is graphically represented.

The adaptive control structures are designed, based on the concept of dynamic inversion and neural networks, for: the dynamics of the translation of the AMB-Rotor, the dynamics of the rotations (angular deviations) of the AMB-Rotor and the dynamics of the rotations of the gyroscopic frames. For all three adaptive control structures, Simulink models are designed and the evolution of the satellite attitude control system (SCAS) variables is graphically represented. These dynamic characteristics are fast, have small overshoots and stationary errors, which highlights the fact that

adaptive control structures based on the concept of dynamic inversion and neural networks provide superior quality indicators to control structures with conventional driving laws.

Chapter 2 presents the structure and equations of an automatic control system of the AMB-Rotor, as well as dynamic models of the rotor, the inner frame and the outer frame of the DGMSCMG type actuator located on a mobile base (satellite). The design of linear servo systems for controlling the angular velocities of gyroscopic frames is also presented. In the following, calculation elements regarding the attitude of the satellites using the quaternion theory are presented.

The attitude of the satellite is controlled with a P.D. controller. designed based on Lyapunov functions, DGMSCMG1 actuator and DGMSCMG2 sensor. First, a P-type law is used to control the AMB-Rotor dynamics and linear servos to control the angular velocities of the gyro frames, then nonlinear models for servos and AMB-Rotor dynamics are used for both actuator and sensor. For both variants, Simulink models are developed and the dynamic characteristics of the SCAS are plotted. In the second variant (with non-linear models), the dynamic characteristics have smaller overshoots, are more slowly variable and with smaller stationary errors.

In chapter 3, dynamic models are elaborated for the actuator-satellite interaction and for the actuator consisting of N=2 DGMSCMGs arranged in parallel and orthogonal configuration, respectively, as well as for the related sensors. Also, dynamic models are developed for the actuator-satellite interaction and for the actuator consisting of N=3 DGMSCMGs arranged in an orthogonal configuration, as well as for the related sensor. Matlab/Simulink models are built for these.

A SCAS is designed with actuators consisting of N=2 and N=3 DGMSCMGs and one DGMSCMG type sensor each, and with the built Simulink models, the dynamic characteristics are drawn.

Chapter 4 elaborates problems related to the dynamics and attitude control of satellites using actuators consisting of N DGVSCMGs. The dynamic model of the attitude S is deduced with an actuator consisting of N=1 DGVSCMG located so that the plane of its outer frame is located in the plane of the undisturbed satellite's elliptical orbit. The dynamics equation of the actuator-satellite interaction is derived. Then, the same problem is addressed for actuators consisting of N=2 DGVSCMGs in parallel and rectangular arrangement, respectively. Attitude control S with actuator consisting of N=3 DGVSCMGs is also addressed.

A satellite attitude control system is designed, with reference model and P.D type controller. using the theory of Lyapunov functions without control of the stored energy of the gyroscopic rotor, with control of the stored energy, as well as equalization of the angular velocities of the gyroscopic rotors, using actuators with N=1, N=2 and N=3 DGVSCMG. And in this case, with the constructed Simulink models the time characteristics are plotted.

CHAPTER 1

DYNAMICS AND AUTOMATIC CONTROL OF DGMSCMG

1.1 EQUATIONS OF MOTION OF THE FREE GYROSCOPIC ROTOR WITH BEARINGS MAGNETIC (AMB-ROTOR)

Compared to conventional bearings, magnetic bearings for high-speed rotors have the advantage of low friction, requiring no lubrication.

The mechanical model of a CMG with a gyroscope frame in magnetic suspension (with magnetic bearings), Active Magnetic Bearing (AMB-rotor) is presented in fig.1.1[70]. On each semi-axis of the gyroscopic stator (not shown in the figure) there are four coils, two in series.
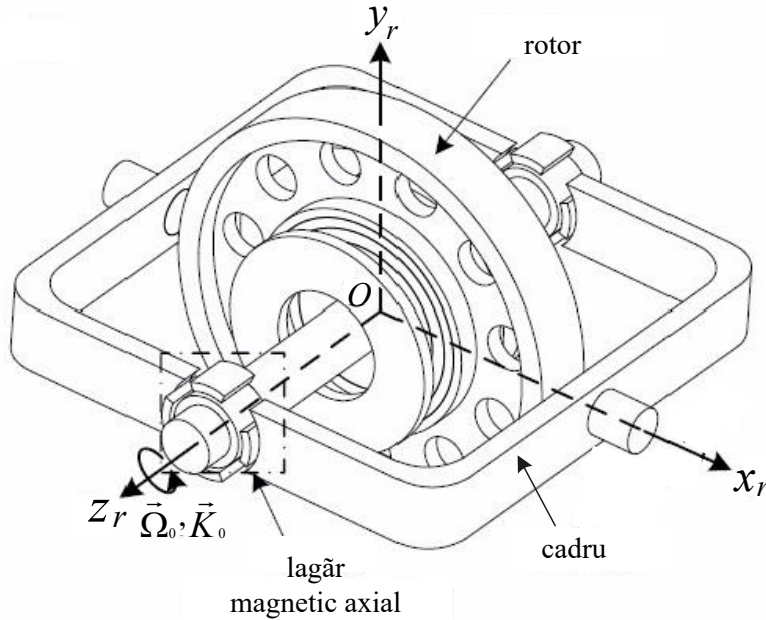
Fig. 1.1. Single frame CMG with magnetic bearing gyro

Fig. 1.2 shows the forces and moments applied to the gyroscopic rotor, and a and b denote the left and right semi-axis of the gyroscopic rotor, respectively;

The balance equations of the forces along the axes ox_r and oy_r are

$$m\ddot{x}_r = F_{cx_r}, m\ddot{y}_r = F_{cy_r},$$
(1.2)

with F_{cx_r} și F_{cy_r} of the forms (1.1) and $m-$ the mass of the gyroscopic rotor.
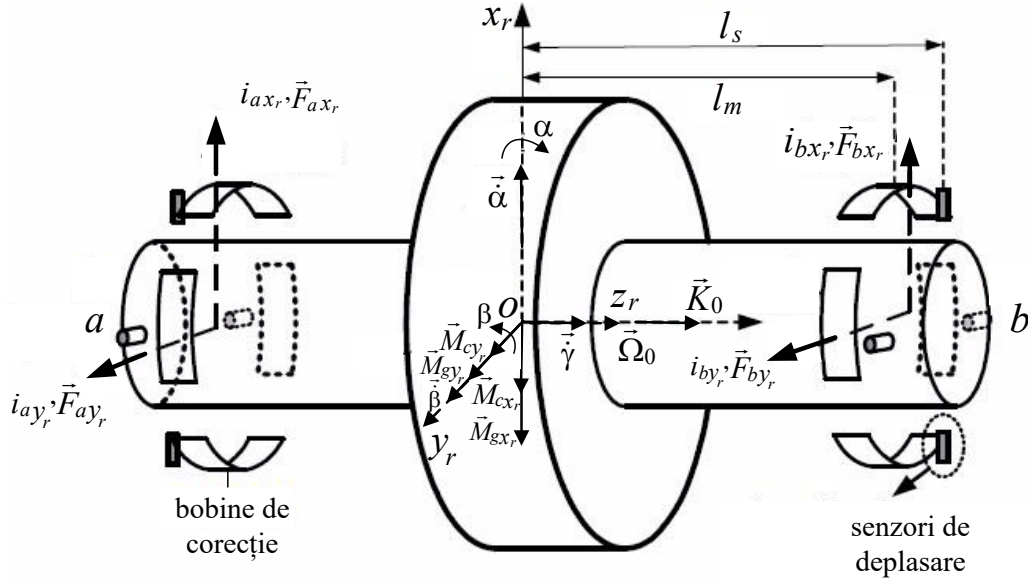
Fig. 1.2. The forces and moments applied to the gyro rotor

Total linear displacements $h_\lambda^{s\delta}$ (the total linear displacements of the sensors) have the expressions

$$h_{xr}^{sa} = x_r - l_s\beta,$$
$$h_{xr}^{sb} = x_r + l_s\beta,$$
$$h_{yr}^{sa} = y_r + l_s\alpha,$$
$$h_{yr}^{sb} = y_r - l_s\alpha,$$

(1.4)

The dynamic model of the linear displacements of the gyroscopic rotor in magnetic suspension along the axes ox_r and oy_r, in the absence of external disturbing forces, it has the following form

$$m\ddot{x}_r = 2k_{i_{ax}}i_x^{ma} + 2k_{h_{ax}}x_r,$$
$$m\ddot{y}_r = 2k_{i_{ay}}i_y^{ma} + 2k_{h_{ay}}y_r.$$

(1.9)

The dynamic model of the angular displacements of the gyroscopic rotor in magnetic suspension is obtained, in the absence of external disturbing moments

$$J_r\ddot{\alpha} + K_0\dot{\beta} = 2l_m k_{i_{ay}}i_\alpha + 2l_m^2 k_{h_{ay}}\alpha,$$
$$J_r\ddot{\beta} - K_0\dot{\alpha} = 2l_m k_{i_{ax}}i_\beta + 2l_m^2 k_{h_{ax}}\beta.$$

(1.16)

The angles α and β are obtained from relations (1.4);

$$\alpha = \frac{h_{yr}^{ma} - h_{yr}^{mb}}{2l_m} = \frac{h_{yr}^{sa} - h_{yr}^{sb}}{2l_s}, \quad \beta = \frac{h_{xr}^{mb} - h_{xr}^{ma}}{2l_m} = \frac{h_{xr}^{sb} - h_{xr}^{sa}}{2l_s};$$

(1.17)

so, α and β are functions of the angular displacements of the gyroscopic rotor along the two axes, measured by the linear displacement sensors arranged on the two axes (ox_r and oy_r).

1.2. NONLINEAR DYNAMIC MODEL OF CMG WITH TWO FRAME AND ROTOR GYROSCOPIC IN MAGNETIC SUSPENSION (DGMSCMG)

1.2.1. DYNAMIC MODEL OF THE SUSPENSION GYROSCOPIC ROTOR MAGNETIC (AMB-ROTOR)

In fig.1.3[89] the triads related to the component dynamic elements of a DGMSCMG are highlighted
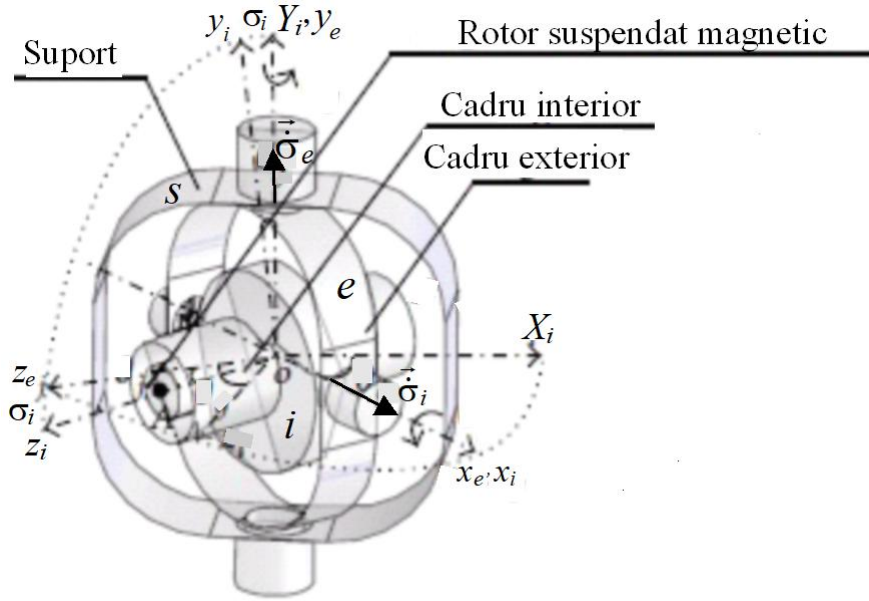
Fig. 1.3. The trihedra related to the dynamic components of DGMSCMG

1.3. THE NONLINEAR DYNAMIC MODEL OF DGMSCMG EXPRESSED IN THE FORM EQUATIONS OF STATE

The nonlinear dynamic model of DGMSCMG is constituted by equations (1.2), (1.37), (1.49) and (1.60); The dynamics of the DGMSCMG will be studied considering the fixed base (velocities and angular accelerations of the base are assumed to be zero). The dynamic model of DGMSCMG becomes

$$\ddot{x}_r = \frac{1}{m} F_{cx_r},$$

$$\ddot{y}_r = \frac{1}{m} F_{cy_r},$$

$$\ddot{\alpha} = \frac{J_{rz}}{J_{rx}} \dot{\sigma}_e \dot{\beta} \sin \sigma_i - \frac{J_{iz} - J_{iy} - J_{rz}}{J_{rx}} \dot{\sigma}_e^2 \sin \sigma_i \cos \sigma_i - \frac{K_0}{J_{rx}} (\dot{\beta} + \dot{\sigma}_e \cos \sigma_i) - \frac{2}{J_{rx}} M_{cx_r} - \frac{1}{J_{rx}} M_{x_i},$$

$$\ddot{\beta} = -2a_1 (J_{iy} - J_{iz}) \dot{\sigma}_i \dot{\sigma}_e \sin \sigma_i \cos^2 \sigma_i + \dot{\sigma}_i \dot{\sigma}_e \sin \sigma_i + \frac{J_{rz}}{J_{rx}} (\dot{\alpha} + \dot{\sigma}_i) \dot{\sigma}_e \sin \sigma_i + \frac{K_0}{J_{rx}} (\dot{\alpha} + \dot{\sigma}_i) +$$

(1.64)

$$+ \frac{1 + a_1 J_{rx} \cos^2 \sigma_i}{J_{rx}} M_{cy_r} - a_1 \cos \sigma_i M_{y_e},$$

$$\ddot{\sigma}_i = \frac{J_{iz} - J_{iy}}{J_{ix}} \dot{\sigma}_e^2 \sin \sigma_i \cos \sigma_i + \frac{1}{J_{ix}} M_{x_i} + \frac{1}{J_{ix}} (M_{cx_r} + M_{gx_r}),$$

$$\ddot{\sigma}_e = 2a_1 (J_{iy} - J_{iz}) \dot{\sigma}_i \dot{\sigma}_e \sin \sigma_i \cos \sigma_i + a_1 M_{y_e} - a_1 \cos \sigma_i (M_{cy_r} + M_{gy_r}),$$

1.5. DGMSCMG DYNAMICS CONTROL USING THE CONCEPT OF DYNAMIC INVERSION

1.5.2. CONTROL OF NONLINEAR DECOUPLED MODELS OF TRANSLATIONAL AND ROTARY MOVEMENTS OF DGMSCMG

To simplify rotor control, one can separate (decouple) the dynamic model of translational motion from that of rotational motion. Thus, the first two equations (1.64), with (1.66), (1.4) and (1.5) (in which $\alpha = \beta = 0, i_\alpha = i_\beta = 0$ and thus $h_{xr}^a = h_{xr}^b = x_r, h_{yr}^a = h_{yr}^b = y_r, i_{xr}^a = i_{xr}^b = i_x, i_{yr}^a = i_{yr}^b = i_y$) also taking into account the perturbations generated by the gravitational force, they become

$$\ddot{x}_r = \frac{2k_{hx}}{m} x_r + \frac{2k_{xr}}{m} i_x + g_{xr},$$

$$\ddot{y}_r = \frac{2k_{hy}}{m} y_r + \frac{2k_{yr}}{m} i_y + g_{yr}, \tag{1.96}$$

From (1.96) the equations are obtained

$$u_1 = \begin{bmatrix} u_{11} \\ u_{12} \end{bmatrix} = \begin{bmatrix} i_x \\ i_y \end{bmatrix} = h_{r1}^{-1}(y_1, v_1) = \underbrace{\begin{bmatrix} \dfrac{m}{2k_{xr}} & 0 \\ 0 & \dfrac{m}{2k_{yr}} \end{bmatrix}}_{B_1^{-1}(x_1)} \left(v_1 - \underbrace{\begin{bmatrix} \dfrac{2k_{hx}}{m} & 0 \\ 0 & \dfrac{2k_{hy}}{m} \end{bmatrix}}_{A_1(x_1)} y_1 - \begin{bmatrix} g_{xr} \\ g_{yr} \end{bmatrix} \right), \tag{1.99}$$

from the equation

$$\ddot{y}_2 = A_2(x_2) + B_2(x_2) u_2; \tag{1.109}$$

by dynamic inversion results

$$u_2 = \begin{bmatrix} u_{21} \\ u_{22} \\ u_{23} \\ u_{24} \end{bmatrix} = \begin{bmatrix} i_\alpha \\ i_\beta \\ i_{xi} \\ i_{ye} \end{bmatrix} = h_{r2}^{-1}(y_2, v_2) = B_2^{-1}(x_2)[v_2 - A_2(x_2)], \tag{1.110}$$

with $v_2 = [v_{21} \quad v_{22} \quad v_{23} \quad v_{24}]^T = \ddot{y}_2 -$ the pseudo-command vector of the angular motion of the gyro rotor.

In fig. 1.7. the structure of an automatic control system of DGMSCMG is presented.
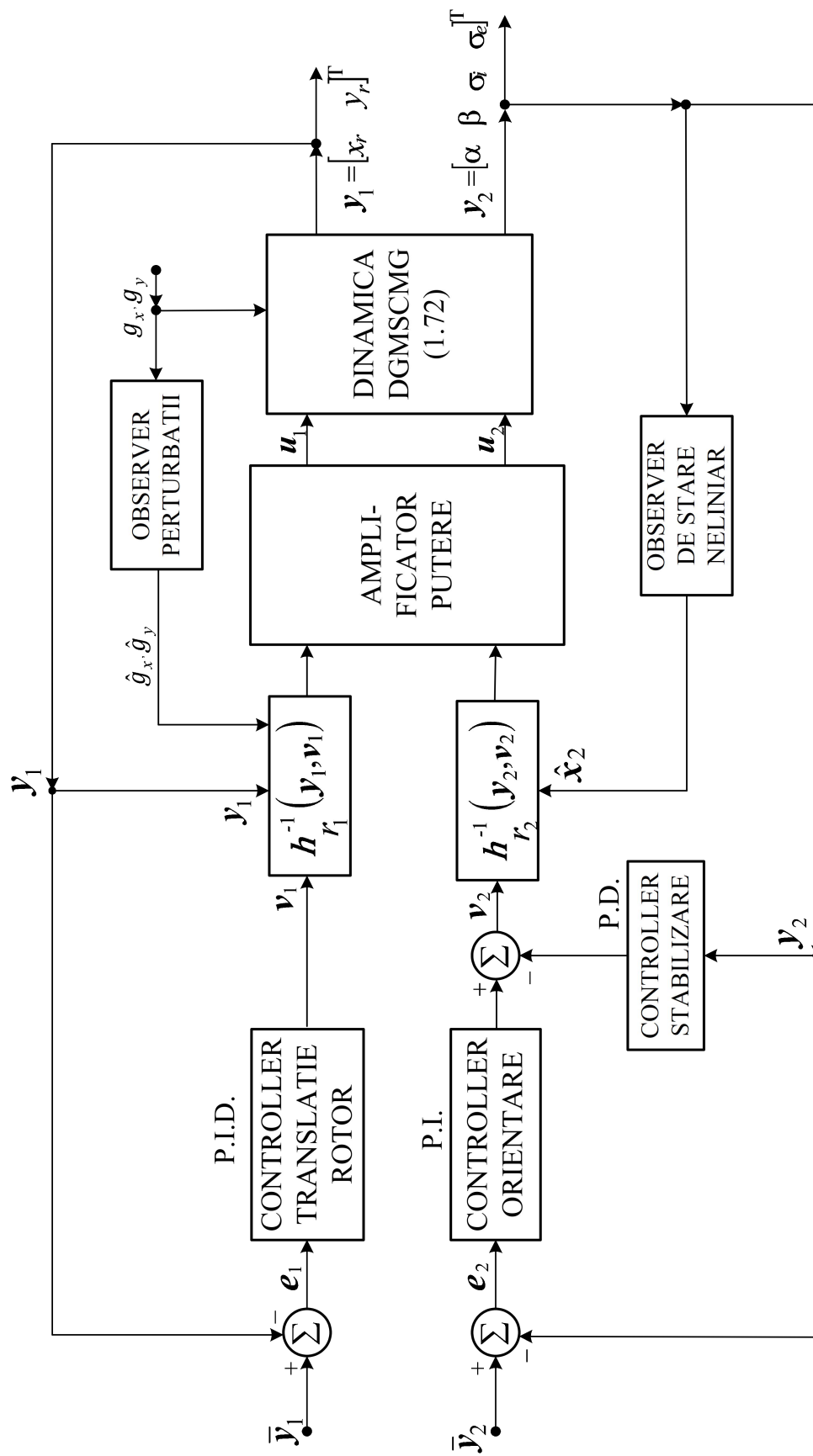
Fig.1.7. Structura sistemului de control automat al DGMSCMG

The Matlab/Simulink model (from fig. 1.8.a) is built for the system with the structure from fig.1.7., with its subsystems from fig.1.8.b and 1.8.c. To obtain the dynamic characteristics from fig.1.9, the Matlab program from Annexe A1.1 was designed and used.
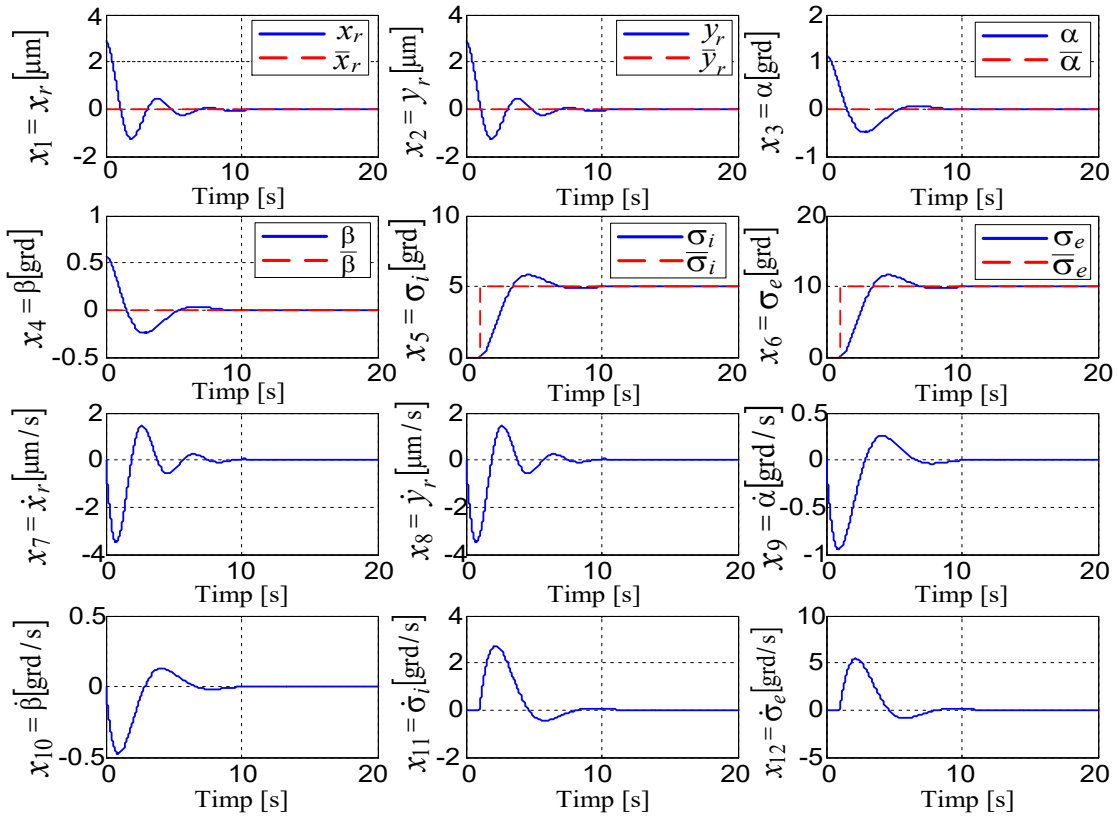
a.
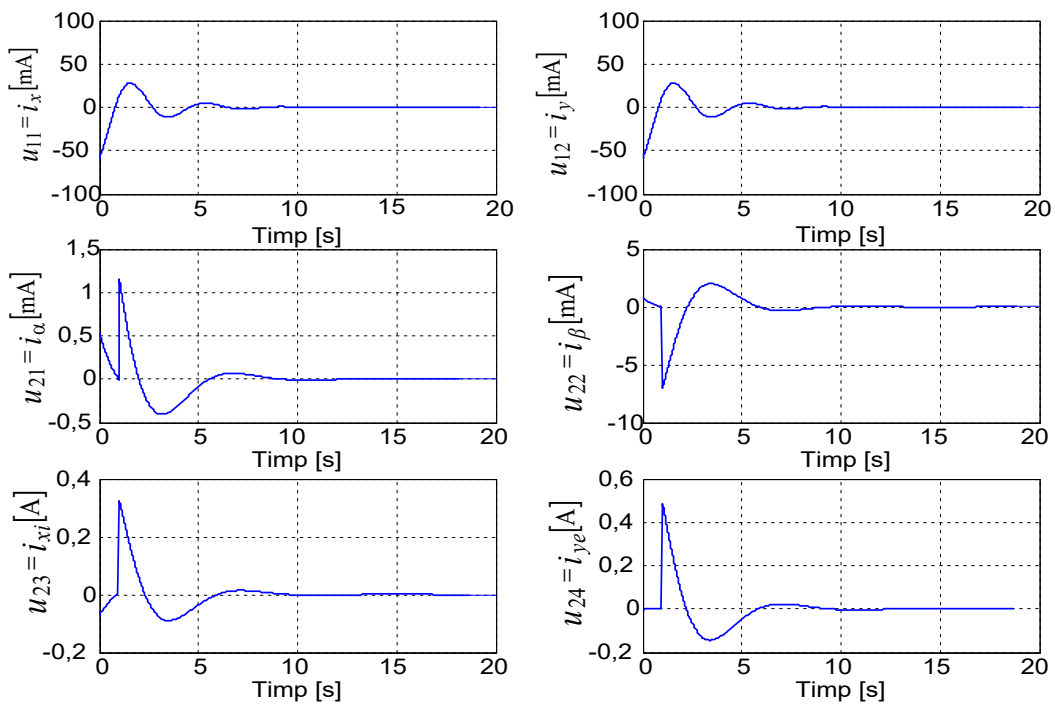
b.
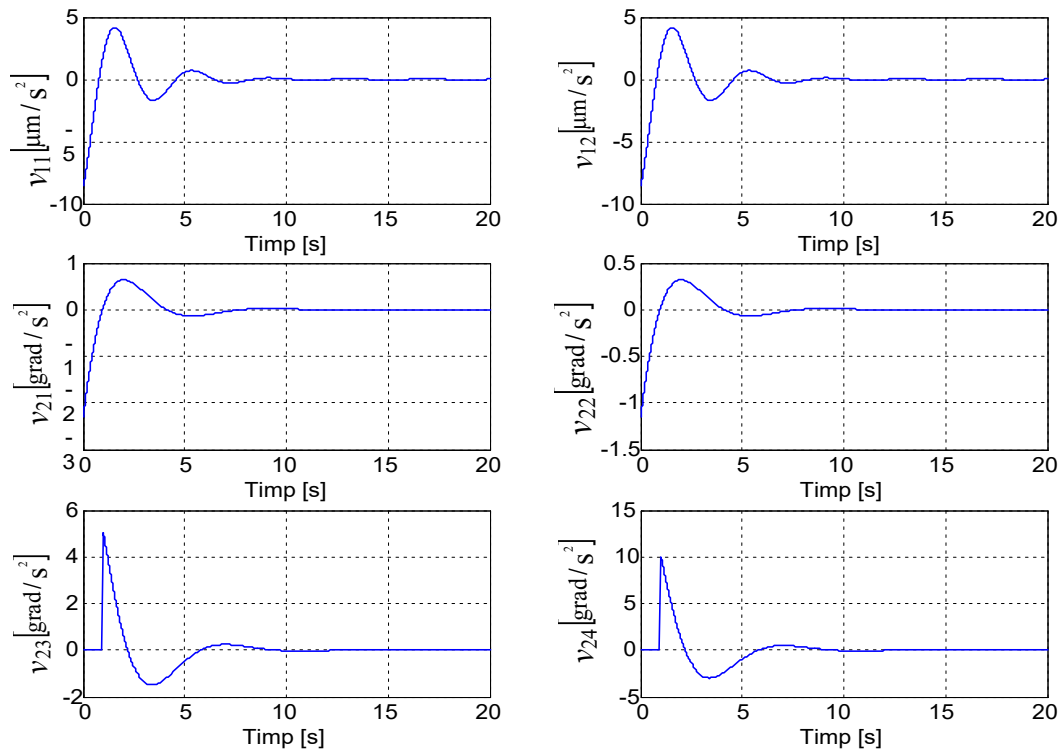
c.
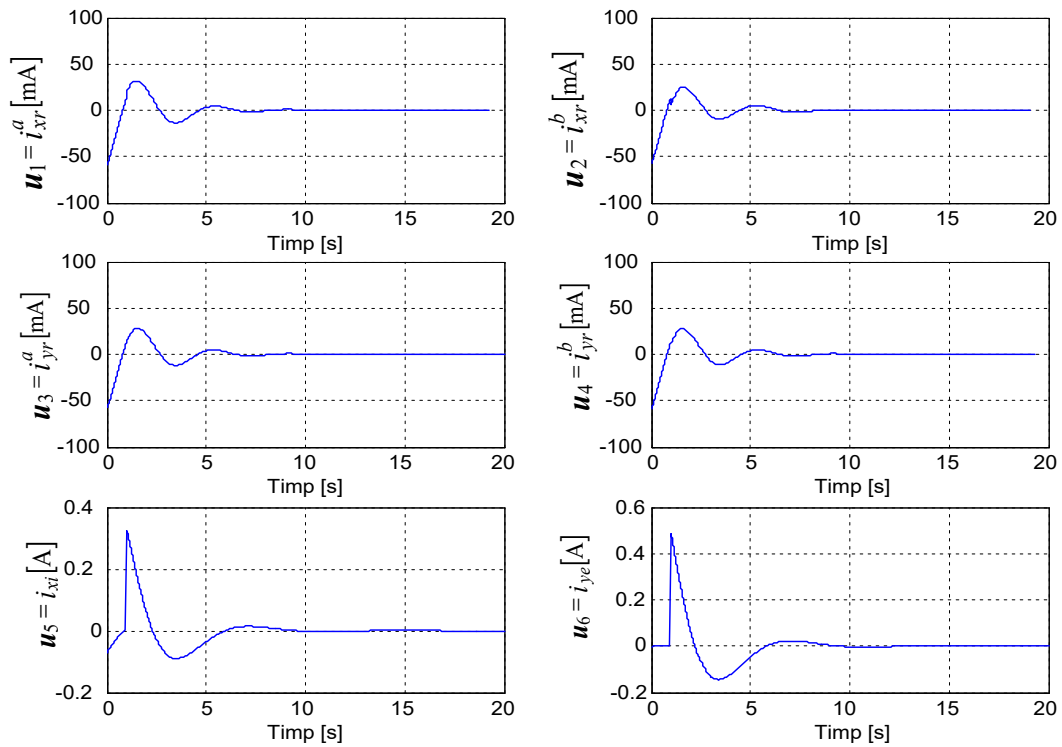
d.

Fig. 1.9. Dynamic characteristics for the automatic control system of DGMSCMG from fig. 1.7

1.5.4. ADAPTIVE CONTROL OF GYROSCOPIC ROTOR DYNAMICS AND ANGULAR VELOCITIES OF GYROSCOPIC FRAMES

For attitude control of satellites by means of DGMSCMGs, control of angular velocities is required $\dot{\sigma}_i$ and $\dot{\sigma}_e$ of the gyroscopic frames, which can be achieved with the structure in fig.1.11.b, where the output is the vector $\boldsymbol{y}_3 = \dot{\boldsymbol{\sigma}} = [\dot{\sigma}_i \quad \dot{\sigma}_e]^T$. The system consists of two servo systems (one for each gyroscopic frame).
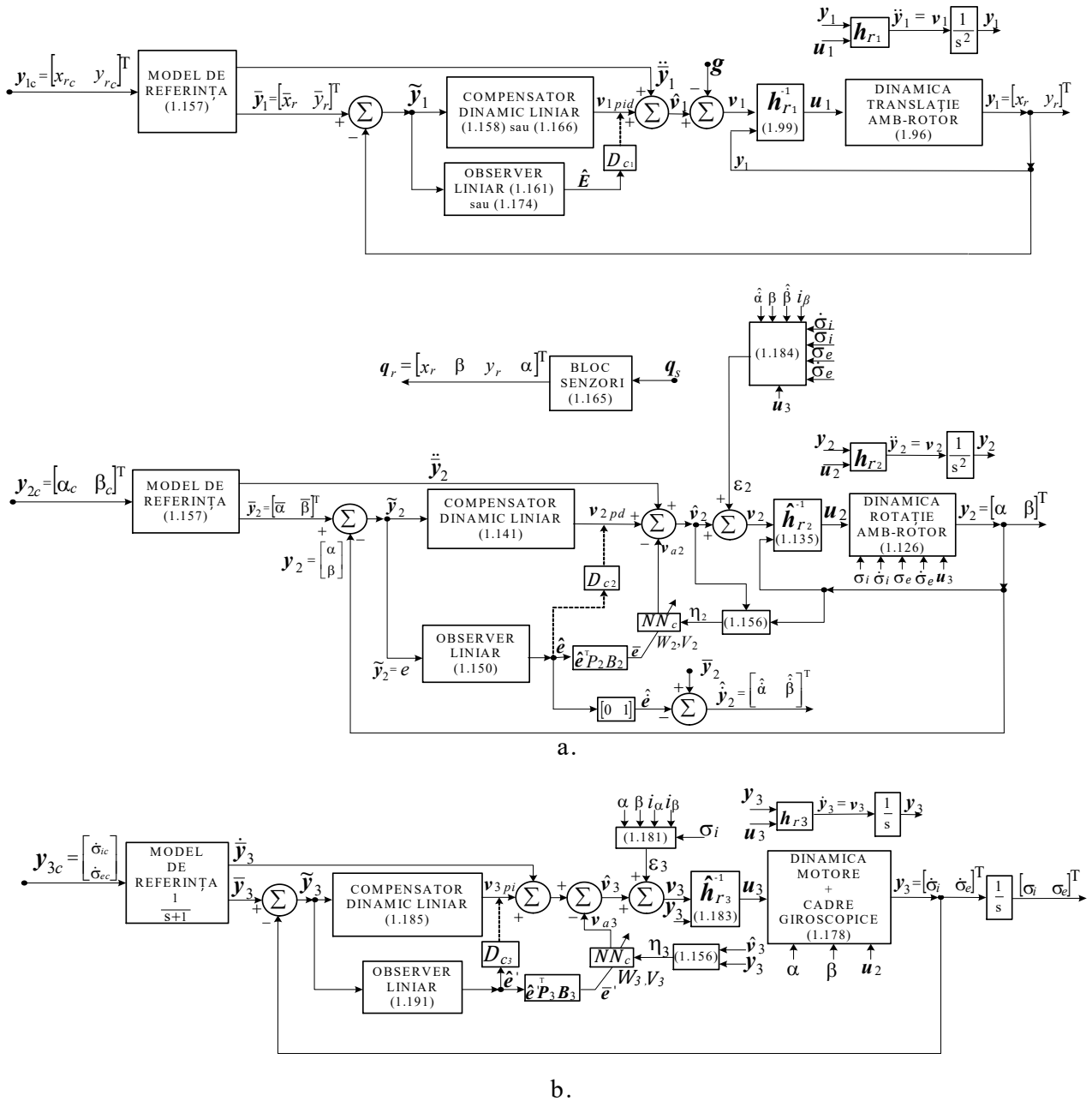
Fig.1.11. DGMSCMG dynamics adaptive control system: a) gyroscopic rotor dynamics adaptive control subsystems; b) adaptive control subsystem of the dynamics of the gyroscopic frames

Fig.1.13 shows the time characteristics of the system from fig.1.11, built with the Matlab/Simulink models and the program from Annexe A1.2
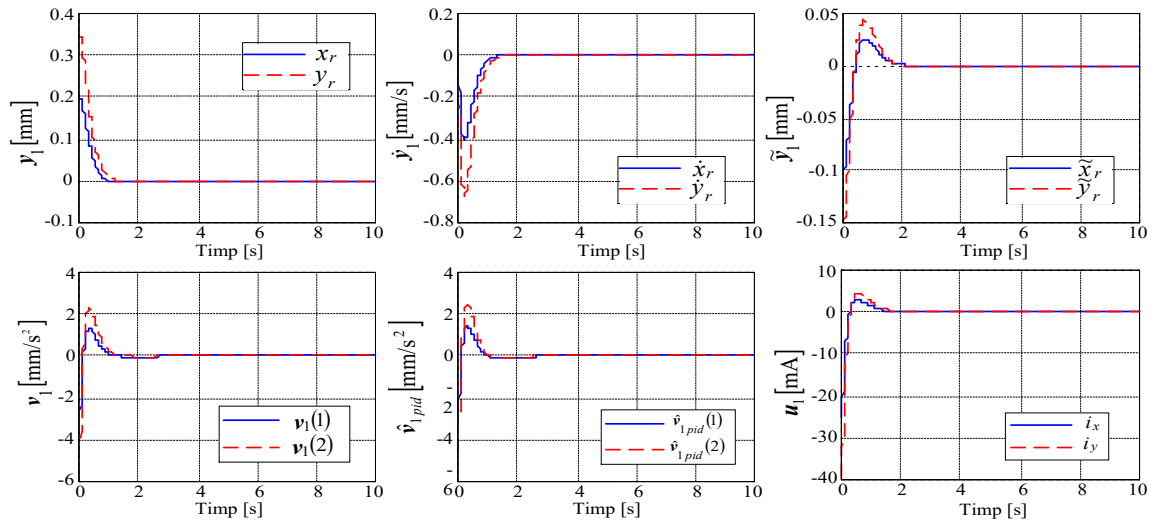
a.
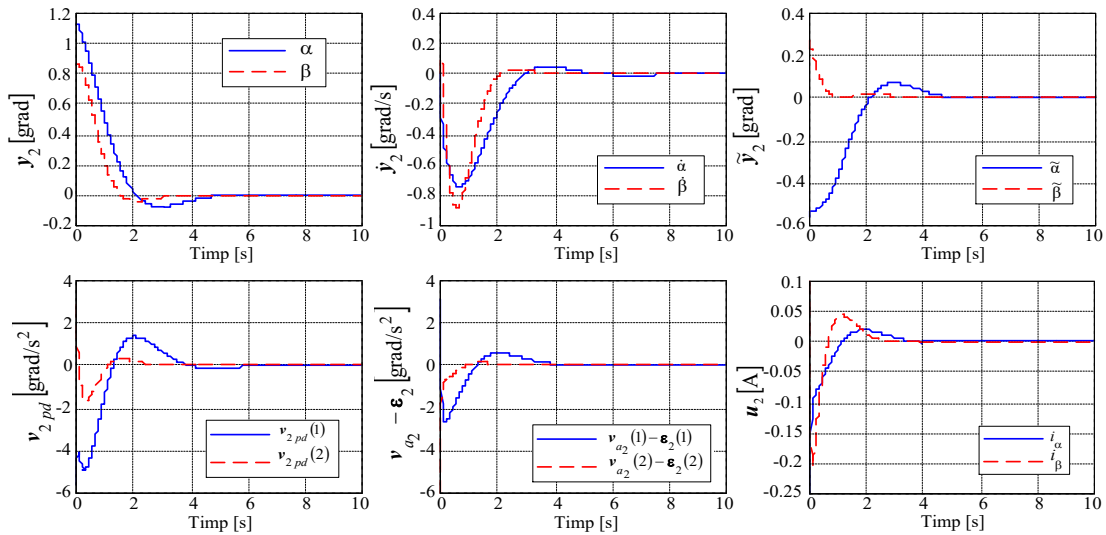
b.
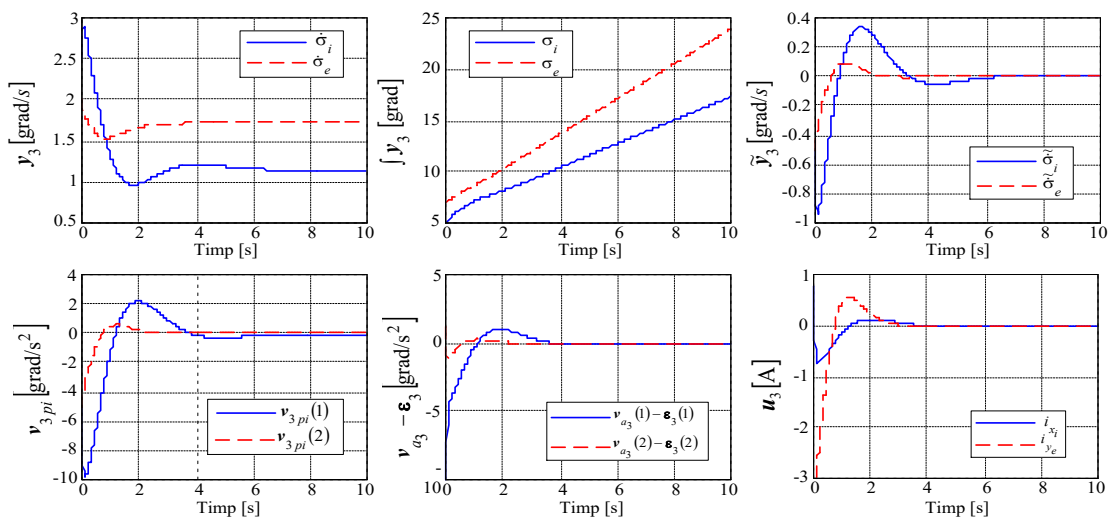
c.

Fig. 1.13. Evolution of system variables from fig.1.11

CHAPTER 2

ATTITUDE CONTROL OF SATELLITES USING ACTUATORS WITH DGMSCMGs

2.1. MODELING OF DGMSCMG DYNAMICS AND SATELLITE DYNAMICS

2.1.5. DYNAMIC MODEL OF THE BASE (SATELLITE)

The dynamics of the base (satellite) is described by the equation

$$J_b \dot{\omega}_b + \omega_b^\times J_b \omega_b = - M_k + M_p, \tag{2.58}$$

in which: J_b is the matrix of the moments of inertia of the base (without DGCMG) with respect to the axes of its trihedral, M_k — the total algebraic control torque vector applied to the base by means of the DGCMG-type CMG, and M_p — the perturbing external algebraic couple vector; $- M_k = M_g$ — the algebraic vector gyroscopic torque. The vector M_g is expressed as the sum of the torques applied to the base, produced by gyroscopic torque by the angular velocities ω_b, ω_i și ω_e applied DGCMG. The projections of the command couples, components of the vector, act on the base M_k.

Also taking into account the absolute kinetic moment K_{gb} produced by DGCMG, the satellite equation becomes

$$J_b \dot{\omega}_b + \frac{dK_{gb}}{dt} + \omega_b^\times J_b \omega_b = M_p; \tag{2.67}$$

K_{gb} is the resultant of the projections of the absolute kinetic moments of the outer frame, the inner frame and the gyroscopic rotor on the trihedral bound to the base (S),

$$K_{gb} = K_{eb} + K_{ib} + K_{rb}, \tag{2.68}$$

The matrix of total moments of inertia is

$$I_b = J_b + \left(A_b^e\right)^\mathrm{T} J_e A_b^e + \left(A_b^i\right)^\mathrm{T} I_i A_b^i. \tag{2.83}$$

Considering the fact that in the composition of the systems in fig. 2.16, fig. 2.17 and fig.2.22 include DGCMG2 (having the role of sensor for angular velocity $\hat{\omega}_b$), the relation (2.83) becomes

$$I_b = J_b + \sum_{j=1}^{2} \left[\left(A_b^{e_j}\right)^\mathrm{T} J_{ej} A_b^{e_j} + \left(A_b^{i_j}\right)^\mathrm{T} I_{i_j} A_b^{i_j} \right]; \tag{2.84}$$

Finally, the satellite equation becomes

$$I_b \dot{\omega}_b + \omega_b^\times I_b \omega_b = - M_k + M_p, \tag{2.86}$$

with

$$M_k = - M_g = \omega_b^\times A_i^b K_0 + A_i^b \omega_i^\times K_0 + A_e^b \omega_e^\times A_i^e K_0, \tag{2.87}$$

which is the very relation (2.65) or

$$M_k = - M_g = \omega_b^\times A_i^b K_0 - A_i^b K_0^\times \omega_i - A_e^b (A_i^e K_0)^\times \omega_e. \tag{2.88}$$

The servo system model for angular velocity control is obtained $\dot{\sigma}_i$ presented in fig. 2.7.

CONTROLLER

$k_{pi} + \dfrac{k_{ii}}{s}$

$\dot\sigma_{ic}$

i_c

k_r

k_i

U

BOBINA MOTOR

$\dfrac{1}{Ls+R}$

C_e

i_m

k_m

M_m^a

ROTOR MOTOR

$\dfrac{1}{J_m s + c_m}$

$\dfrac{1}{n}$

$\dot\sigma_m$

$\dfrac{1}{s}$

σ_m

$\dfrac{1}{n}$

σ

k_e

M_i^c

CADRU GIROSCOPIC

$\dfrac{1}{J_{ix}s + c_i}$

M_{ix}

$\dot\sigma_i$

$\dfrac{1}{s}$

σ_i

MOTOR

R.M.

MOTOR - R.M.
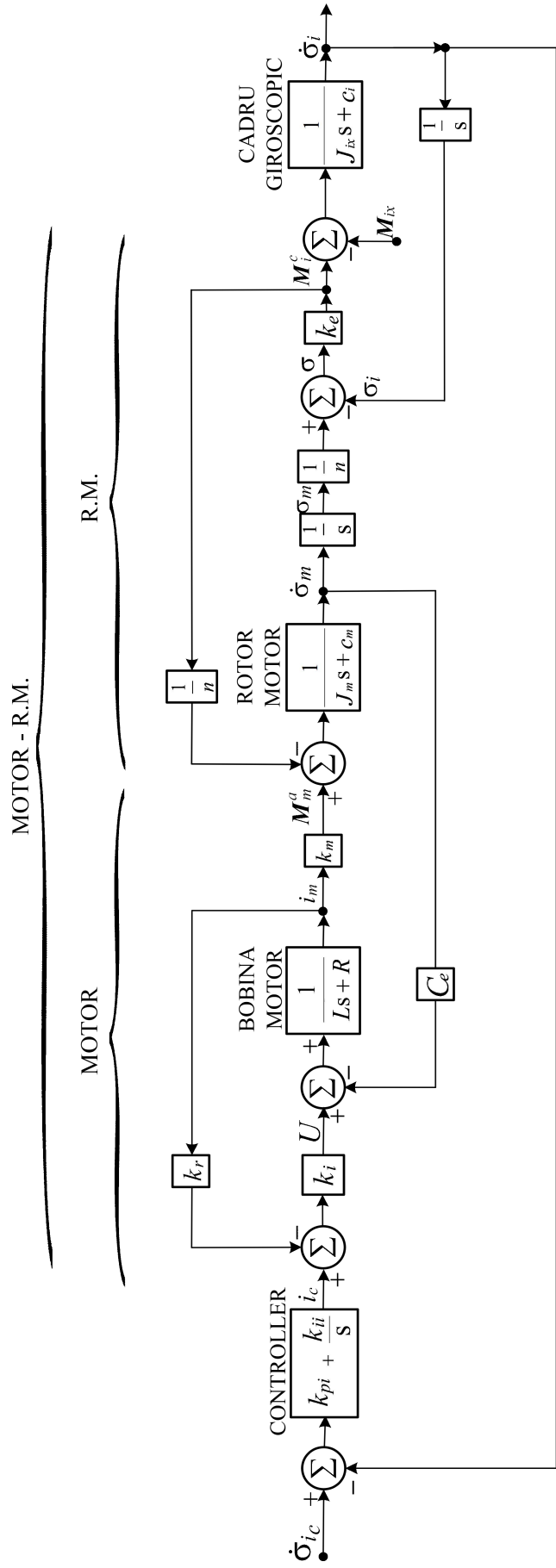
Fig.2.7. Modelul servosistemului liniar pentru controlul vitezei unghiulare $\dot\sigma_i$

2.2. ATTITUDE CONTROL OF SATELLITES

2.2.1. DETERMINATION OF THE ATTITUDE OF SATELLITES

The orbit of the satellite is elliptical; The Earth is located in one of the foci of the ellipse. The inertial trihedron $O_iX_iY_iZ_i$ has the axis O_iX_i oriented in the direction of the Vernal equinox, the axis O_iZ_i to the geographic north pole of the Earth and the axis O_iY_i perpendicular to the other two with which it forms a right orthogonal trihedron $O_iX_iY_iZ_i$. The local orbital trihedron $ox_oy_oz_o$ has the axes oriented as follows: oy_o in the direction that connects the satellite S (with the origin in o) to the center of the Earth O_i, oz_o is oriented in the sense of the antinormal and ox_o is oriented so as to complete the right orthogonal trihedron $ox_oy_oz_o$. Fig. 2.8 shows the inertial triads $O_iX_iY_iZ_i$, local orbital $ox_oy_oz_o$ and "Satellite" ($ox_by_bz_b$).
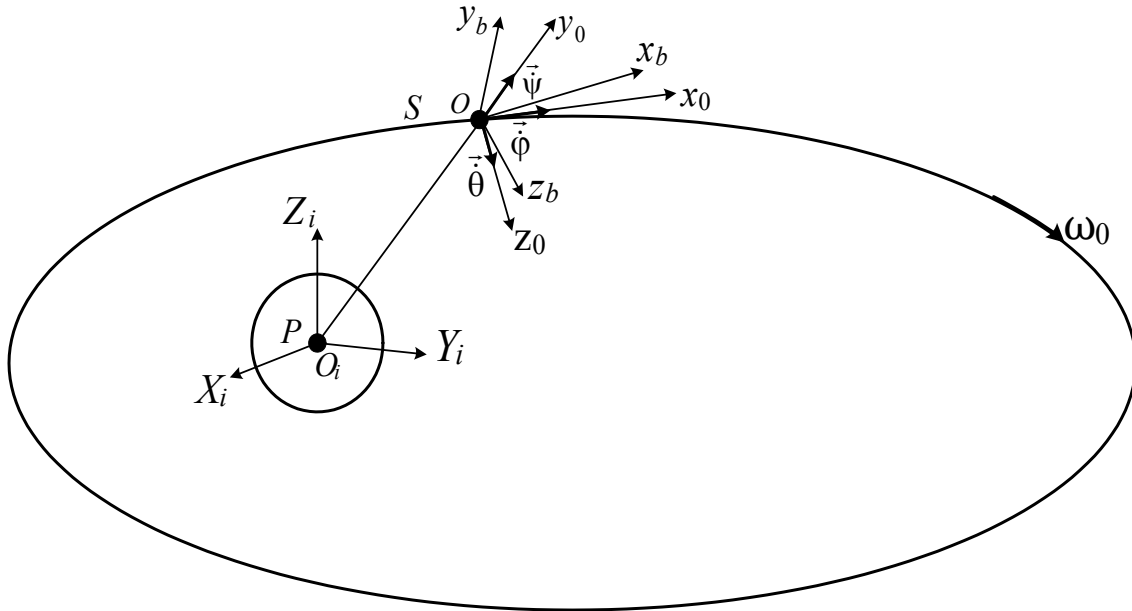
Fig. 2.8. Inertial trihedral, local orbital and "Satellite"

Fig. 2.10 shows: inertial coordinate systems (trieds). $\mathcal{J}$ ($O_iX_iY_iZ_i$), S (base, satellite, $ox_by_bz_b$) and the reference one $\mathcal{R}$ ($o_Rx_Ry_Rz_R$) (in particular the local orbital trihedral $ox_oy_oz_o$); absolute angular velocities $\vec{\omega}_b$ and relative $\vec{\omega}_s$ of the satellite, as well as its angular velocity of transport $\vec{\omega}_0$;

The relationship between absolute angular velocities ω_b, relative ω_s and transport ω_0 is

$$\omega_b = \omega_s + A(\boldsymbol{q}, q_4)\, \omega_0. \tag{2.127}$$
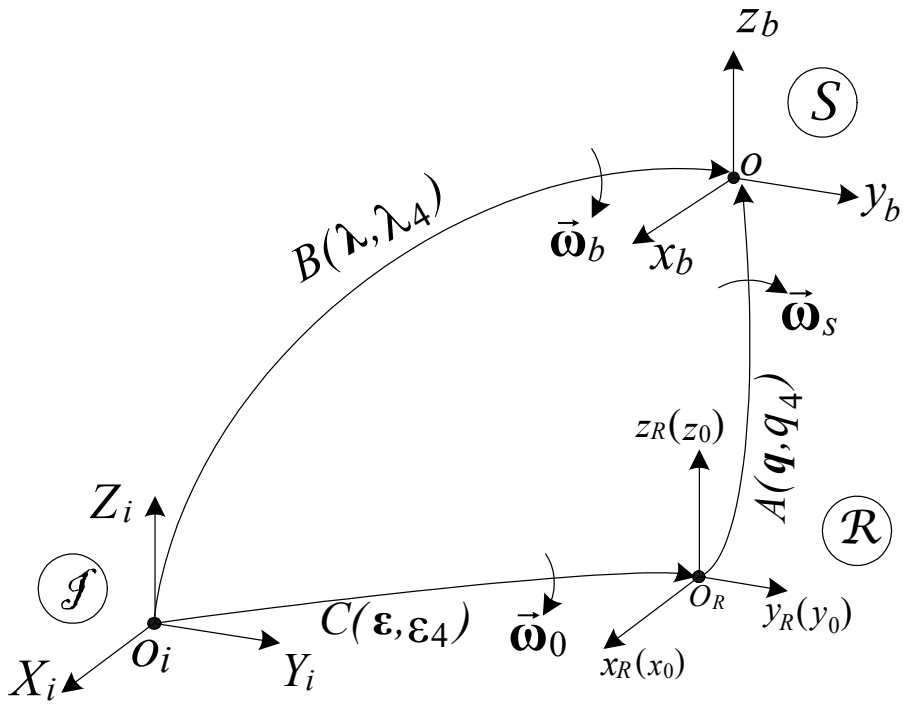
Fig. 2.10. Coordinate systems, rotation matrices and quaternions

Fig. 2.12 shows the block diagram of the satellite attitude calculation system.
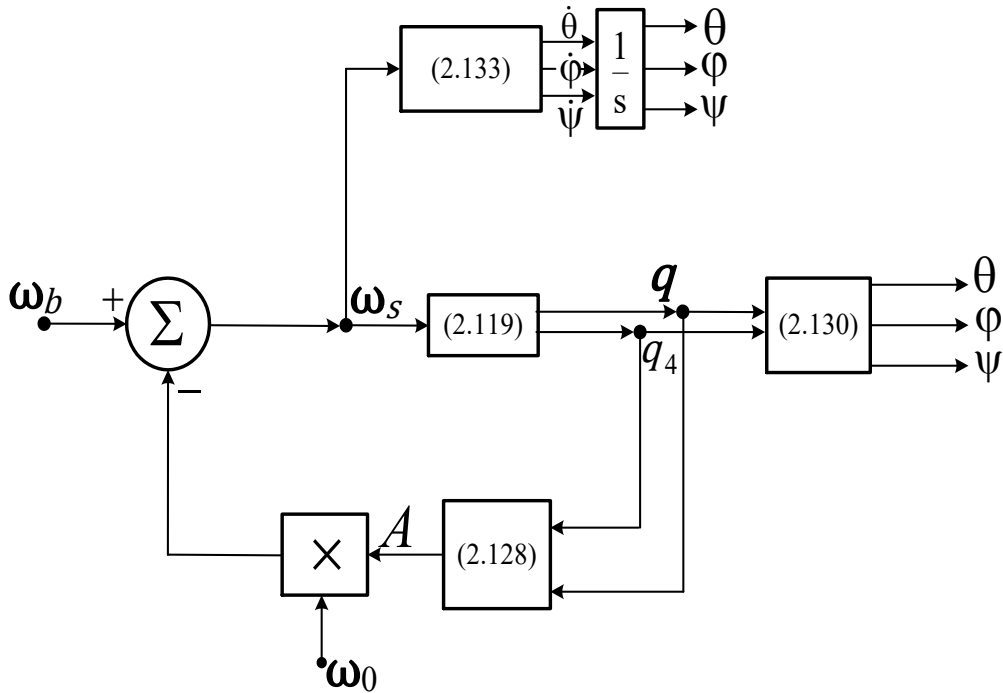
Fig. 2.12. Block diagram of the attitude calculation system S

2.2.2. ATTITUDE CONTROL OF SATELLITES USING ACTUATOR WITH
N=1 DGMSCMG

In fig. 2.13, the triads linked to the gyroscopic rotor, the inner frame, the outer frame and the one linked to the base are highlighted (satellite $ox_b y_b z_b$); this figure is consistent with fig.2.2 and fig.2.4. Exterior frame plan $e(ox_e y_e)$ lies in the local orbital plane $(ox_o y_o)$, if $\sigma_i = \sigma_e = 0$ and the satellite (S), mean the trihedral $S(ox_b y_b z_b)$ is superimposed on the trihedral $ox_o y_o z_o$ (v.fig.2.8).
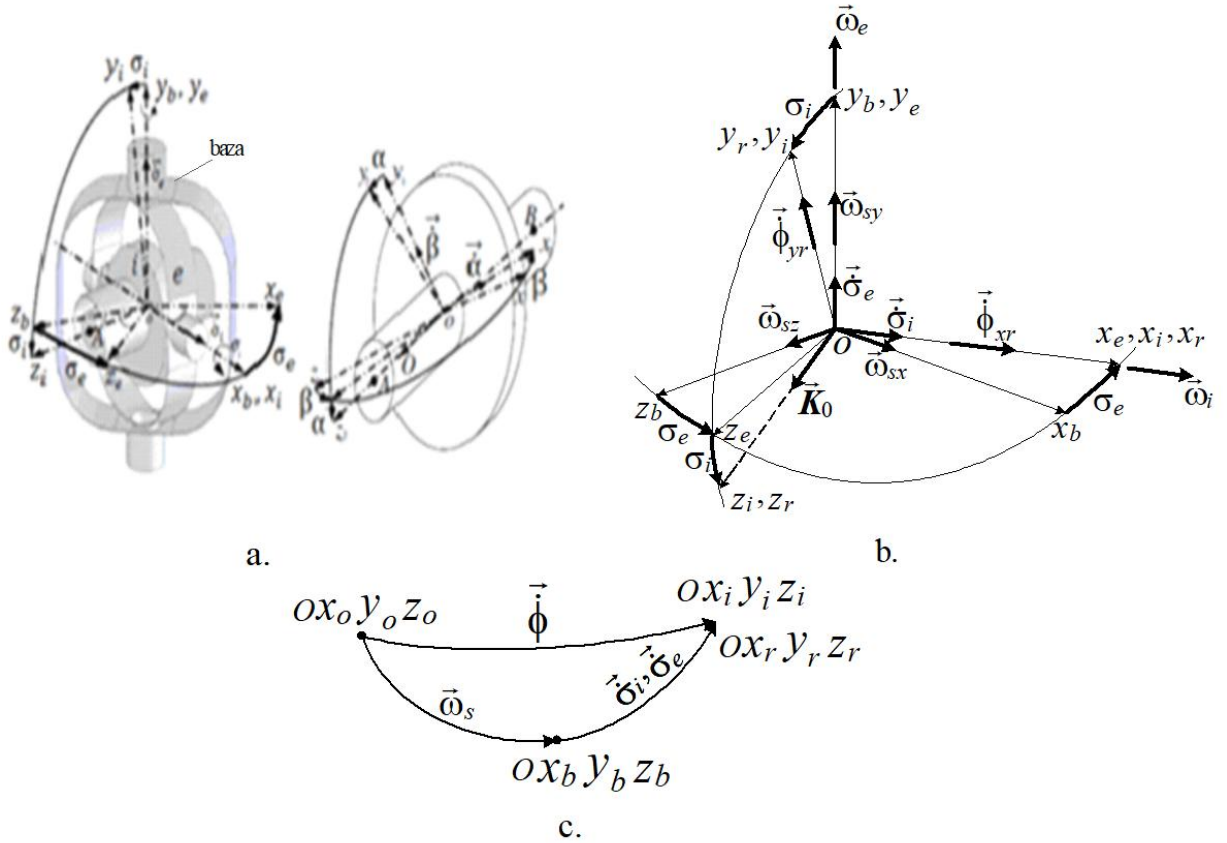
Fig. 2.13. The trihedra connected to the rotor, to the two gyroscopic and base frames (S)

The absolute angular velocities of the rotor and the inner gyroscopic frame relative to the local orbital trihedron $ox_o y_o z_o$ are the resultants of the relative angular velocities $\dot{\sigma}_i$ and $\dot{\sigma}_e$ (against the base of the trihedral $ox_b y_b z_b$) and of the transport ones (of the base, S, against the local orbital trihedron; the components of the vector $\boldsymbol{\omega}_s$); according fig.2.13.b şi 2.13.c,

$$\dot{\phi}_{x_r} \simeq \dot{\phi}_{x_i} = \dot{\sigma}_i + \omega_{sx} \cos \sigma_e - \omega_{sz} \sin \sigma_e,$$
$$\dot{\phi}_{y_r} \simeq \dot{\phi}_{y_i} = (\dot{\sigma}_e + \omega_{sy}) \cos \sigma_i + (\omega_{sx} \sin \sigma_e + \omega_{sz} \cos \sigma_e) \sin \sigma_i,$$
(2.135)

According to fig.2.13.b, the angular velocities calculated by the attitude controller of S are $\omega_i = \dot{\phi}_{x_r} \simeq \dot{\phi}_{x_i}$ and $\omega_e = \dfrac{\dot{\phi}_{y_r}}{\cos \sigma_i} \simeq \dfrac{\dot{\phi}_{y_i}}{\cos \sigma_i}$. Substituting in them (2.135), the relative angular velocities applied to the gyroscopic frame actuation servo systems are obtained

$$\dot{\sigma}_{i1c} = \omega_i - (\omega_{sx} \cos \sigma_{e_1} - \omega_{sz} \sin \sigma_{e_1}),$$

$$\dot{\sigma}_{e1c} = \omega_e - \omega_{sy} - (\omega_{sx} \sin \sigma_{e_1} + \omega_{sz} \cos \sigma_{e_1}) \tan \sigma_{i_1}. \tag{2.144}$$

Fig. 2.14 shows the subsystems for modeling the dynamics of the actuator-satellite interaction, the automatic control of the dynamics of the gyroscopic rotor and the servo systems for actuating the gyroscopic frames of the MSDGCMG1. Fig. 2.15 shows the subsystems for modeling the dynamics of the DGMSCMG2-satellite sensor interaction and the dynamics of the sensor, and in Fig. 2.16 – the structure of the automatic attitude control system of the satellite, with DGMSCMG1 actuator and DGMSCMG2 sensor for measuring the satellite's absolute angular velocity.

Because $\boldsymbol{\omega}_b = [\omega_{bx} \quad \omega_{by} \quad \omega_{bz}]^\mathrm{T}$, $\boldsymbol{\omega}_i = [\omega_i \quad 0 \quad 0]^\mathrm{T}$ and $\boldsymbol{\omega}_e = [0 \quad \omega_e \quad 0]^\mathrm{T}$, the matrices result

$$\boldsymbol{\omega}_b^\times = \begin{bmatrix} 0 & -\omega_{bz} & \omega_{by} \\ \omega_{bz} & 0 & -\omega_{bx} \\ -\omega_{by} & \omega_{bx} & 0 \end{bmatrix}, \boldsymbol{\omega}_i^\times = \begin{bmatrix} 0 & 0 & 0 \\ 0 & 0 & -\omega_i \\ 0 & \omega_i & 0 \end{bmatrix}, \boldsymbol{\omega}_e^\times = \begin{bmatrix} 0 & 0 & \omega_e \\ 0 & 0 & 0 \\ -\omega_e & 0 & 0 \end{bmatrix}. \tag{2.145}$$

Disturbed satellite, rotating with relative angular velocity $\boldsymbol{\omega}_s$, respectively with the absolute angular velocity $\boldsymbol{\omega}_b$(v. fig.2.10), must be returned to the initial position with the angular velocity $-\boldsymbol{\omega}_s$; for this, the actuator (DGMSCMG 1) must apply a torque to the satellite $\boldsymbol{M}_k = -\boldsymbol{M}_g$, which depends only on the angular velocity $\boldsymbol{\omega}_b$, to bring the satellite through an aperiodic evolution to the angular velocity $\boldsymbol{\omega}_0$ (according to equation (2.86) and relation (2.127)). But, according to (2.88), with $\boldsymbol{K}_0 = [0 \quad 0 \quad K_0]^\mathrm{T}$, $\boldsymbol{M}_k = \boldsymbol{M}_k(\boldsymbol{\omega}_b, \boldsymbol{\omega}_i, \boldsymbol{\omega}_e)$ and, as a result, the satellite will rotate with an angular velocity $\widehat{\boldsymbol{\omega}}_b \neq \boldsymbol{\omega}_b$. Therefore, a second DGMSCMG (DGMSCMG2) is used as an angular velocity sensor $\widehat{\boldsymbol{\omega}}_b$.

DGMSCMG 2 being located on the base (satellite), it reacts to the angular velocity $\widehat{\boldsymbol{\omega}}_b$ by the gyroscopic torque $\boldsymbol{M}_{ks}$ (acts as a sensor for angular velocity $\widehat{\boldsymbol{\omega}}_b$). Indeed, if no angular velocities are applied to its gyroscopic frames, mean $\omega_i = \omega_e = 0$, then, according to (2.88),

$$\boldsymbol{M}_{ks} = -\boldsymbol{M}_{gs} = \widehat{\boldsymbol{\omega}}_b^\times A_{is}^b \boldsymbol{K}_{0s} = -\left(A_{is}^b \boldsymbol{K}_{0s}\right)^\times \widehat{\boldsymbol{\omega}}_b, \tag{2.146}$$

Relations of the form (2.144), for the sensor, become

$$\dot{\sigma}_{i2c} = -(\omega_{sx} \cos \sigma_{e_2} - \omega_{sz} \sin \sigma_{e_2}),$$

$$\dot{\sigma}_{e2c} = -\omega_{sy} - (\omega_{sx} \sin \sigma_{e_2} + \omega_{sz} \cos \sigma_{e_2}) \tan \sigma_{i_2}. \tag{2.149}$$

The control low by the relative attitude of the satellite (expressed by the quaternion vector $\boldsymbol{q}$) it is chosen, for example, of type P.D. after $\boldsymbol{q}$; taking into account the equations of the kinematics of the quaternions (2.119), the control can be performed according to $\boldsymbol{q}$ and $\boldsymbol{\omega}_s$; if the desired attitude is chosen, then the system in fig. 2.16 must perform in a stabilized regime $\boldsymbol{q} = \boldsymbol{q}_d$, $\boldsymbol{\omega}_s = \boldsymbol{\omega}_{sd} = 0_{3\times1}$ and, implicitly, from (2.127), according to fig.2.10, $\boldsymbol{\omega}_b = \boldsymbol{\omega}_s + A(\boldsymbol{q}_d, q_{4d})\boldsymbol{\omega}_0$, $\dot{\sigma}_{i1c} = \dot{\sigma}_{e1c} = \dot{\sigma}_{i1} = \dot{\sigma}_{e1} = \omega_i = \omega_e = 0$ şi, implicitly, $\boldsymbol{M}_k$ it is reduced only to the component (2.146); according to the satellite dynamics equation (2.86), $\widehat{\boldsymbol{\omega}}_b \to \boldsymbol{\omega}_b$ and $\boldsymbol{M}_k \to \boldsymbol{M}_{ks}$.
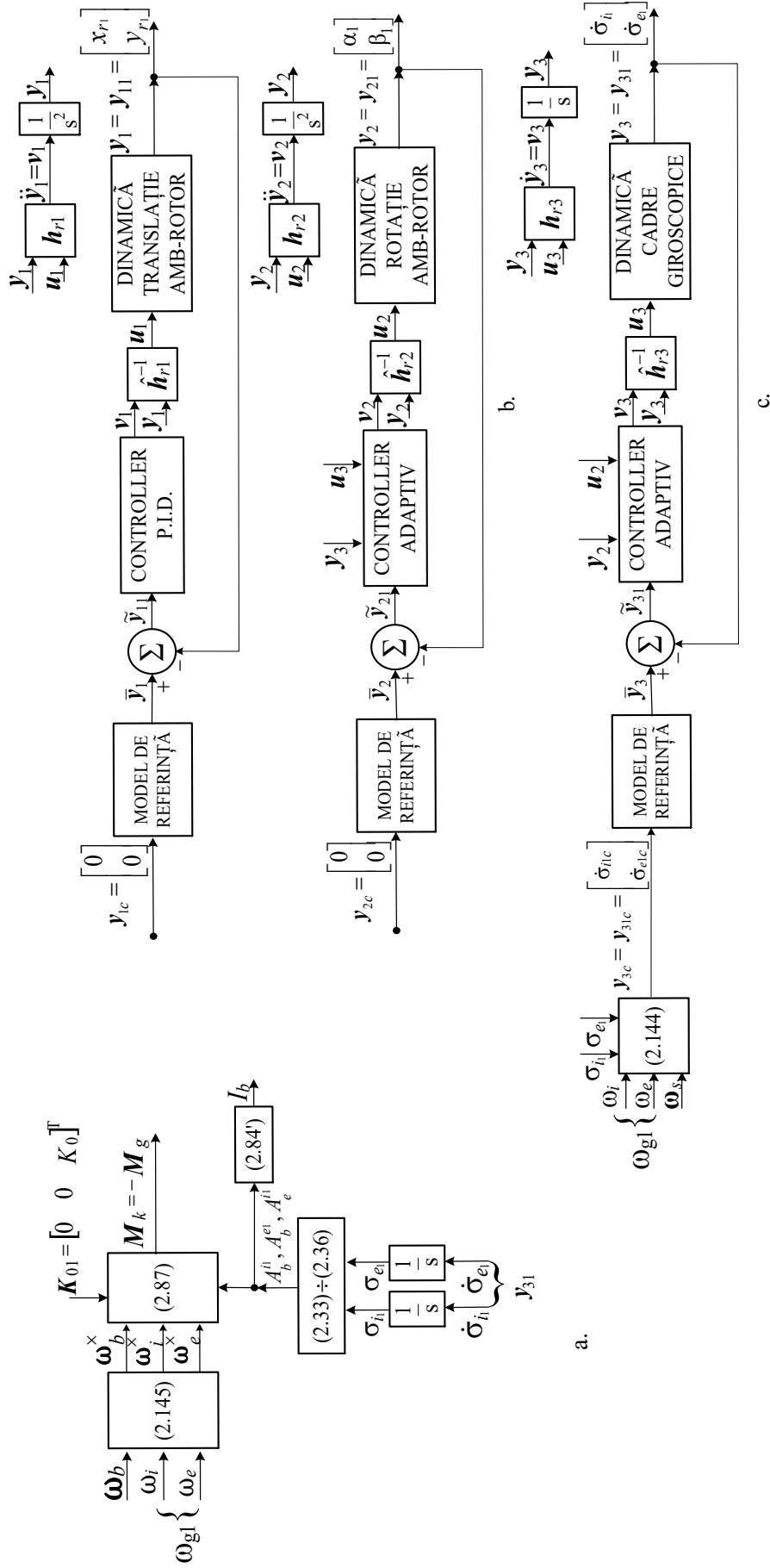
Fig.2.14. Subsisteme pentru modelarea dinamicii interactiunii actuator (DGMSCMGI)-satelit (a), a controlului automat al dinamicii translatiei si rotatiei AMB-Rotor (b) si a servosistemelor pentru actionarea cadrelor giroscopice (c)

24

fig.2.14.b, cu

$y_1 = y_{12} = [x_{r2} \quad y_{r2}]^T$

$y_2 = y_{22} = [\alpha_2 \quad \beta_2]^T$

$y_3 = y_{32} = [\dot{\sigma}_{i2} \quad \dot{\sigma}_{e2}]^T$

y_{12}

y_{22}

fig.2.14.c, cu

$y_2 = y_{22} = [\alpha_2 \quad \beta_2]^T$

$y_3 = y_{32} = [\dot{\sigma}_{i2} \quad \dot{\sigma}_{e2}]^T$

y_{32}

$y_{32c} = \begin{bmatrix} \dot{\sigma}_{i2c} \\ \dot{\sigma}_{e2c} \end{bmatrix}^T$

σ_{e2}

σ_{i2}

(2.149)

$\omega_i = 0$

$\omega_e = 0$

ω_s

b.

$K_{02} = [0 \quad 0 \quad K_0]^T$

$M_{ks} = -M_{gs}$

(2.146)

$\hat{\omega}_b^\times$

(2.170')

$\hat{\omega}_b$

$A_{i2}^b = (A_b^{i2})^T$

(2.33),(2.34),(2.36)

A_b^{i2}, A_b^{e2}

(2.84')

I_b

σ_{e2}

σ_{i2}

$\dfrac{1}{s}$

$\dfrac{1}{s}$

$\dot{\sigma}_{e2}$

$\dot{\sigma}_{i2}$

y_{32}

a.

Fig.2.15. Subsisteme pentru modelarea interacțiunii satelit-senzor (DGMSCMG2) (a) și a dinamicii senzorului (b)

25
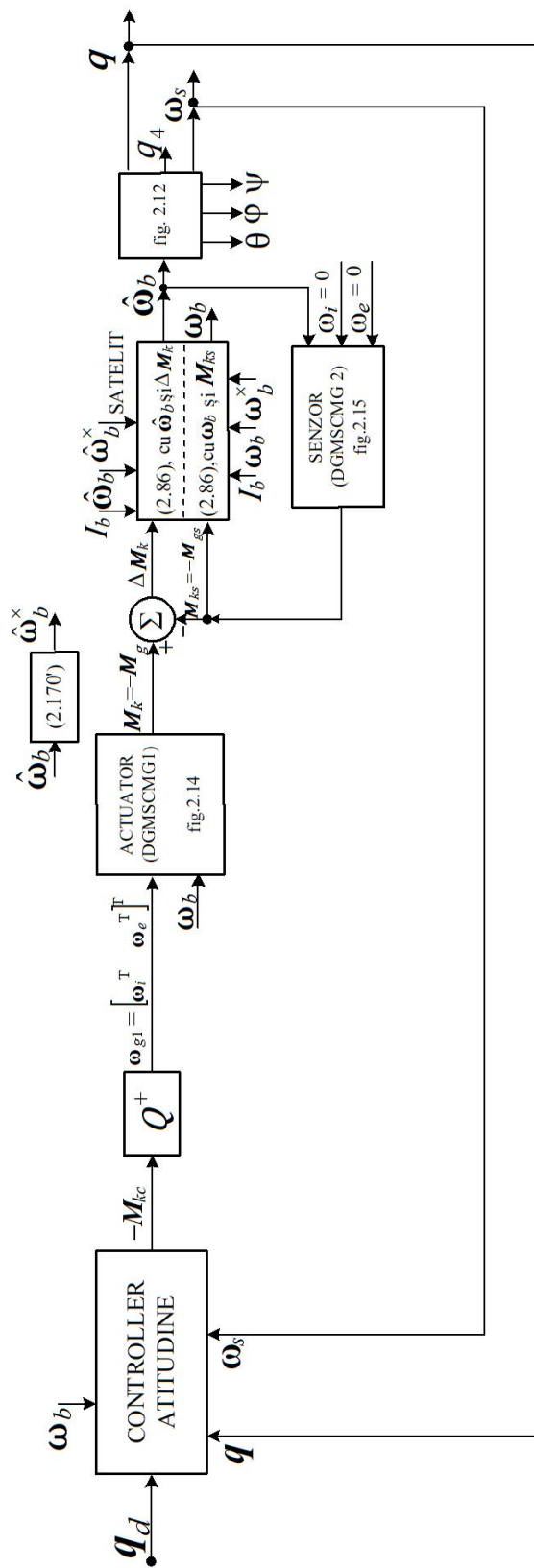
Fig.2.16. Sistem de control al atitudinii satelitului cu DGMSCMG 1 și DGMSCMG 2

2.2.3. DESIGN OF THE ATTITUDE CONTROLLER

With Lyapunov function [101]

$$V = \frac{1}{2}\boldsymbol{\omega}_{se}^T I_b \boldsymbol{\omega}_{se} + 2k_p \ln(1 + \boldsymbol{q}_e^T \boldsymbol{q}_e),\ k_p > 0; \tag{2.150}$$

the control law ensures the achievement of convergences $\boldsymbol{\omega}_{se} = \boldsymbol{\omega}_{sd} - \boldsymbol{\omega}_s \to [0\ \ 0\ \ 0]^T$ and $[\boldsymbol{q}_e\ \ q_{e4}]^T = M(\boldsymbol{q}_d, q_{4d})[\boldsymbol{q}\ \ q_4]^T \to [0\ \ 0\ \ 0\ \ 1]^T$ when $t \to \infty$, with $\boldsymbol{\omega}_{sd}$ – the desired angular velocity of the satellite relative to the local orbital trihedral, $\boldsymbol{q}_d$ – the desired quaternion, and $\boldsymbol{q}_e$ – attitude deviation quaternion, $\boldsymbol{q}_e = [q_{e1}\ \ q_{e2}\ \ q_{e3}]^T$, solution of the equation

$$\dot{\boldsymbol{q}}_e = F(\boldsymbol{q}_e)\boldsymbol{\omega}_{se}, \tag{2.151}$$

with $F(\boldsymbol{q}_e)$ formal [92]

$$F(\boldsymbol{q}_e) = \frac{1}{2}\left[\frac{1}{2}(1 + \boldsymbol{q}_e^T \boldsymbol{q}_e)I_{3\times3} + \boldsymbol{q}_e^\times\right], \tag{2.152}$$

$$\boldsymbol{q}_e^\times = \begin{bmatrix} 0 & -q_{e3} & q_{e2} \\ q_{e3} & 0 & -q_{e1} \\ -q_{e2} & q_{e1} & 0 \end{bmatrix}; M(\boldsymbol{q}_d, q_{4d}) = \begin{bmatrix} q_{4d} & q_{3d} & -q_{2d} & -q_{1d} \\ -q_{3d} & q_{4d} & q_{1d} & -q_{2d} \\ q_{2d} & -q_{1d} & q_{4d} & -q_{3d} \\ q_{1d} & q_{2d} & q_{3d} & q_{4d} \end{bmatrix} \tag{2.153}$$

$\dot{V} < 0$ expresses the condition that the closed circuit system is asymptotically stable.

$$I_b \dot{\boldsymbol{\omega}}_{sd} + k_d \boldsymbol{\omega}_{se} + k_p \boldsymbol{q}_e + \boldsymbol{\omega}_b^\times (I_b \boldsymbol{\omega}_b + A_{i1}^b \boldsymbol{K}_0) + \omega_0 I_b \boldsymbol{\omega}_s^\times (\text{col } 3)_A - \boldsymbol{M}_p = -\boldsymbol{M}_{kc}. \tag{2.166}$$

Using $\boldsymbol{M}_{kc}$, calculated with (2.166), from (2.164) results

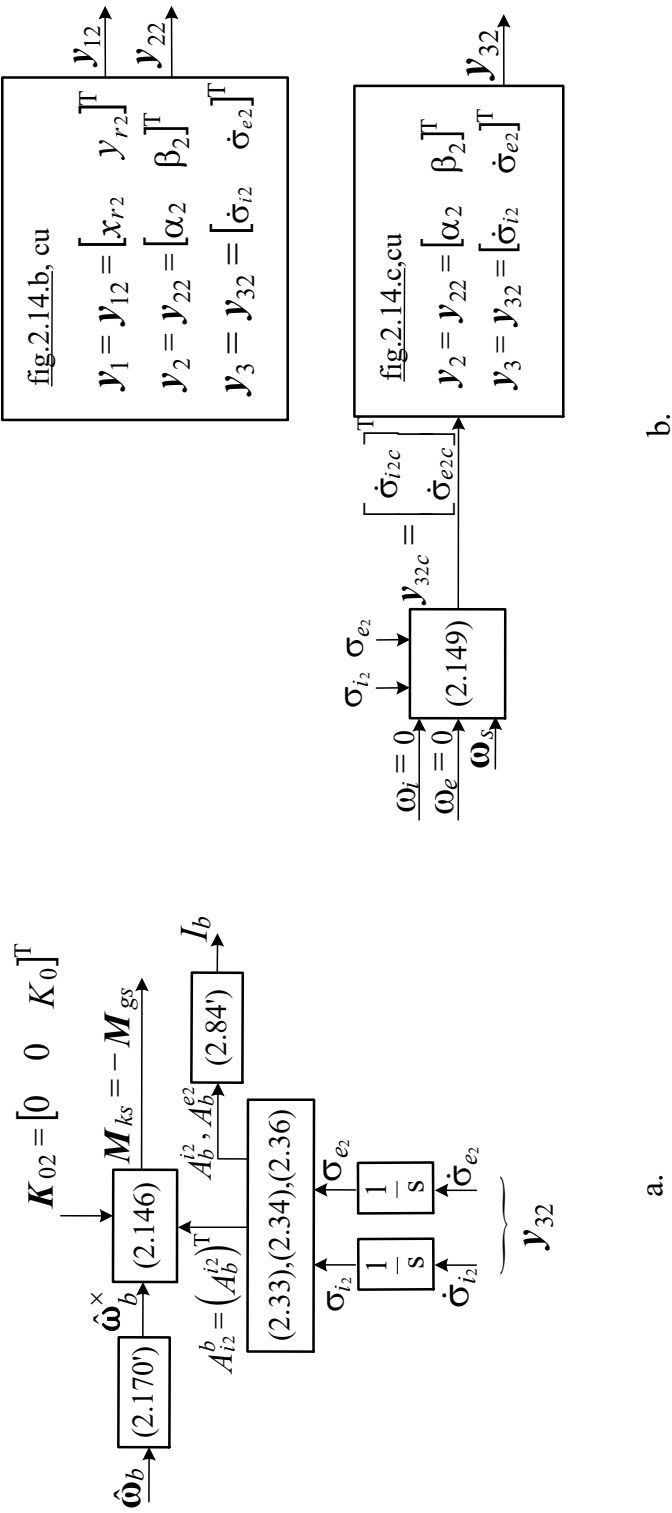$$[\boldsymbol{\omega}_i^T\ \ \boldsymbol{\omega}_e^T]^T = -Q^+ \boldsymbol{M}_{kc}, \tag{2.167}$$

with $\boldsymbol{\omega}_i = [1\ 0\ 0]^T \omega_i$, $\boldsymbol{\omega}_e = [0\ 1\ 0]^T \omega_e$ and Q^+ – the pseudoinverse of the matrix Q;

$$Q^+ = (Q^T Q)^{-1} Q^T. \tag{2.168}$$

Noting with $\boldsymbol{M}'_{kc}$ – totally disruptive moment,

$$\boldsymbol{M}'_{kc} = \boldsymbol{\varepsilon} = \boldsymbol{\omega}_b^\times (I_b \boldsymbol{\omega}_b + A_{i1}^b \boldsymbol{K}_0) + \omega_0 I_b \boldsymbol{\omega}_s^\times (\text{col } 3)_A - \boldsymbol{M}_p, \tag{2.169}$$

The structure of the satellite's automatic attitude control system, with a P.D. type controller. is given in fig. 2.17. In the absence of angular velocities $\boldsymbol{\omega}_i$ and $\boldsymbol{\omega}_e$ (for $\omega_i = \omega_e = 0$), the angular velocity of S is $\boldsymbol{\omega}_b$, mean that obtained for the automatic attitude control system S open on its direct path (for S perturbed and uncontrolled); $\hat{\boldsymbol{\omega}}_b$ is the angular velocity of the system in closed loop (S controlled). The equal $\boldsymbol{\omega}_b = \hat{\boldsymbol{\omega}}_b$ is achieved when ω_i and ω_e become null, relation equivalent to $\boldsymbol{M}_k = \boldsymbol{M}_{ks}$.

CONTROLLER DE ATITUDINE

ACTUATOR - SENZOR - SATELIT

ACTUATOR (DGMSCMG1) fig.2.14

SENZOR (DGMSCMG 2) fig.2.15

MODEL DE REFERINȚĂ
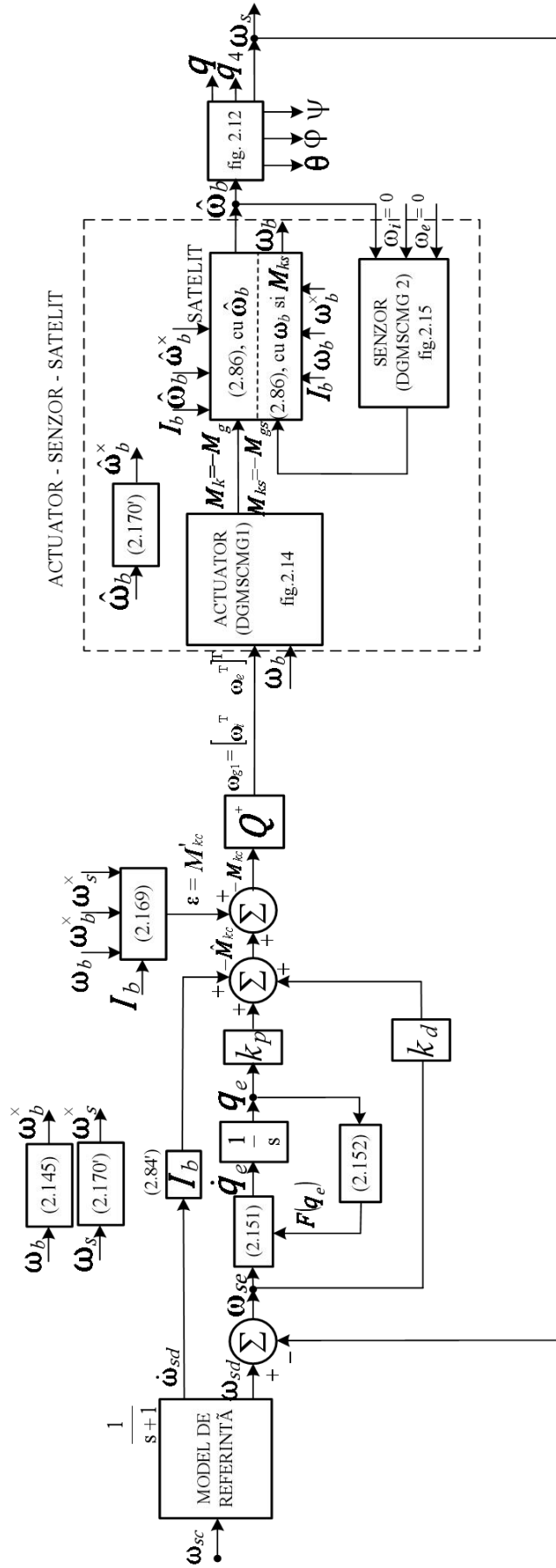
Fig.2.17. Sistem de control automat al atitudinii S, cu controller de tip P.D.,actuator DGMSCMG 1 si senzor DGMSCMG 2

Fig. 2.19 shows the dynamic characteristics of this system using the calculation program from Annex A2.1.
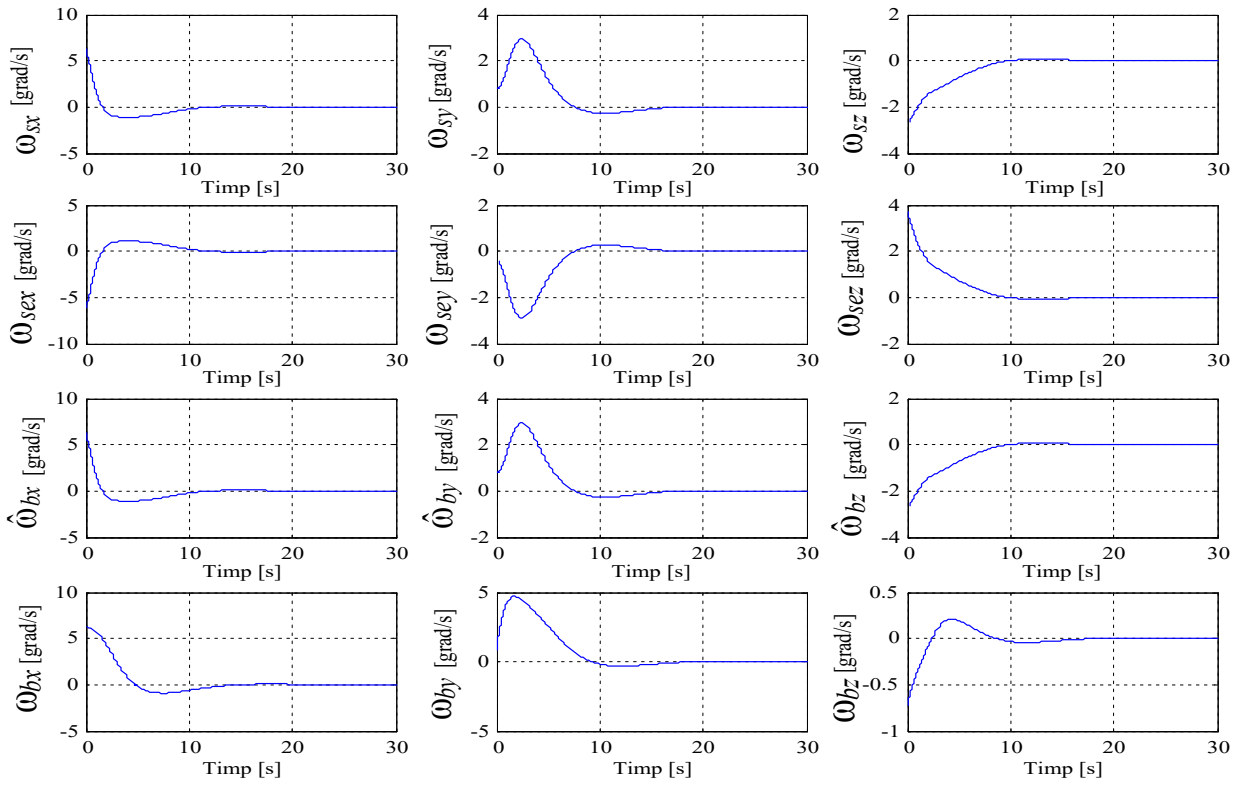
a.
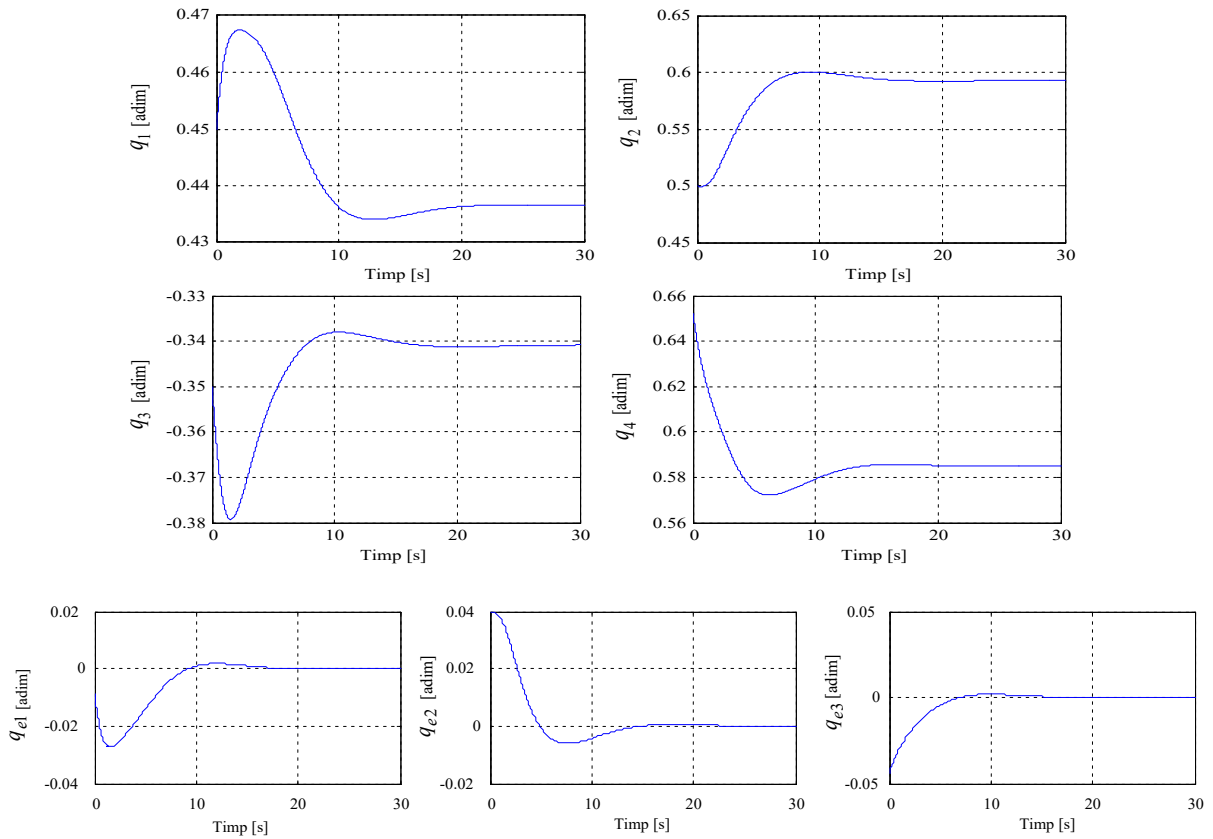
b.
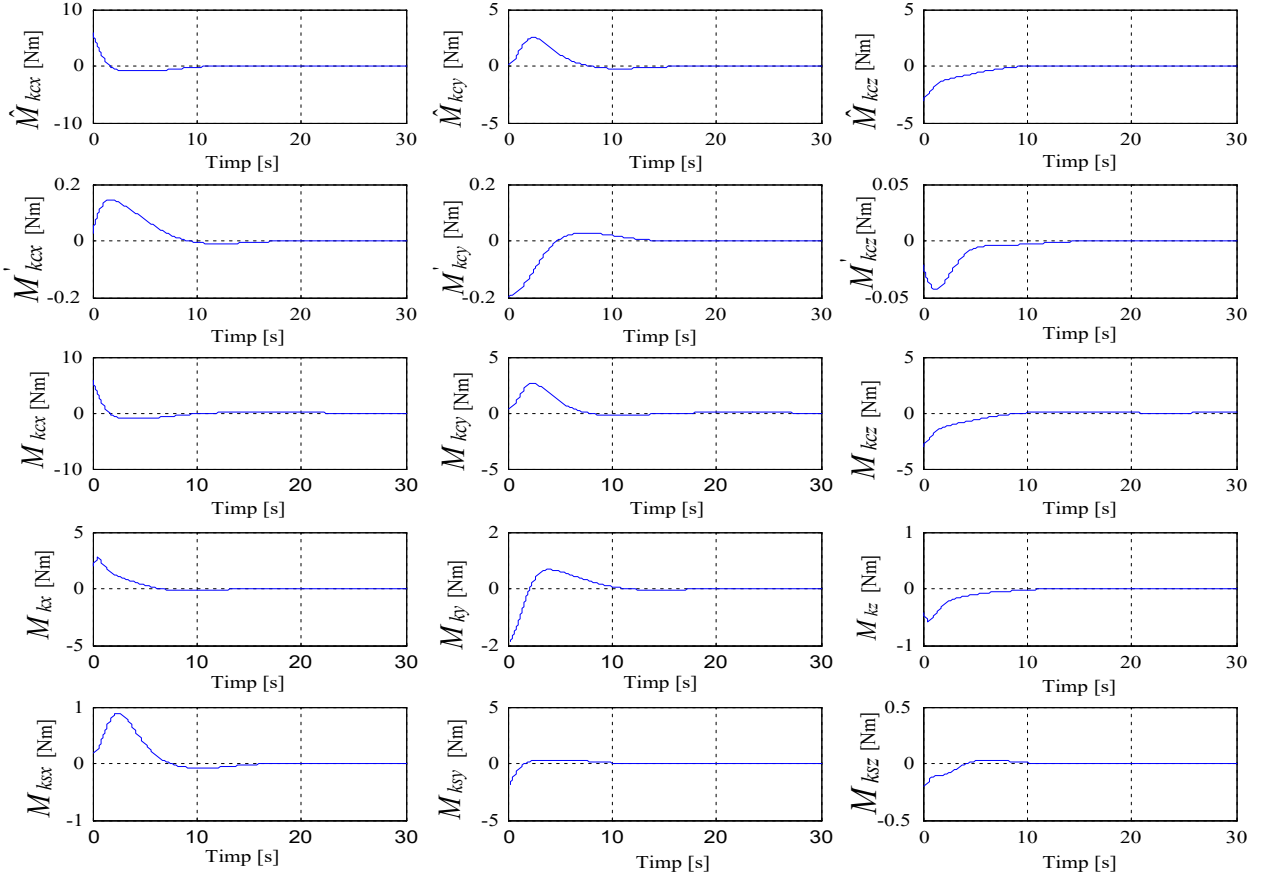
c.
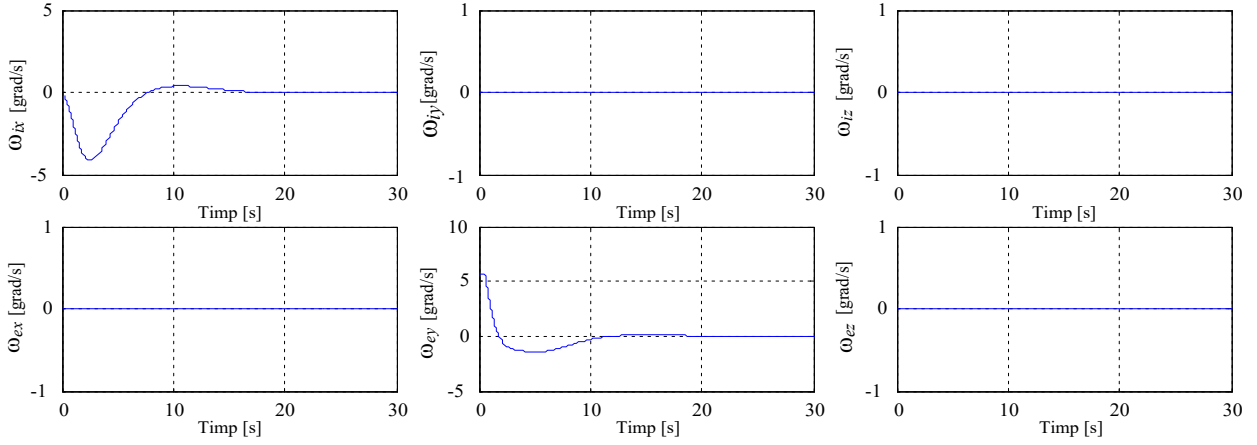
d.
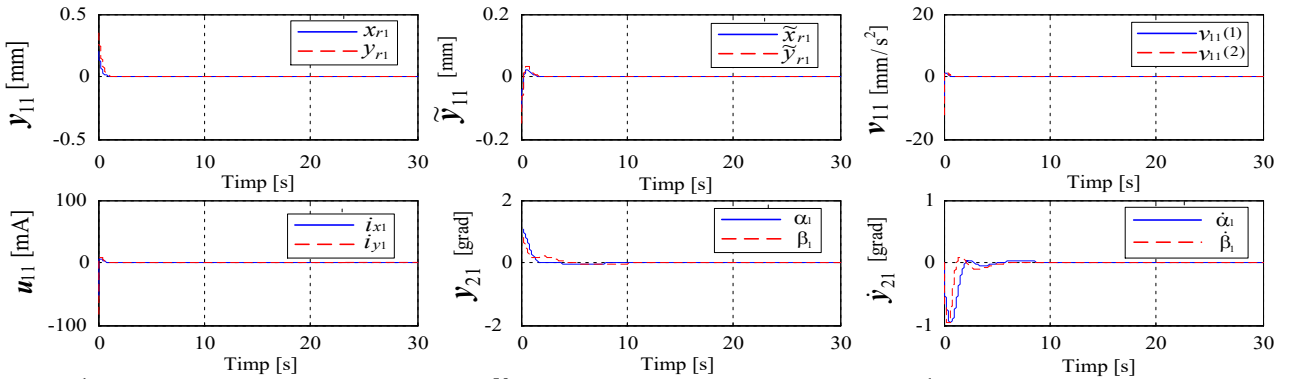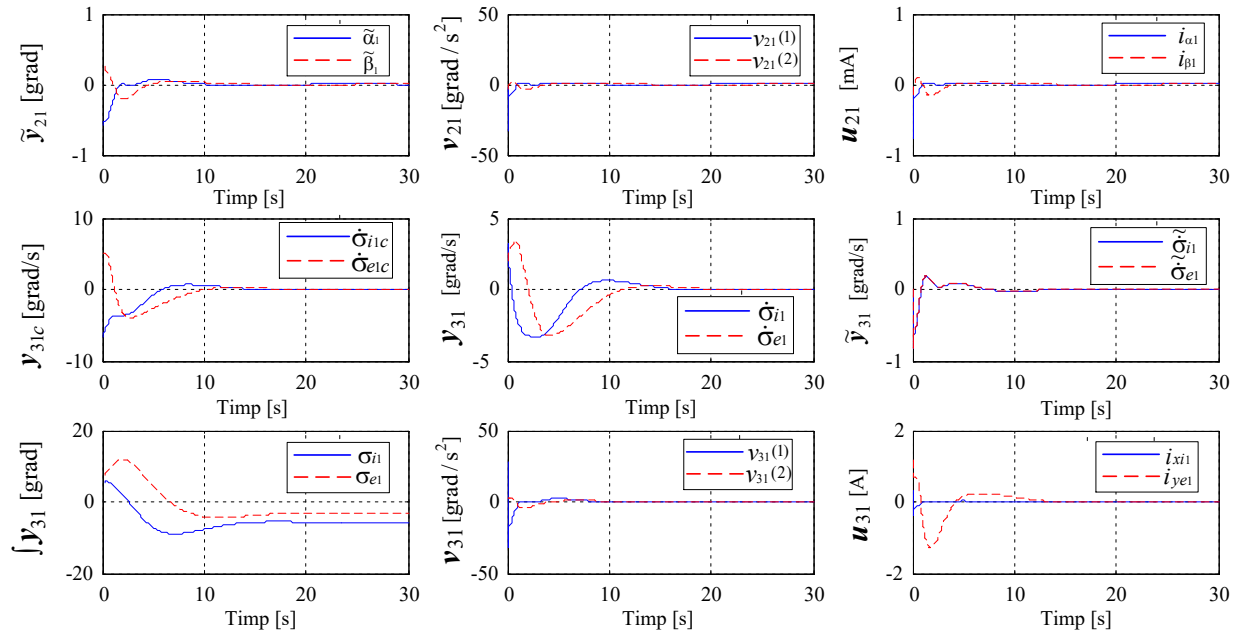
e.
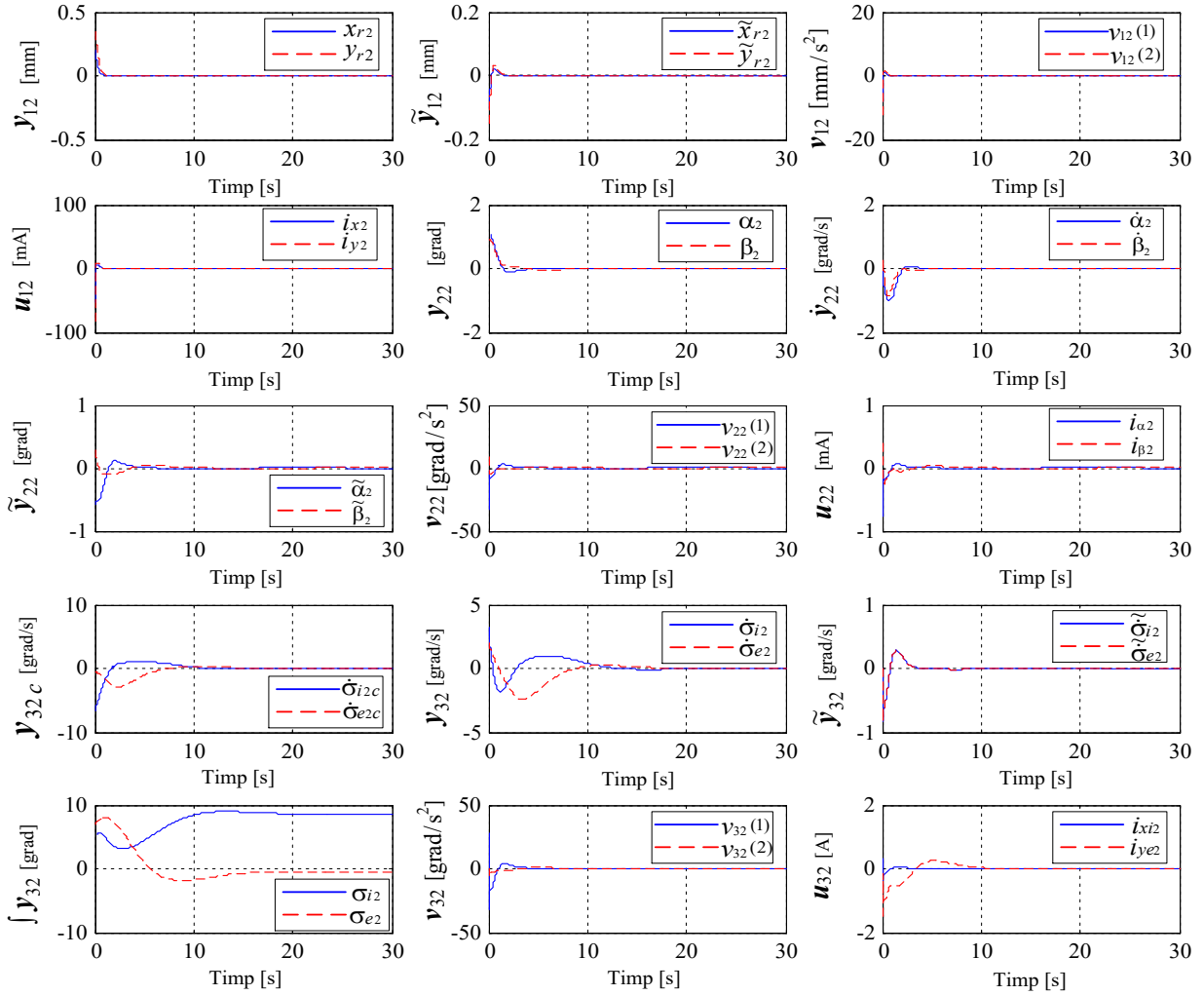
f.

Fig.2.21. The evolution of the SCAS variables, with the dynamic models

of the actuator from fig.2.14 and the sensor from fig.2.15

CHAPTER 3

ATTITUDE CONTROL OF SATELLITES USING ACTUATORS WITH N-DGMSCMGS

3.1. ACTUATOR DYNAMICS WITH N=2 DGMSCMGs IN PARALLEL CONFIGURATION

Fig.3.1. Subsisteme pentru modelarea dinamicii interacțiunii actuator–satelit (a) și a dinamicii actuatorului constituit din N=2 DGMSCMG-uri (b), în configurație paralelă/rectangulară

Fig.3.1 shows the subsystems for modeling the dynamics of the actuator-satellite interaction (a) and the dynamics of the actuator consisting of N=2 DGMSCMGs, in parallel configuration (b), and in fig.3.2 the subsystems for modeling the satellite-sensor interaction (a) and sensor dynamics (b).
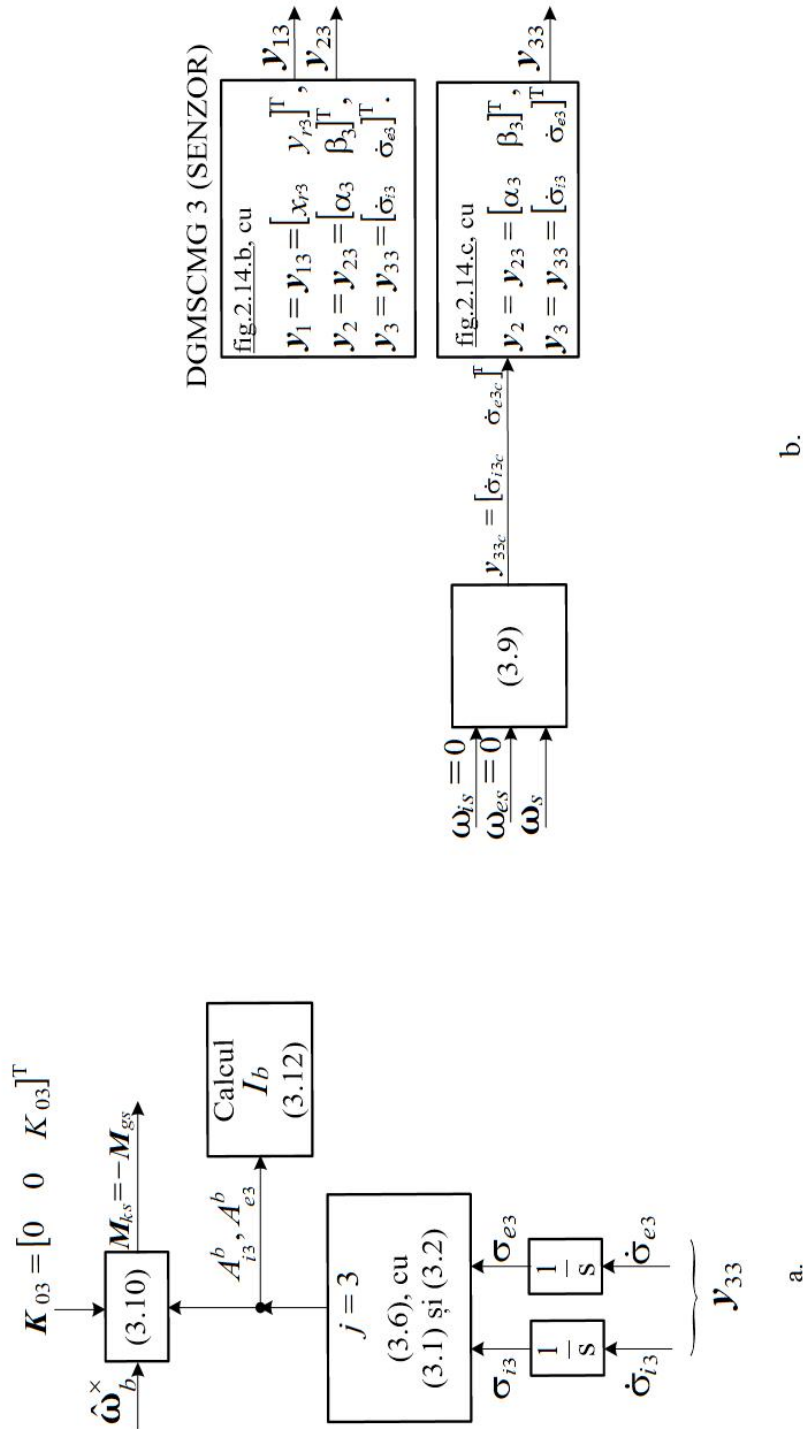
Fig.3.2. Subsisteme pentru modelarea interacţiunii satelit–senzor (a) şi a dinamicii senzorului DGMSCMG 3 (b), în cazul utilizării unui actuator constituit din N=2 DGMSCMG-uri, în configuraţie paralelă sau rectangulară

3.3. ACTUATOR DYNAMICS WITH N=3 DGMSCMGS IN CONFIGURATION ORTHOGONAL

The command moment applied to the base (S) is

$$\boldsymbol{M}_{k1} = -\boldsymbol{M}_{g1} = \boldsymbol{\omega}_b^\times A_{r1}^b \boldsymbol{K}_{01} + A_{i1}^b \boldsymbol{\omega}_{i1}^\times A_{r1}^{i1} \boldsymbol{K}_{01} + A_{e1}^b \boldsymbol{\omega}_{e1}^\times A_{r1}^{e1} \boldsymbol{K}_{01};$$ (3.20)

according to fig.3.6.b,

$$\boldsymbol{K}_{01} = [K_0 \quad 0 \quad 0]^T, \boldsymbol{\omega}_{i1} = [0 \quad 0 \quad \omega_{i1}]^T, \boldsymbol{\omega}_{e1} = [0 \quad \omega_{e1} \quad 0]^T;$$ (3.21)

the calculated angular velocities of the gyroscopic frames relative to the base (S) can be deduced

$$\dot{\sigma}_{i1c} = \omega_{i1} - (\omega_{sx}\sin\sigma_{e1} + \omega_{sz}\cos\sigma_{e1}),$$

$$\dot{\sigma}_{e1c} = \omega_{e1} - \omega_{sy} + (\omega_{sx}\cos\sigma_{e1} - \omega_{sz}\sin\sigma_{e1})\text{tg}\,\sigma_{i1}.$$ (3.25)

A structure with N=3 DGMSCMGs in orthogonal configuration is shown in fig.3.6.a; in fig.3.6.b, 3.6.c and 3.6.d are represented the rotations of the frames and gyroscopic rotors for each of the three CMGs.
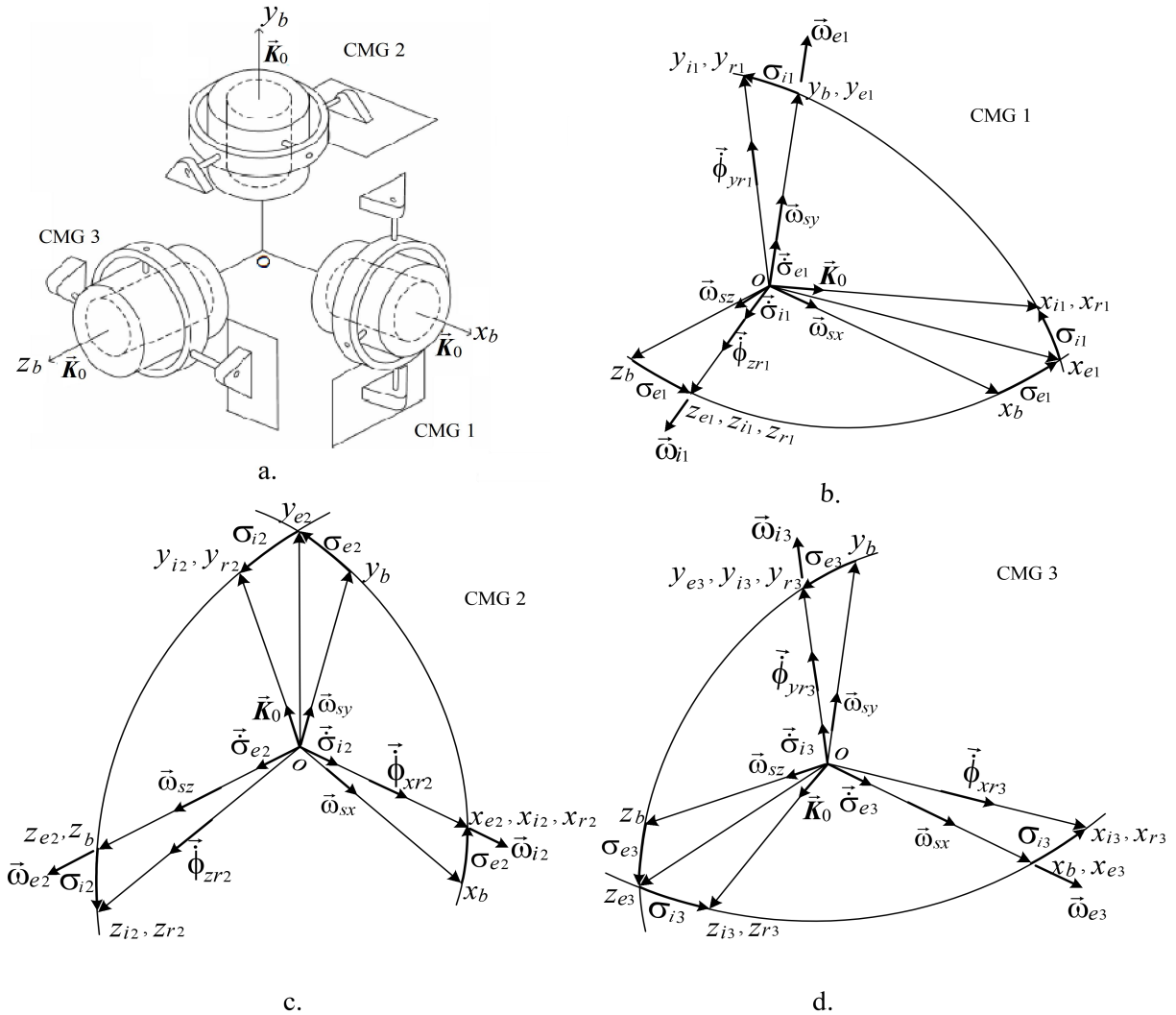
Fig.3.6. Orthogonal configuration with N=3 DGMSCMGs, rotations of their dynamic components and angular sizes

Similarly, for CMG 2, according to fig. 3.6.c,

$$\boldsymbol{M}_{k2} = -\boldsymbol{M}_{g2} = \boldsymbol{\omega}_b^{\times} A_{r2}^b \boldsymbol{K}_{02} + A_{i2}^b \boldsymbol{\omega}_{i2}^{\times} A_{r2}^{i2} \boldsymbol{K}_{02} + A_{e2}^b \boldsymbol{\omega}_{e2}^{\times} A_{r2}^{e2} \boldsymbol{K}_{02}; \tag{3.28}$$

according to fig.3.6.c,

$$\boldsymbol{K}_{02} = [0 \quad K_0 \quad 0]^{\mathrm{T}}, \boldsymbol{\omega}_{i2} = [\omega_{i2} \quad 0 \quad 0]^{\mathrm{T}}, \boldsymbol{\omega}_{e2} = [0 \quad 0 \quad \omega_{e2}]^{\mathrm{T}}; \tag{3.29}$$

the calculated angular velocities of the gyroscopic frames relative to the base (S) can be deduced

$$\dot{\sigma}_{i2c} = \omega_{i2} - (\omega_{sx}\cos\sigma_{e2} + \omega_{sy}\sin\sigma_{e2}),$$

$$\dot{\sigma}_{e2c} = \omega_{e2} - \omega_{sz} + (-\omega_{sx}\sin\sigma_{e2} + \omega_{sy}\cos\sigma_{e2})\mathrm{tg}\,\sigma_{i2}. \tag{3.33}$$

For CMG 3, according to fig.3.6.d,

$$\boldsymbol{M}_{k3} = -\boldsymbol{M}_{g3} = \boldsymbol{\omega}_b^{\times} A_{r3}^b \boldsymbol{K}_{03} + A_{i3}^b \boldsymbol{\omega}_{i3}^{\times} A_{r3}^{i3} \boldsymbol{K}_{03} + A_{e3}^b \boldsymbol{\omega}_{e3}^{\times} A_{r3}^{e3} \boldsymbol{K}_{03}; \tag{3.36}$$

$$\boldsymbol{K}_{03} = [0 \quad 0 \quad K_0]^{\mathrm{T}}, \boldsymbol{\omega}_{i3} = [0 \quad \omega_{i3} \quad 0]^{\mathrm{T}}, \boldsymbol{\omega}_{e3} = [\omega_{e3} \quad 0 \quad 0]^{\mathrm{T}}; \tag{3.37}$$

the calculated angular velocities of the gyroscopic frames relative to the base (S) can be deduced

$$\dot{\sigma}_{i3c} = \omega_{i3} - (\omega_{sy}\cos\sigma_{e3} + \omega_{sz}\sin\sigma_{e3}),$$

$$\dot{\sigma}_{e3c} = \omega_{e3} - \omega_{sx} + (-\omega_{sy}\sin\sigma_{e3} + \omega_{sz}\cos\sigma_{e3})\mathrm{tg}\,\sigma_{i3}. \tag{3.41}$$

Fig.3.7 shows the subsystems for modeling the actuator-satellite interaction (a) and the dynamics of the actuator consisting of N=3 DGMSCMGs, in orthogonal configuration (b).

For the angular velocity sensor $\boldsymbol{\omega}_b$, with layout for example as DGMSCMG 1, modeling scheme is given in fig.3.8; this scheme consists of two subsystems: one for modeling the satellite-sensor interaction (a) and another for modeling the sensor dynamics (b). This sensor models the equation

$$\boldsymbol{M}_{ks} = -\boldsymbol{M}_{gs} = \hat{\boldsymbol{\omega}}_b^{\times} A_{i4}^b \boldsymbol{K}_{04}. \tag{3.42}$$

$\boldsymbol{M}_k$ is the resultant of the moments generated by the N=3 DGMSCMGs arranged in an orthogonal configuration, and $\boldsymbol{M}_g$ is the resultant gyroscopic torque;

$$\boldsymbol{M}_k = -\boldsymbol{M}_g = \boldsymbol{\omega}_b^{\times} \sum_{j=1}^{3} A_{ij}^b \boldsymbol{K}_{0j} - \sum_{j=1}^{3} A_{ij}^b \boldsymbol{K}_{0j}^{\times} \boldsymbol{\omega}_{ij} - \sum_{j=1}^{3} A_{ej}^b \left(A_{ij}^{ej} \boldsymbol{K}_{0j}\right)^{\times} \boldsymbol{\omega}_{ej}, \tag{3.44}$$

Calculation relations of angular velocities $\dot{\sigma}_{i4c}$ and $\dot{\sigma}_{e4c}$ are qualitatively of the forms (3.33), where σ_{e2} becomes σ_{e4}, σ_{i2} become σ_{i4} and $\omega_{i4} = \omega_{e4} = \omega_{is} = \omega_{es} = 0$;

$$\dot{\sigma}_{i4c} = -(\omega_{sx}\cos\sigma_{e4} + \omega_{sy}\sin\sigma_{e4}),$$

$$\dot{\sigma}_{e4c} = -\omega_{sz} + (-\omega_{sx}\sin\sigma_{e4} + \omega_{sy}\cos\sigma_{e4})\mathrm{tg}\,\sigma_{i4}. \tag{3.47}$$

The matrix of total moments of inertia of the satellite equipped with 3 DGMSCMGs is calculated with the formula

$$I_b = J_b + \sum_{j=1}^{4} \left(A_b^{ej}\right)^{\mathrm{T}} J_{ej} A_b^{ej} + \sum_{j=1}^{4} \left(A_b^{ij}\right)^{\mathrm{T}} I_{ij} A_b^{ij}, \tag{3.48}$$
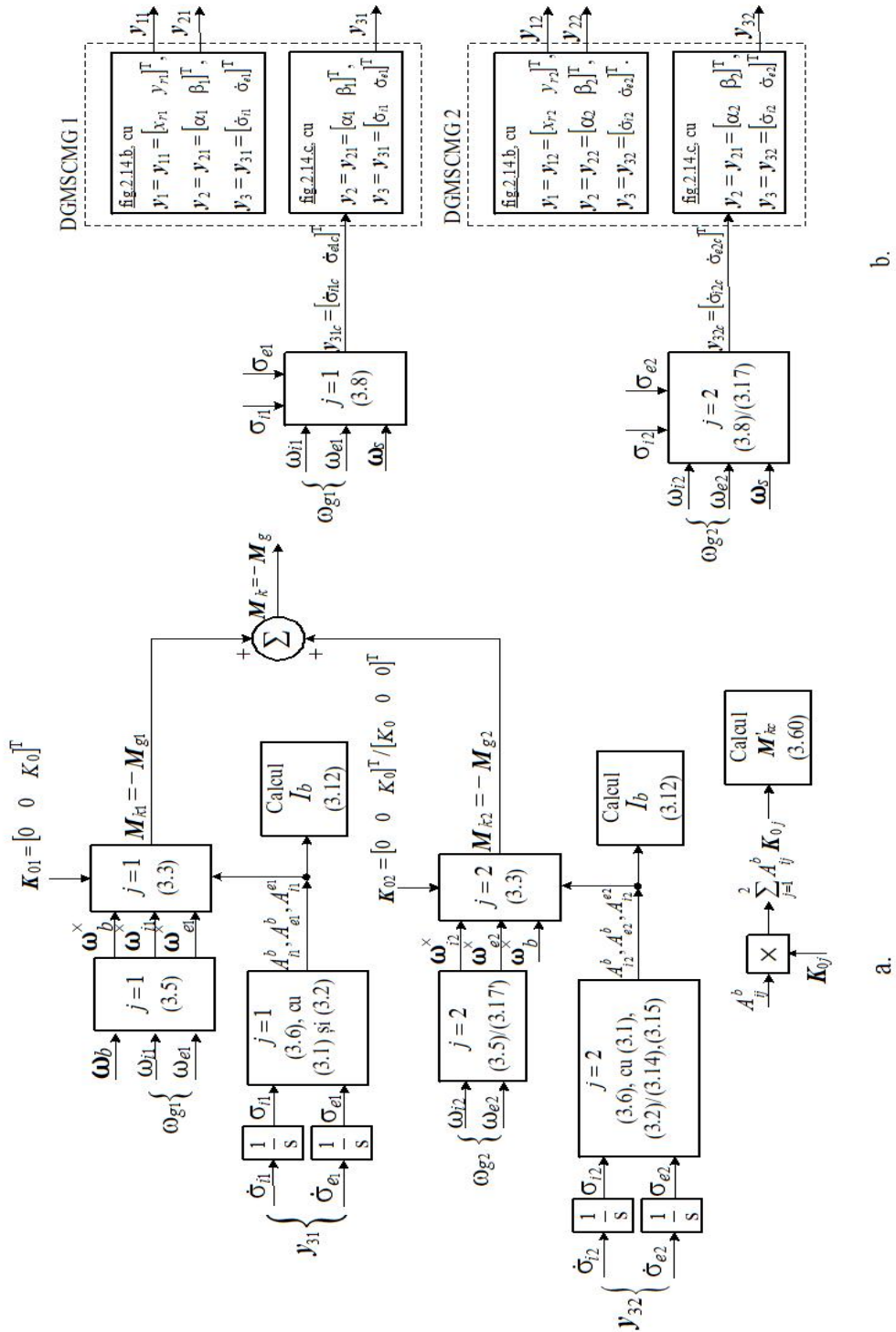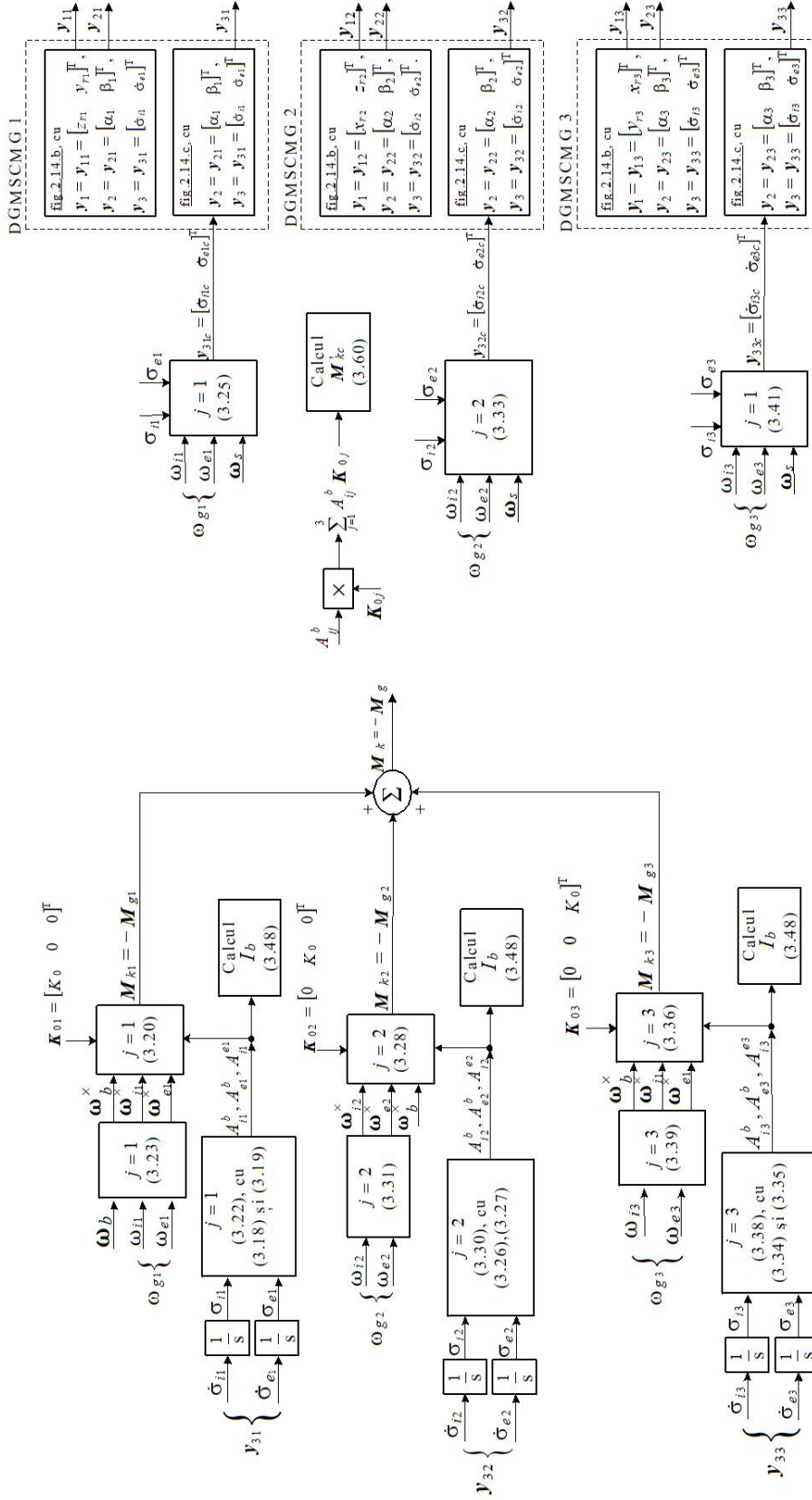
Fig.3.7. Subsisteme pentru modelarea dinamicii interacțiunii actuator–satelit (a) și a dinamicii actuatorului constituit din N=3 DGMSCMG-uri, în configurație rectangulară (b)

36

DGMSCMG 4 (SENZOR)

fig.2.14.b, cu
$y_1 = y_{14} = [x_{r4} \quad z_{r4}]^T$,
$y_2 = y_{24} = [\alpha_4 \quad \beta_4]^T$,
$y_3 = y_{34} = [\dot{\sigma}_{i4} \quad \dot{\sigma}_{e4}]^T$.

y_{14}
y_{24}

fig.2.14.c, cu
$y_2 = y_{24} = [\alpha_4 \quad \beta_4]^T$,
$y_3 = y_{34} = [\dot{\sigma}_{i4} \quad \dot{\sigma}_{e4}]^T$,

y_{34}

$y_{34c} = [\dot{\sigma}_{i4c} \quad \dot{\sigma}_{e4c}]^T$

(3.47)

$\omega_{is} = 0$
$\omega_{es} = 0$
ω_s

b.

$K_{04} = [0 \quad K_{04} \quad 0]^T$

$M_{ks} = -M_{gs}$

Calcul I_b (3.48)

A^b_{i4}, A^b_{e4}

(3.42)

$\hat{\omega}^\times_b$

(3.45), cu (3.46)

σ_{e4}
$\frac{1}{s}$
$\dot{\sigma}_{e4}$

y_{34}

σ_{i4}
$\frac{1}{s}$
$\dot{\sigma}_{i4}$

a.
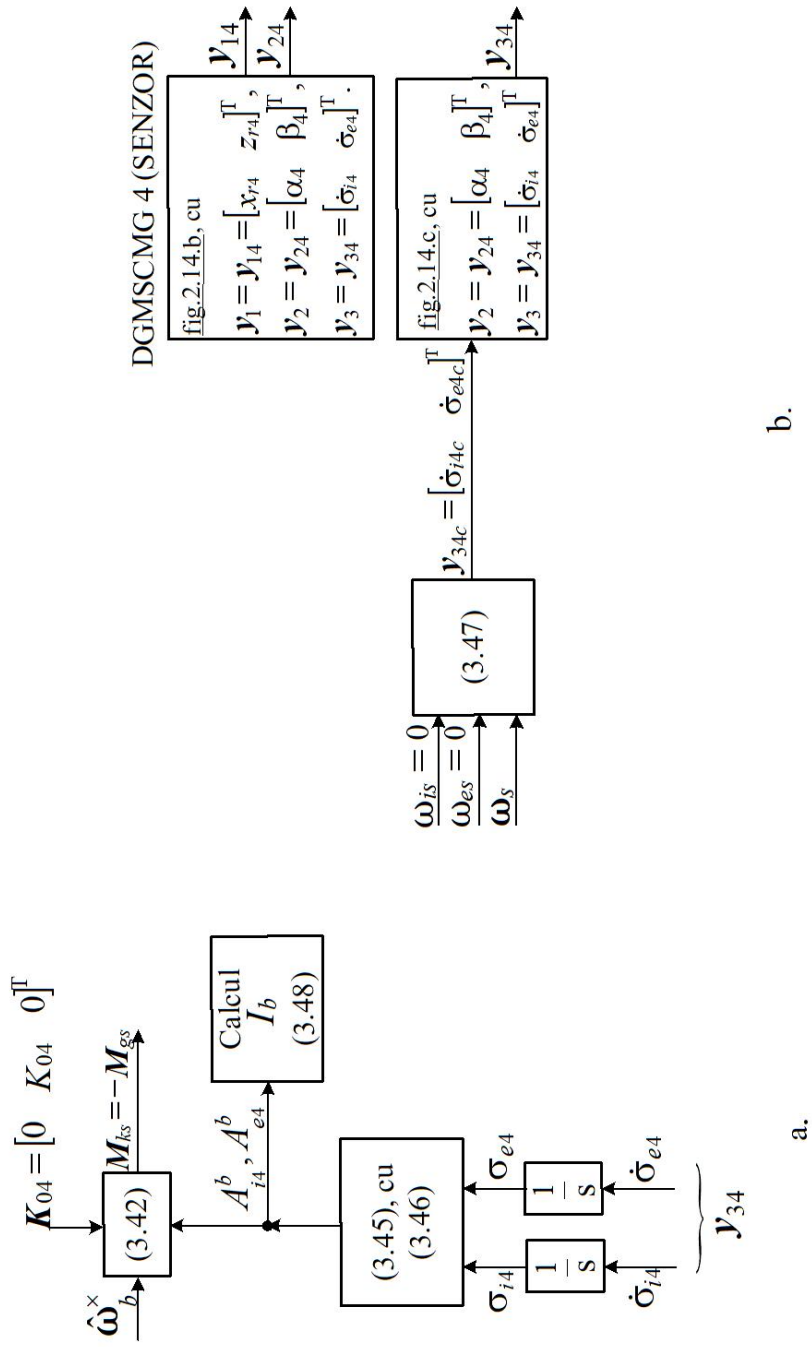
Fig.3.8. Subsisteme pentru modelarea interacțiunii satelit–senzor (a) și a dinamicii senzorului DGMSCMG 4 (b)

3.4. SATELLITE ATTITUDE CONTROL USING A P.D. TYPE CONTROLLER AND ACTUATOR WITH N DGMSCMGs

As in the case of using an actuator with a single CMG (for example of DGMSCMG type), for designing the controller (control laws) a Lyapunov function of the form is chosen [101]

$$V = \frac{1}{2}\boldsymbol{\omega}_{se}^{\mathrm{T}}I_b\boldsymbol{\omega}_{se} + 2k_p\ln\left(1 + \boldsymbol{q}_e^{\mathrm{T}}\boldsymbol{q}_e\right), k_p > 0, \tag{3.50}$$

The condition of stability of the closed circuit system is imposed for the attitude control of the satellite,

$$\dot{V} = \boldsymbol{\omega}_{se}^{\mathrm{T}}I_b\dot{\boldsymbol{\omega}}_{se} + k_p\boldsymbol{\omega}_{se}^{\mathrm{T}}\boldsymbol{q}_e =- k_d\boldsymbol{\omega}_{se}^{\mathrm{T}}\boldsymbol{\omega}_{se} < 0, \tag{3.55}$$

Fig. 3.10 shows the block diagram of the actuator-sensor-satellite subsystem.
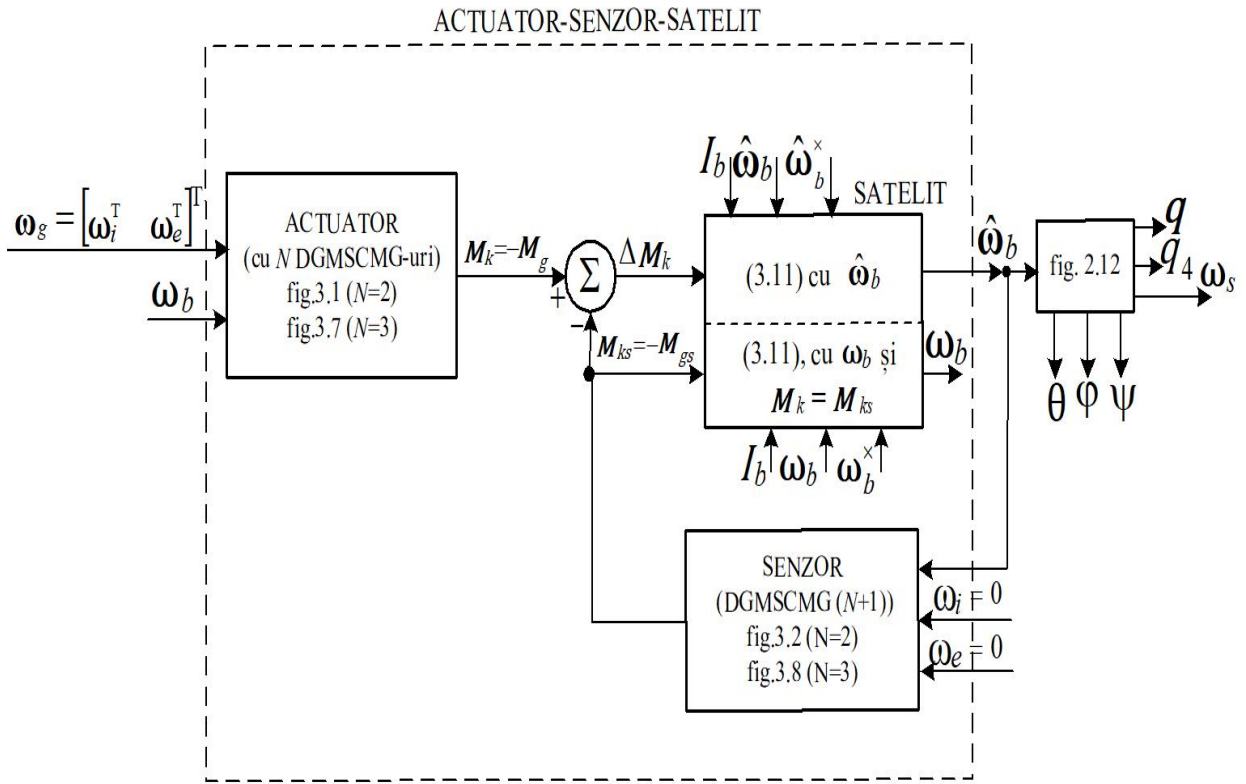
Fig. 3.10. Actuator-sensor-satellite subsystem

The structure of the satellite's automatic attitude control system, with a P.D. type controller. and reference model, with an actuator consisting of DGMSCMGs and a sensor (DGMSCMG ()) is given in fig.3.11.
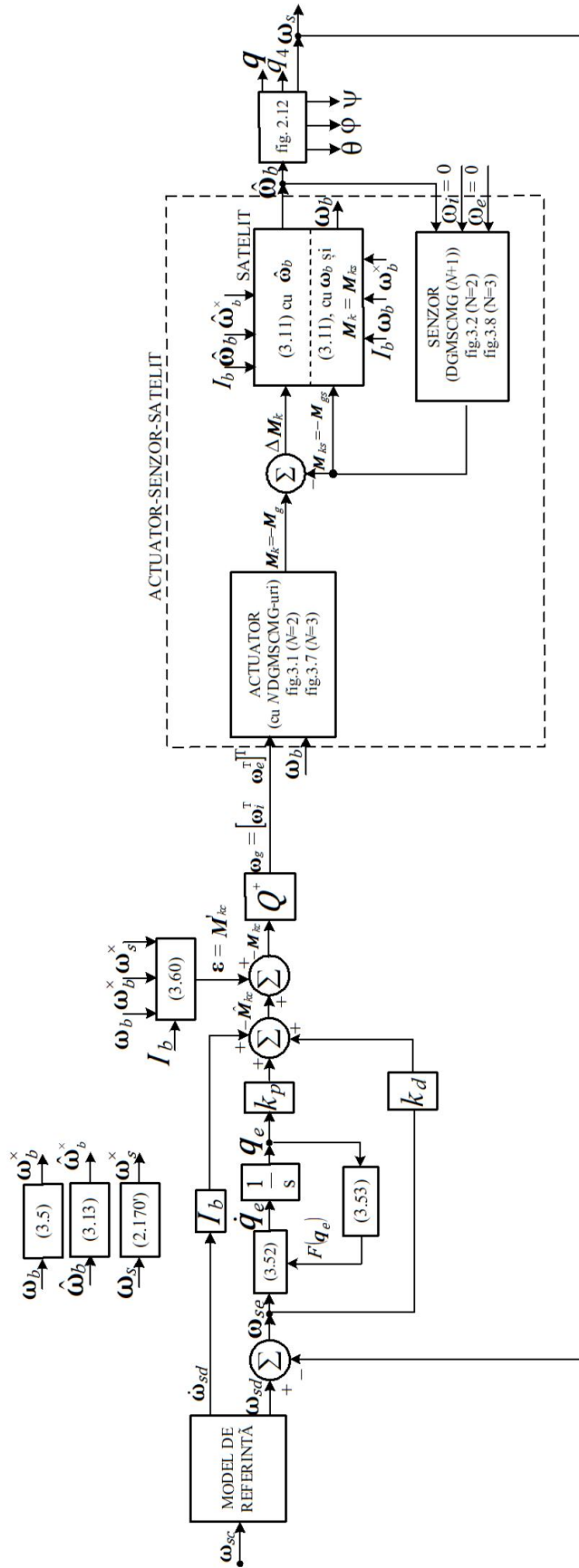
Fig.3.11. Sistem de control automat al atitudinii S, cu controller de tip P.D., actuator cu N DGMSCMG-uri și senzor de tip DGMSCMG ($N+1$)

In fig.3.18, the dynamic characteristics of the system from fig.3.11 are represented, with an actuator consisting of N=3 DGMSCMGs arranged in an orthogonal configuration. The numerical calculation program is given in annex A.3.3.

a.

b.
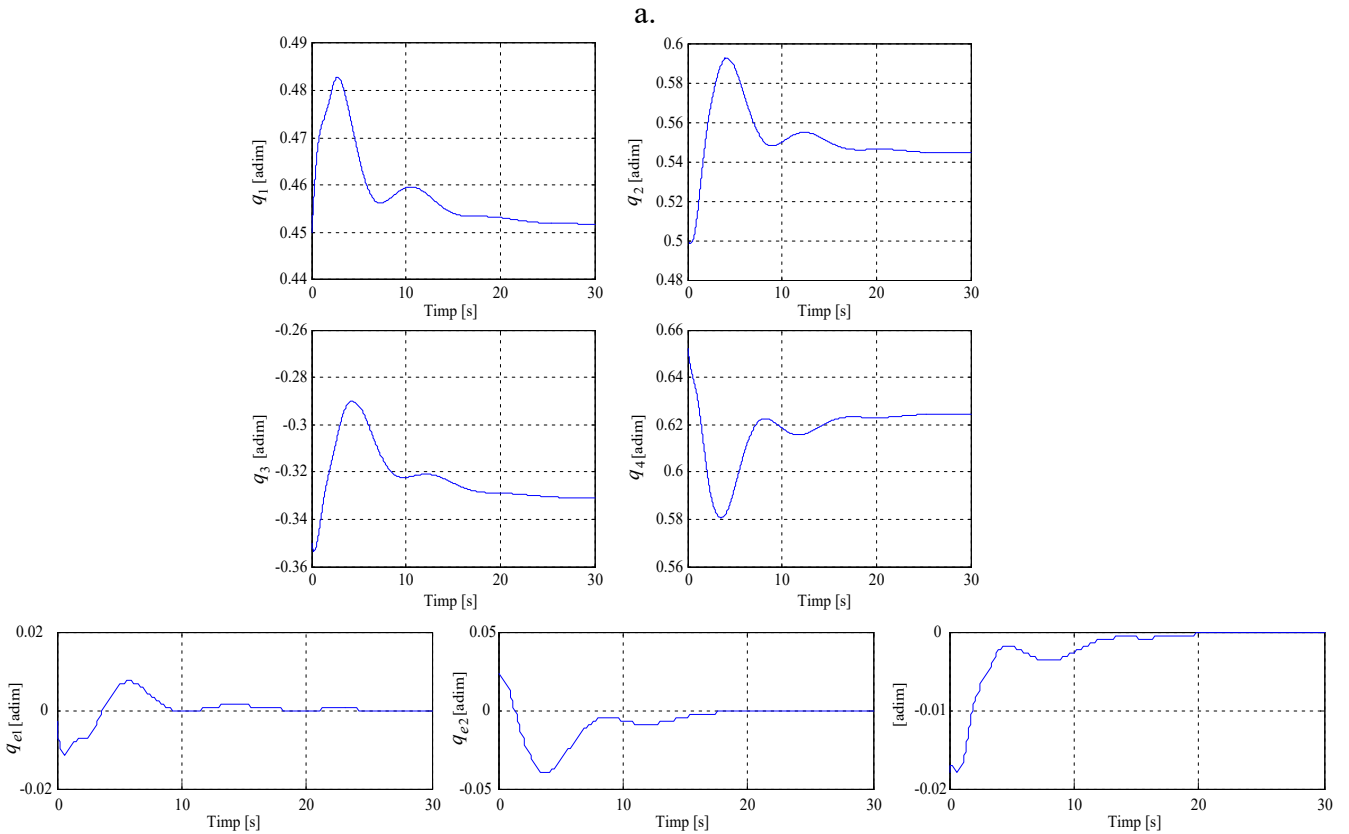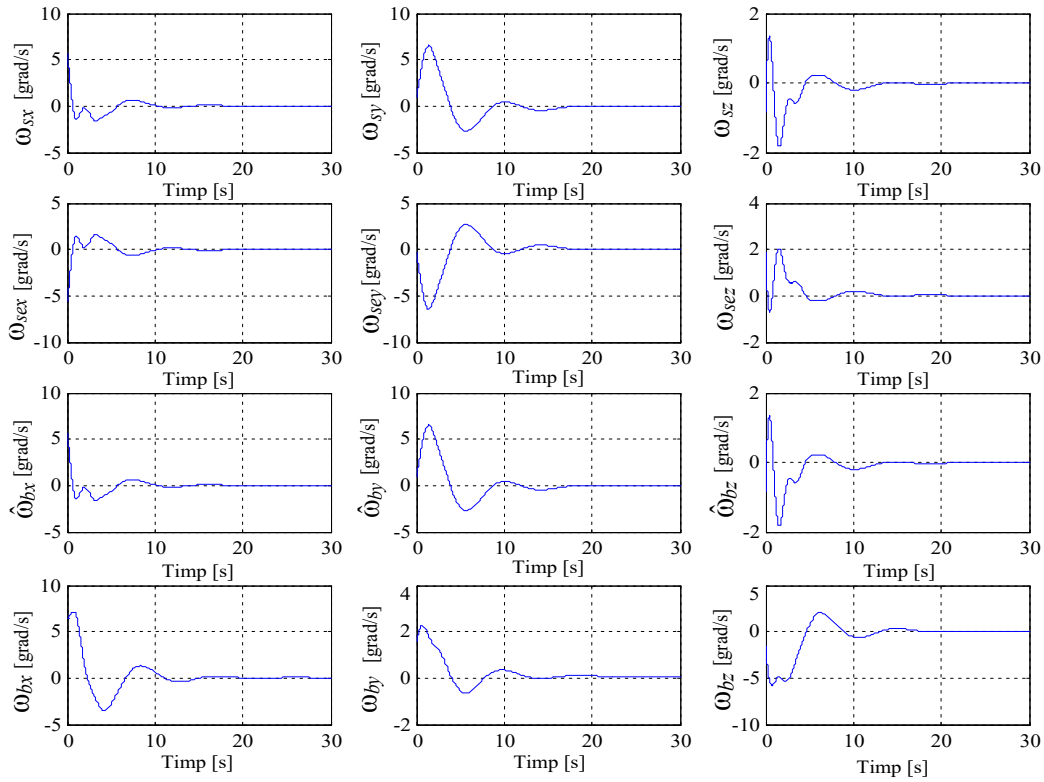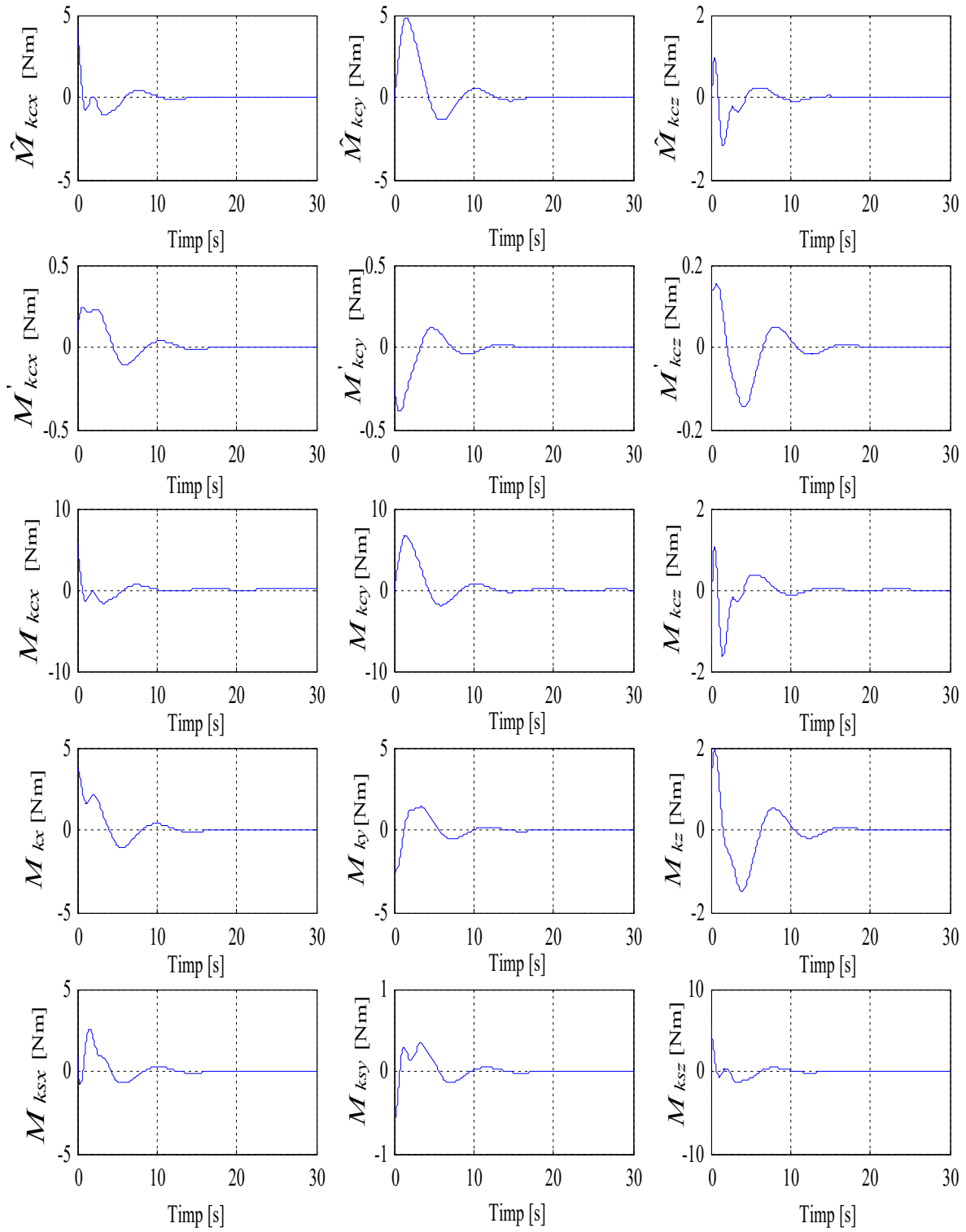
c.
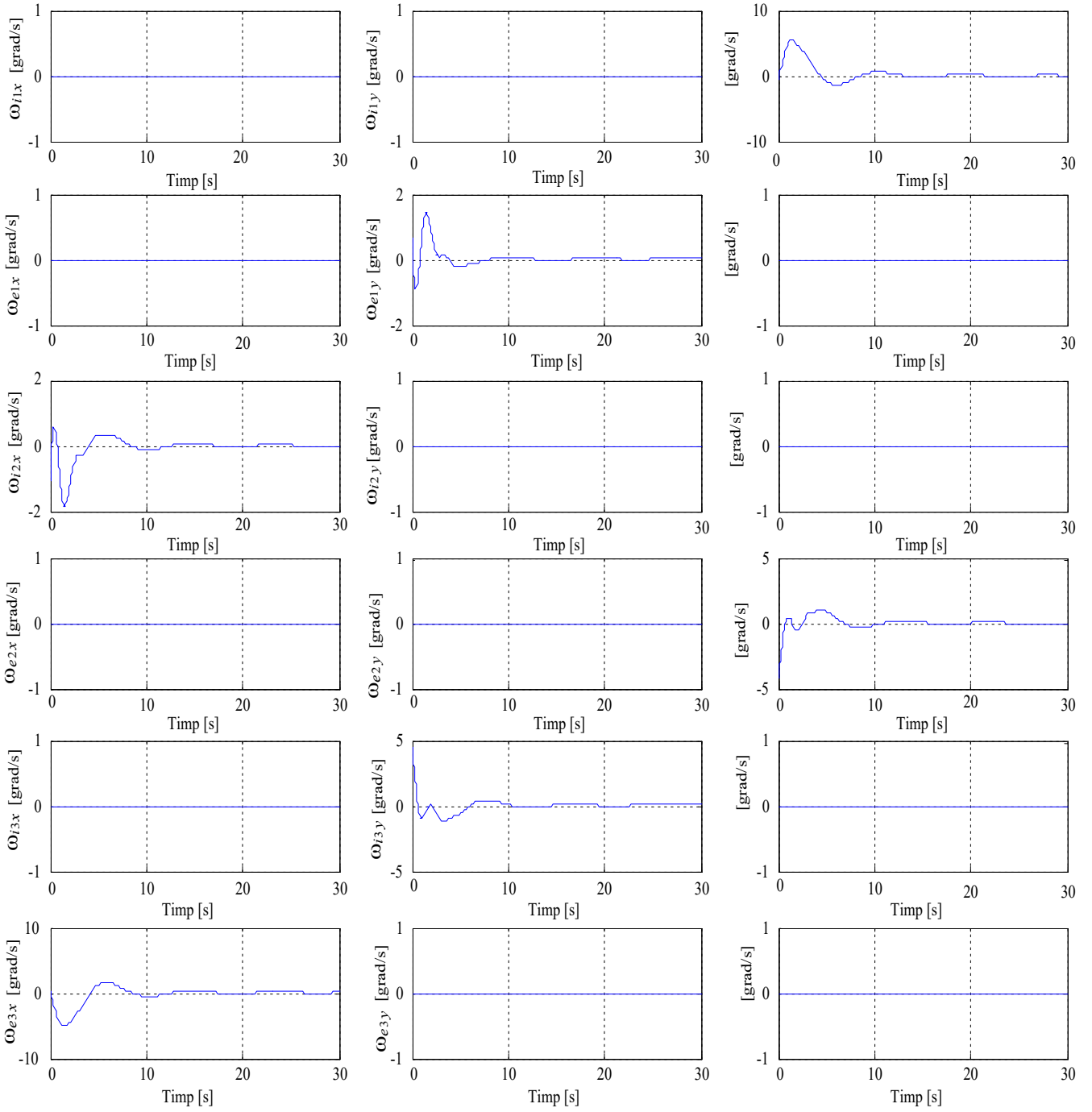
d.
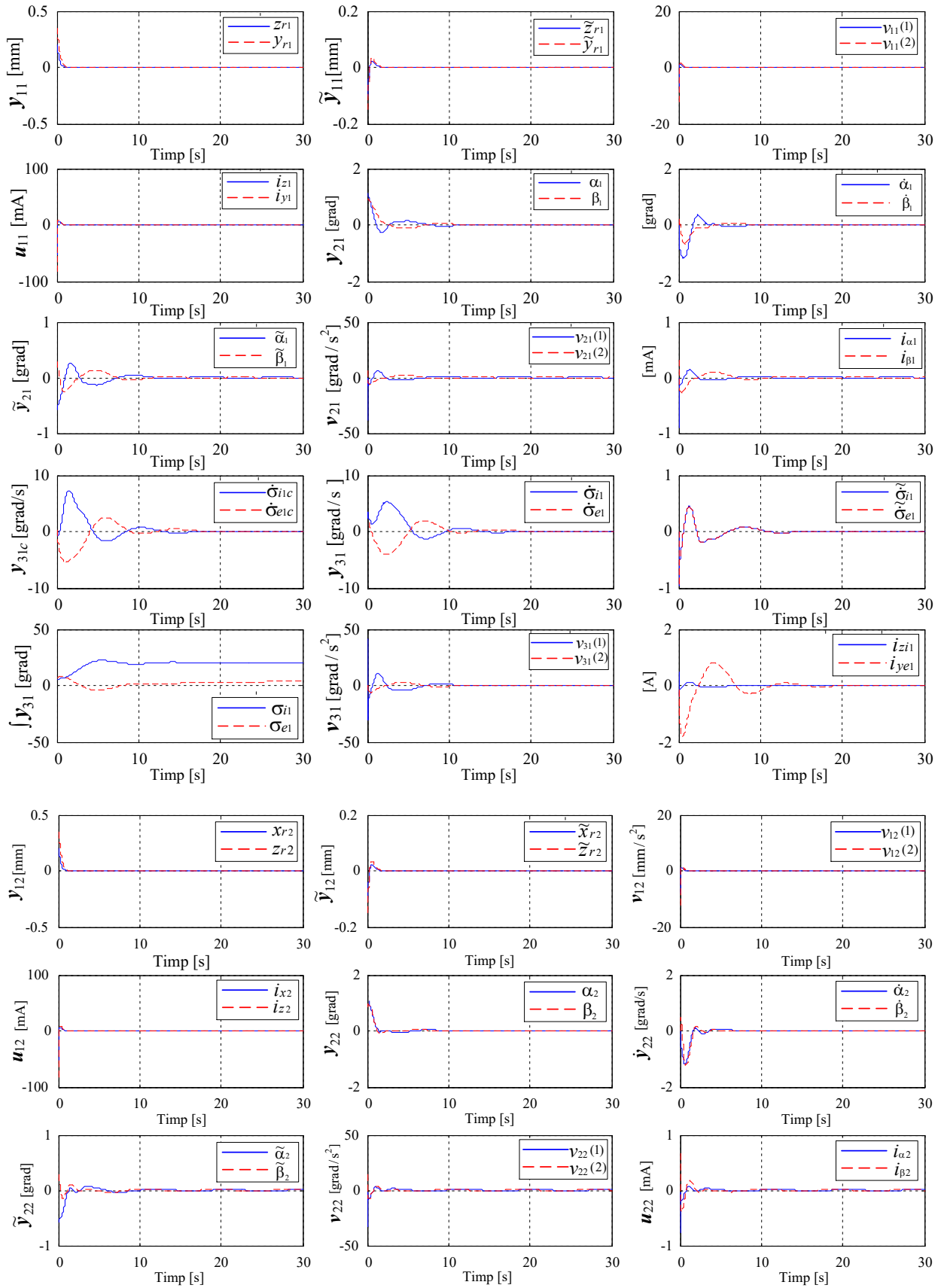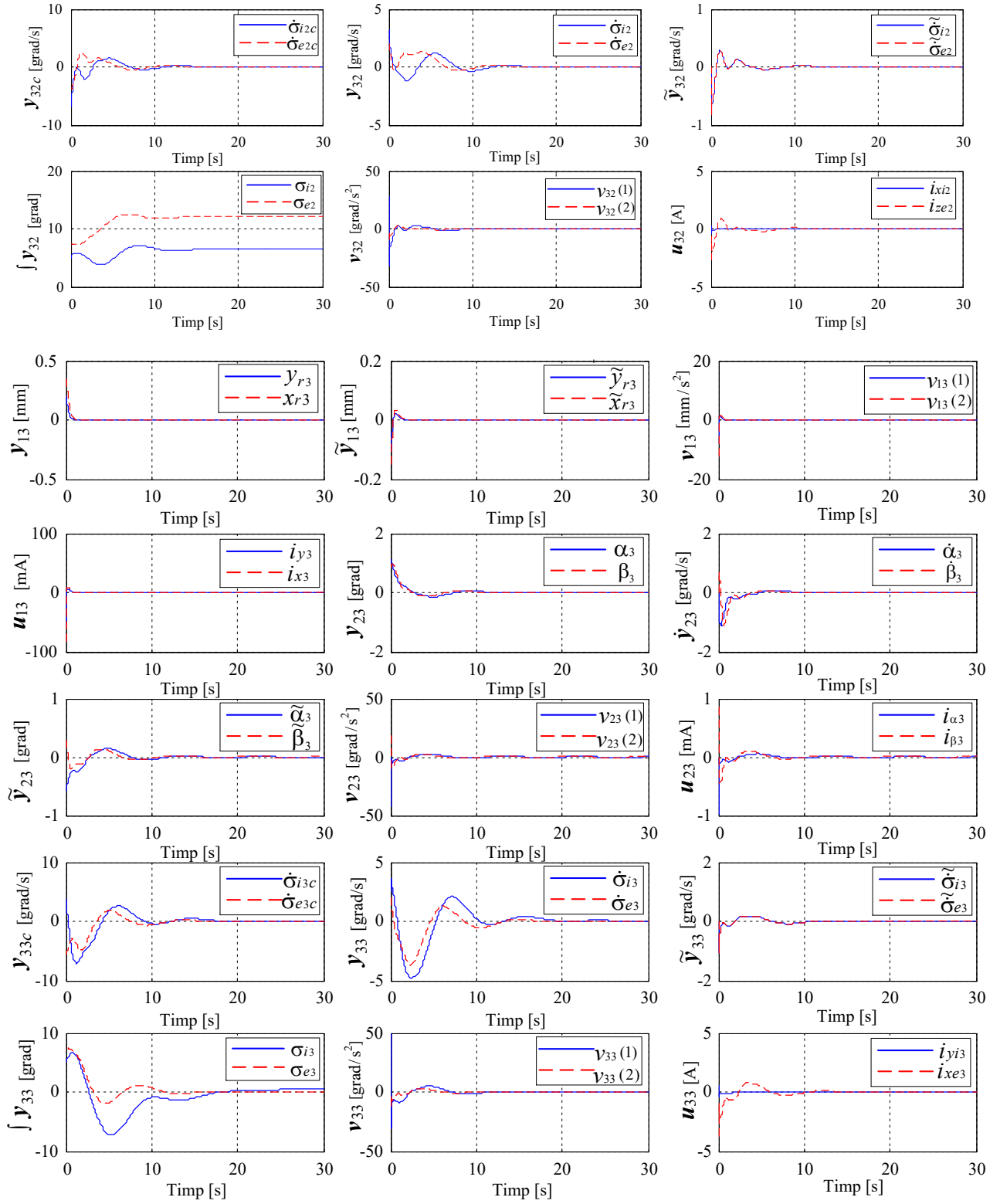
e.
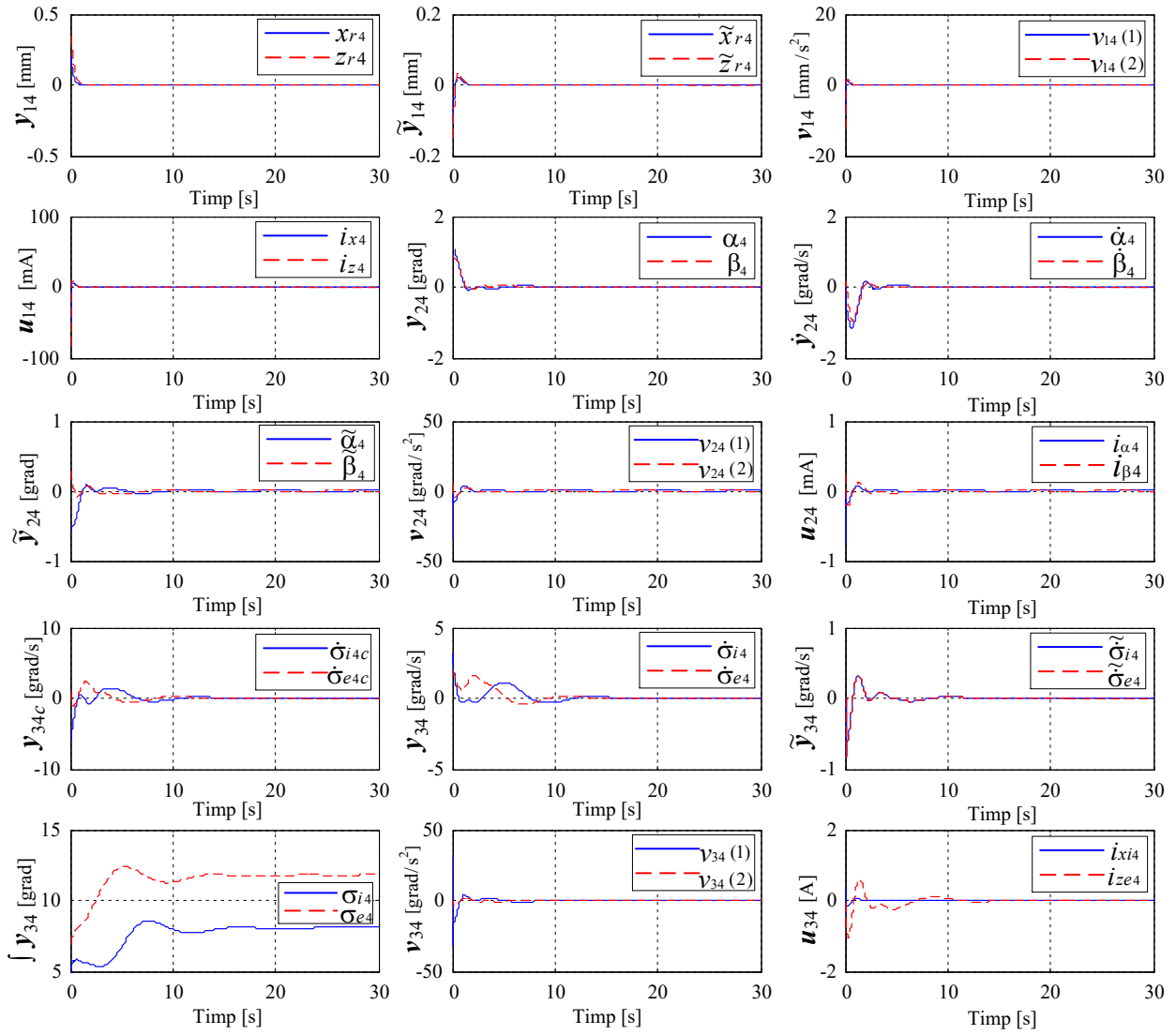
f.

Fig. 3.18. The dynamic characteristics of the system in fig. 3.11, with an actuator consisting of N=3 DGMSCMGs in an orthogonal configuration

CHAPTER 4

ATTITUDE CONTROL OF SATELLITES USING ACTUATORS WITH DGVSCMG-URI

4.1. SATELLITE DYNAMICS USING A DGVSCMG

The rotor of the two-frame CMG, with mechanical bearings related to the gyroscopic rotor, has a variable angular velocity of its own rotation (variable spin), controlled by means of a servo system. That is why it is called DGVSCMG.

The relative angular velocities e with respect to b, i with respect to e and that of the self-rotation of the gyroscopic rotor are respectively $\dot{\sigma}_e, \dot{\sigma}_i$ and Ω, and the absolute angular velocities (relative to the reference trihedral, local orbital $ox_oy_oz_o$) of the outer frame (e), inner frame (i) and rotor are respectively $\mathbf{\Omega}_e, \mathbf{\Omega}_i, \mathbf{\Omega}_r$ (fig.4.1.b).

a.   b.
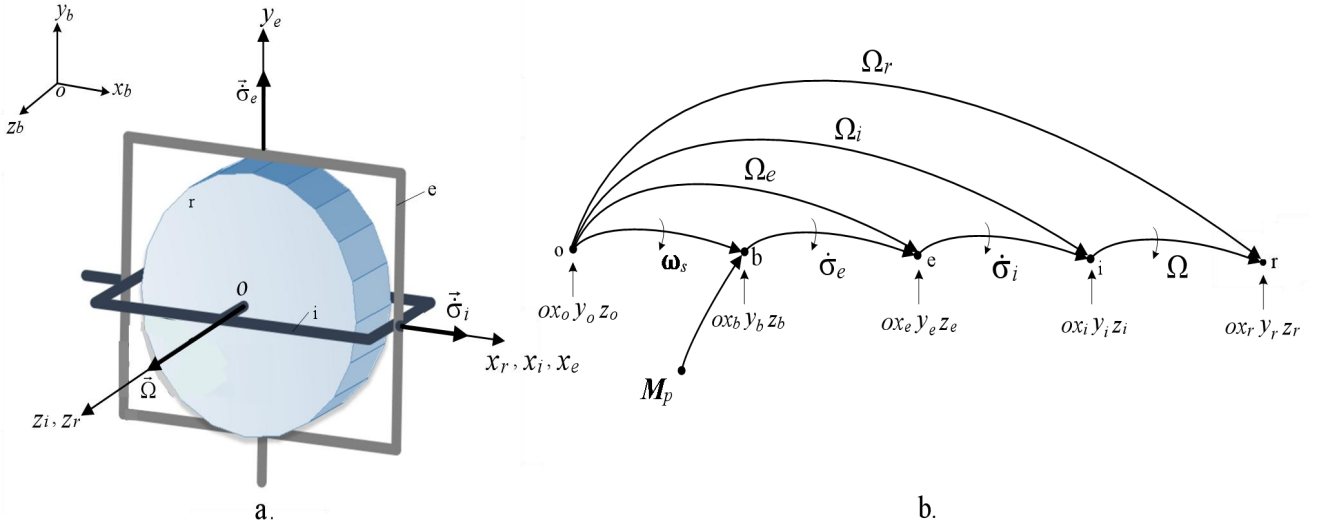
Fig.4.1. DGVSCMG and its dynamic component interdependencies graph

With (4.8) and (4.10) relations (4.3)(4.5) become [81]

$$\mathbf{\Omega}_e = \mathbf{\omega}_s + \dot{\sigma}_e\widehat{\mathbf{g}}_e, \tag{4.11}$$

$$\mathbf{\Omega}_i = \mathbf{\omega}_s + \dot{\sigma}_e\widehat{\mathbf{g}}_e + \dot{\sigma}_i\widehat{\mathbf{g}}_i, \tag{4.12}$$

$$\mathbf{\Omega}_r = \mathbf{\omega}_s + \dot{\sigma}_e\widehat{\mathbf{g}}_e + \dot{\sigma}_i\widehat{\mathbf{g}}_i + \Omega\widehat{\mathbf{g}}_r, \tag{4.13}$$

where the vectors of the vertices of the trihedra related respectively to the outer frame, the inner frame and the gyroscopic rotor have the expressions

$$\widehat{\mathbf{g}}_e = [0 \quad 1 \quad 0]^T, \widehat{\mathbf{g}}_i = [\cos\sigma_e \quad 0 \quad -\sin\sigma_e]^T, \widehat{\mathbf{g}}_r = [\cos\sigma_i\sin\sigma_e \quad -\sin\sigma_i \quad \cos\sigma_i\cos\sigma_e]^T. \tag{4.14}$$

As a result, the equation of dynamics of the satellite-actuator system becomes

$$I_b\dot{\mathbf{\omega}}_s = -\mathbf{\omega}_s^\times I_b\mathbf{\omega}_s - \mathbf{M}_c + \mathbf{M}_p, \tag{4.22}$$

in which

$$I_b = J_b + (A_b^e)^{\mathrm{T}} J_e A_b^e + \left(A_b^i\right)^{\mathrm{T}} I_i A_b^i; \tag{4.23}$$

$$- M_c = M_g = J_r \Omega \widehat{g}_r^\times \omega_s + J_r \Omega (\widehat{g}_r^\times \widehat{g}_i) \dot{\sigma}_i + J_r \Omega (\widehat{g}_r^\times \widehat{g}_e) \dot{\sigma}_e - J_r \widehat{g}_r \dot{\Omega}. \tag{4.24}$$

The last term is generated by the moment of inertia of the gyro rotor.

Equation (4.22) is equivalent to the following

$$I_b \dot{\omega}_s = - M_{kc}, \quad M_{kc} = \widehat{M}_{kc} + M_{kc}'; \quad - M_{kc}' = \varepsilon = - (\omega_s^\times I_b - J_r \Omega \widehat{g}_r^\times) \omega_s + M_p; \tag{4.25}$$

$$- \widehat{M}_{kc} = \widehat{M}_{gc} = J_r \Omega (\widehat{g}_r^\times \widehat{g}_i) \widehat{\dot{\sigma}}_{ic} + J_r \Omega (\widehat{g}_r^\times \widehat{g}_e) \widehat{\dot{\sigma}}_{ec} - J_r \widehat{g}_r \widehat{\dot{\Omega}}_c. \tag{4.26}$$

With the notations

$$Q_i = J_r \Omega (\widehat{g}_r^\times \widehat{g}_i), \quad Q_e = J_r \Omega (\widehat{g}_r^\times \widehat{g}_e), \quad Q_r = - J_r \widehat{g}_r, \tag{4.27}$$

So the SERVO applied command vector is calculated with the formula

$$u_c = [\dot{\sigma}_{ic} \quad \dot{\sigma}_{ec} \quad \dot{\Omega}_c]^{\mathrm{T}} = - Q^+ M_{kc} = \widehat{h}_r^{-1}(M_{kc}, y). \tag{4.31}$$

The satellite equation is of the form (4.22), with M_c of the form (4.24) or of the form

$$- M_c = M_g = J_r \Omega \widehat{g}_r^\times \omega_s + Q u_k, \quad u_k = [\dot{\sigma}_i \quad \dot{\sigma}_e \quad \dot{\Omega}]^{\mathrm{T}}, \tag{4.32}$$

the matrices result

$$Q_i = J_r \begin{bmatrix} \Omega \sin\sigma_i \sin\sigma_e \\ \Omega \cos\sigma_i \\ \Omega \sin\sigma_i \cos\sigma_e \end{bmatrix}, \quad Q_e = J_r \begin{bmatrix} -\Omega \cos\sigma_i \cos\sigma_e \\ 0 \\ \Omega \cos\sigma_i \sin\sigma_e \end{bmatrix}, \quad Q_r = J_r \begin{bmatrix} -\cos\sigma_i \sin\sigma_e \\ \sin\sigma_i \\ -\cos\sigma_i \cos\sigma_e \end{bmatrix}. \tag{4.35}$$

4.2. SATELLITE DYNAMICS USING ACTUATORS FORMED OF N=2 DGVSCMGs
4.2.2. ACTUATOR CONSISTING OF N=2 DGVSCMGs IN CONFIGURATION ORTHOGONAL

The two DGVSCMGs in the actuator are arranged on the satellite with the axes of the outer frames perpendicular;

For this case, the matrices Q_i, Q_e and Q_r are

$$Q_i = J_r \begin{bmatrix} \Omega_1 \sin\sigma_{i1} \sin\sigma_{e1} & \Omega_2 \sin\sigma_{i2} \cos\sigma_{e2} \\ \Omega_1 \cos\sigma_{i1} & \Omega_2 \sin\sigma_{i1} \sin\sigma_{e1} \\ \Omega_1 \sin\sigma_{i1} \cos\sigma_{e1} & \Omega_2 \cos\sigma_{i2} \end{bmatrix},$$

$$Q_e = J_r \begin{bmatrix} -\Omega_1 \cos\sigma_{i1} \cos\sigma_{e1} & \Omega_2 \cos\sigma_{i2} \sin\sigma_{e2} \\ 0 & -\Omega_2 \cos\sigma_{i2} \cos\sigma_{e2} \\ \Omega_1 \sin\sigma_{i1} \sin\sigma_{e1} & 0 \end{bmatrix}, \tag{4.60}$$

$$Q_r = J_r \begin{bmatrix} -\cos\sigma_{i1} \sin\sigma_{e1} & -\cos\sigma_{i2} \cos\sigma_{e2} \\ \sin\sigma_{i1} & -\cos\sigma_{i2} \sin\sigma_{e2} \\ -\cos\sigma_{i1} \cos\sigma_{e1} & \sin\sigma_{i2} \end{bmatrix}.$$

4.3. SATELLITE DYNAMICS USING N=3 DGVSCMG ACTUATORS IN ORTHOGONAL CONFIGURATION

DGVSCMG 1 and DGVSCMG 2 are located on the satellite as in the case studied in $\oint 4.2.2$, and DGVSCMG 3 is located as in fig.4.4.a (the plane of the undisturbed outer frame is parallel to the plane $ox_b z_b$, axis of rotation of this frame ox_{e3} being parallel to the axis ox_b). So, for the first two DGVSCMGs, all the results from $\oint 4.2.2$, which will be supplemented with similar ones for DGVSCMG 3.

The matrices Q_i, Q_e and Q_r have the first two columns identical to those in (4.60), and the third column is respectively given by the products $\Omega_3 \widehat{\boldsymbol{g}}_{r3}^{\times} \widehat{\boldsymbol{g}}_{i3}, \Omega_3 \widehat{\boldsymbol{g}}_{r3}^{\times} \widehat{\boldsymbol{g}}_{e3}$ and $\widehat{\boldsymbol{g}}_{r3}$; the matrices result

$$Q_i = J_r \begin{bmatrix} \Omega_1 \sin\sigma_{i1}\sin\sigma_{e1} & \Omega_2 \sin\sigma_{i2}\cos\sigma_{e2} & \Omega_3 \cos\sigma_{i3} \\ \Omega_1 \cos\sigma_{i1} & \Omega_2 \sin\sigma_{i2}\sin\sigma_{e2} & \Omega_3 \sin\sigma_{i3}\cos\sigma_{e3} \\ \Omega_1 \sin\sigma_{i1}\cos\sigma_{e1} & \Omega_2 \cos\sigma_{i2} & \Omega_3 \sin\sigma_{i3}\sin\sigma_{e3} \end{bmatrix},$$

$$Q_e = J_r \begin{bmatrix} -\Omega_1 \cos\sigma_{i1}\cos\sigma_{e1} & \Omega_2 \cos\sigma_{i2}\sin\sigma_{e2} & 0 \\ 0 & -\Omega_2 \cos\sigma_{i2}\cos\sigma_{e2} & \Omega_3 \cos\sigma_{i3}\sin\sigma_{e3} \\ \Omega_1 \sin\sigma_{i1}\sin\sigma_{e1} & 0 & -\Omega_3 \cos\sigma_{i3}\cos\sigma_{e3} \end{bmatrix}, \qquad (4.78)$$

$$Q_r = J_r \begin{bmatrix} -\cos\sigma_{i1}\sin\sigma_{e1} & -\cos\sigma_{i2}\cos\sigma_{e2} & \sin\sigma_{i3} \\ \sin\sigma_{i1} & -\cos\sigma_{i2}\sin\sigma_{e2} & -\cos\sigma_{i3}\cos\sigma_{e3} \\ -\cos\sigma_{i1}\cos\sigma_{e1} & \sin\sigma_{i2} & -\cos\sigma_{i3}\sin\sigma_{e3} \end{bmatrix}.$$

4.4. AUTOMATIC ATTITUDE CONTROL USING DGVSCMGs, WITH REFERENCE MODEL AND P.D.-TYPE CONTROLLER

For the design of the control law (controller) type P.D. the Lyapunov function is chosen[92]

$$V = \frac{1}{2} \boldsymbol{\omega}_{se}^{\mathrm{T}} I_b \boldsymbol{\omega}_{se} + 2k_p \ln (1 + \boldsymbol{q}_e^{\mathrm{T}} \boldsymbol{q}_e), k_p > 0; \qquad (4.79)$$

Automatic attitude control S without stored energy control

The calculation relation of the matrix pseudoinverse Q is

$$Q^+ = (Q^{\mathrm{T}} Q)^{-1} Q^{\mathrm{T}}. \qquad (4.87)$$

In order to avoid the appearance of singularities, other relations are used to calculate Q^+. One of these is [96]

$$Q^+ = Q^{\mathrm{T}} (Q Q^{\mathrm{T}} + \lambda \mathrm{E})^{-1}; \qquad (4.88)$$

In [79] the local gradient method was used, based on "zero movement"; the control law is of the form

$$\boldsymbol{u}_c = -Q^+ \boldsymbol{M}_{kc} + \boldsymbol{W}\boldsymbol{Z}, \qquad (4.92)$$
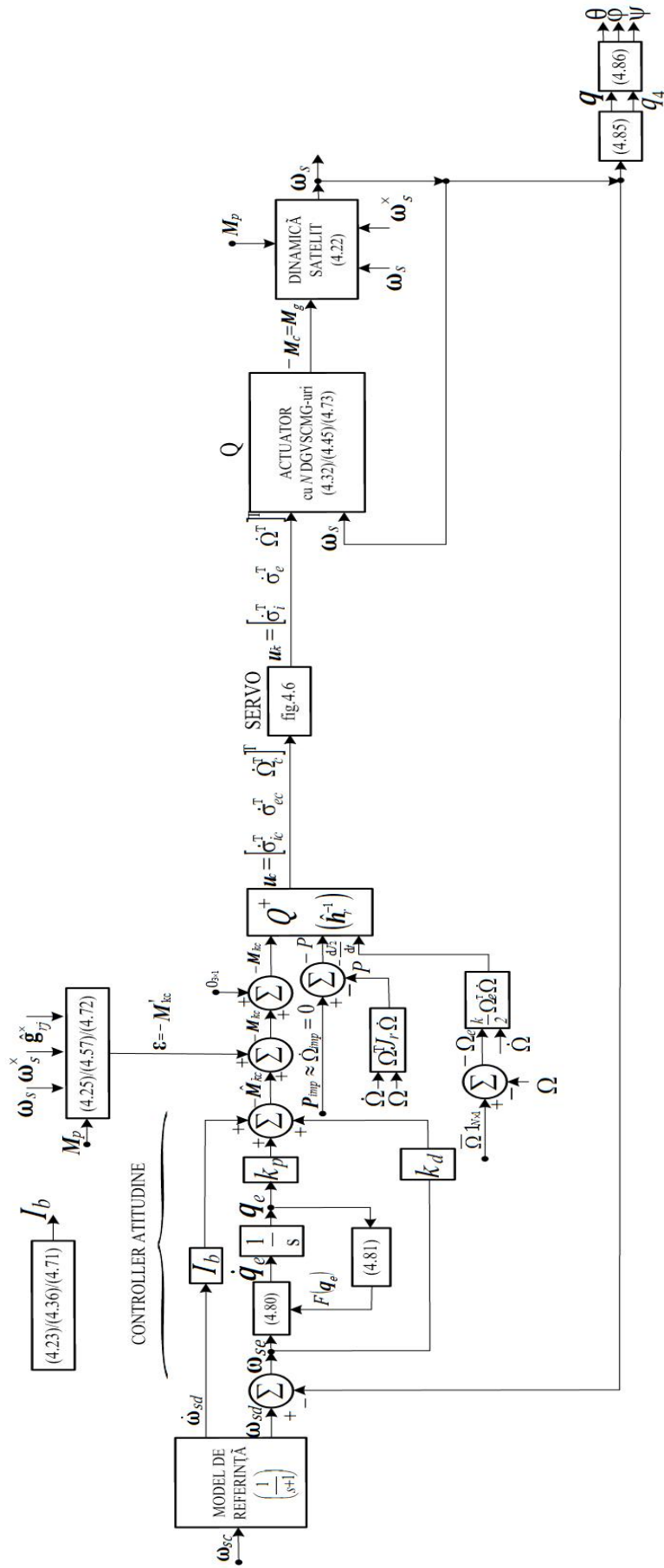
Fig.4.5. Sistem de control automat al atitudinii S cu N DGVSCMG-uri
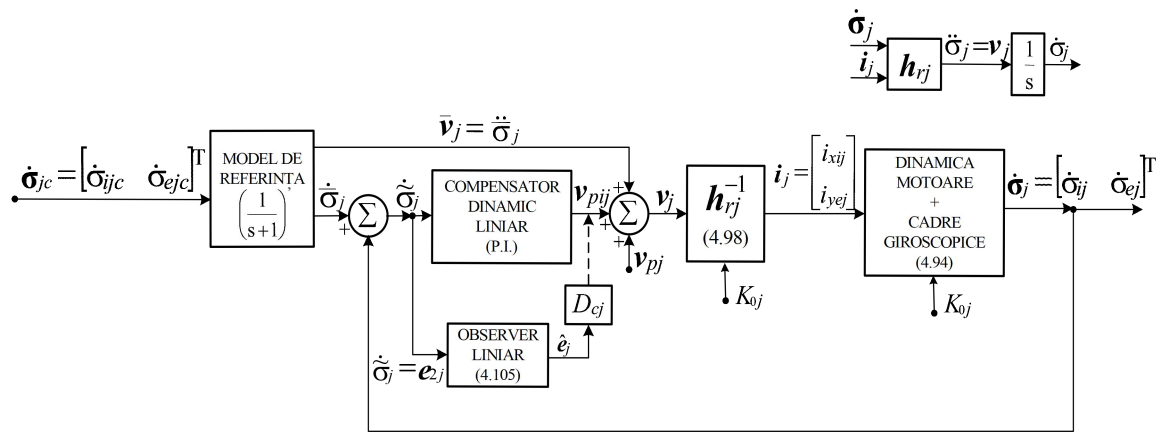
a.
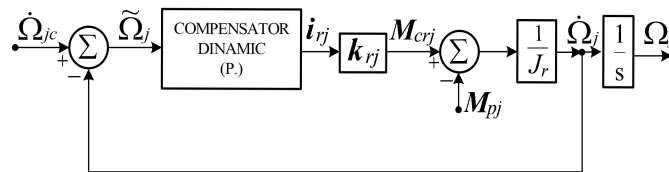
b.

Fig.4.6. Servo systems for controlling angular velocities of gyroscopic frames (a) and
of the angular accelerations of the gyroscopic rotors (b)

In fig. 4.11, the time characteristics of the actuator system consisting of N=3 DGVSCMGs in orthogonal arrangement are plotted.
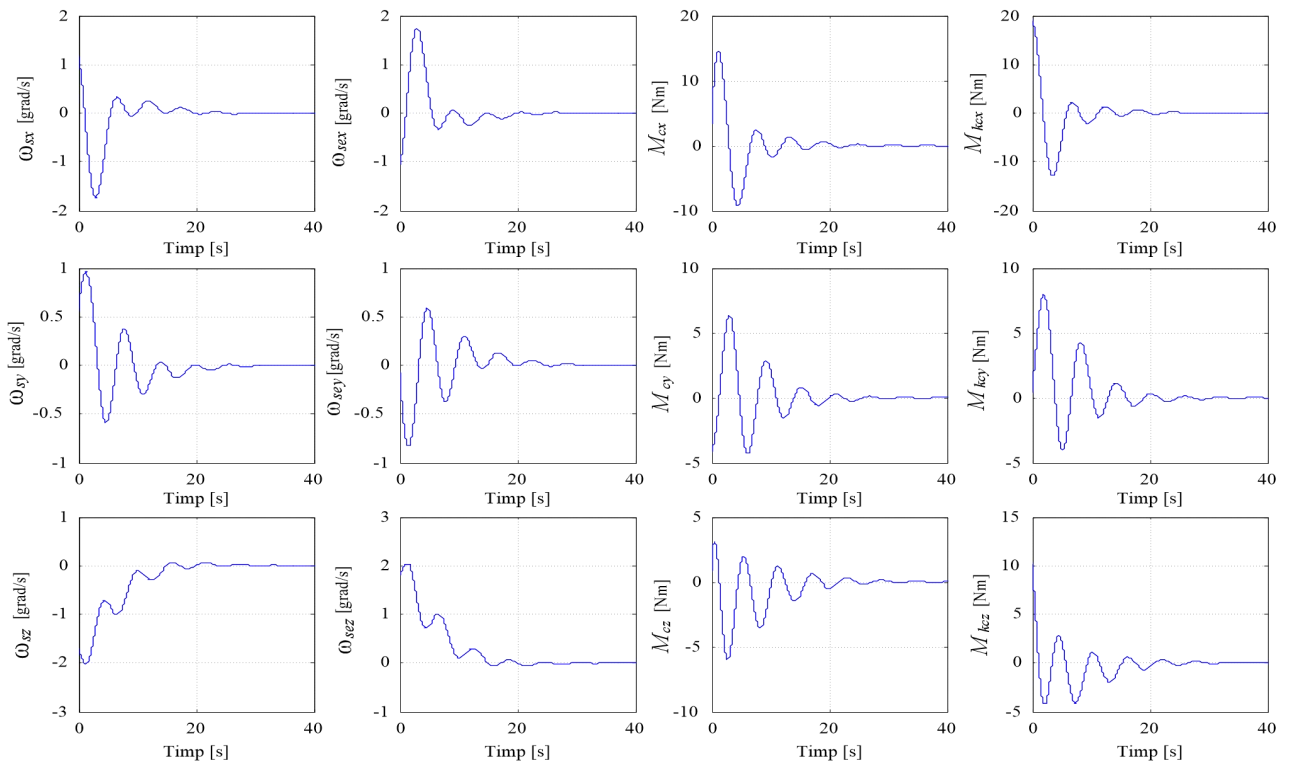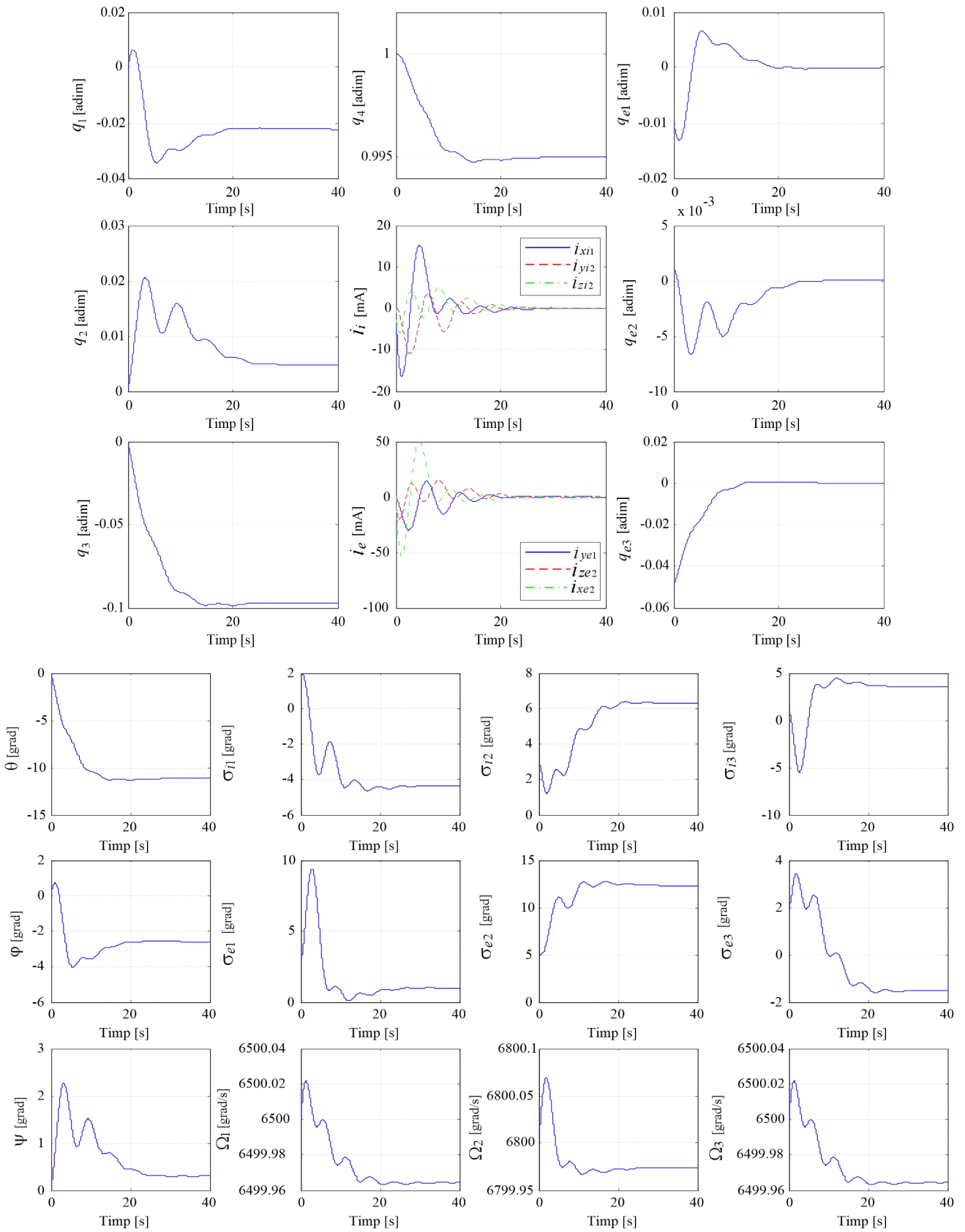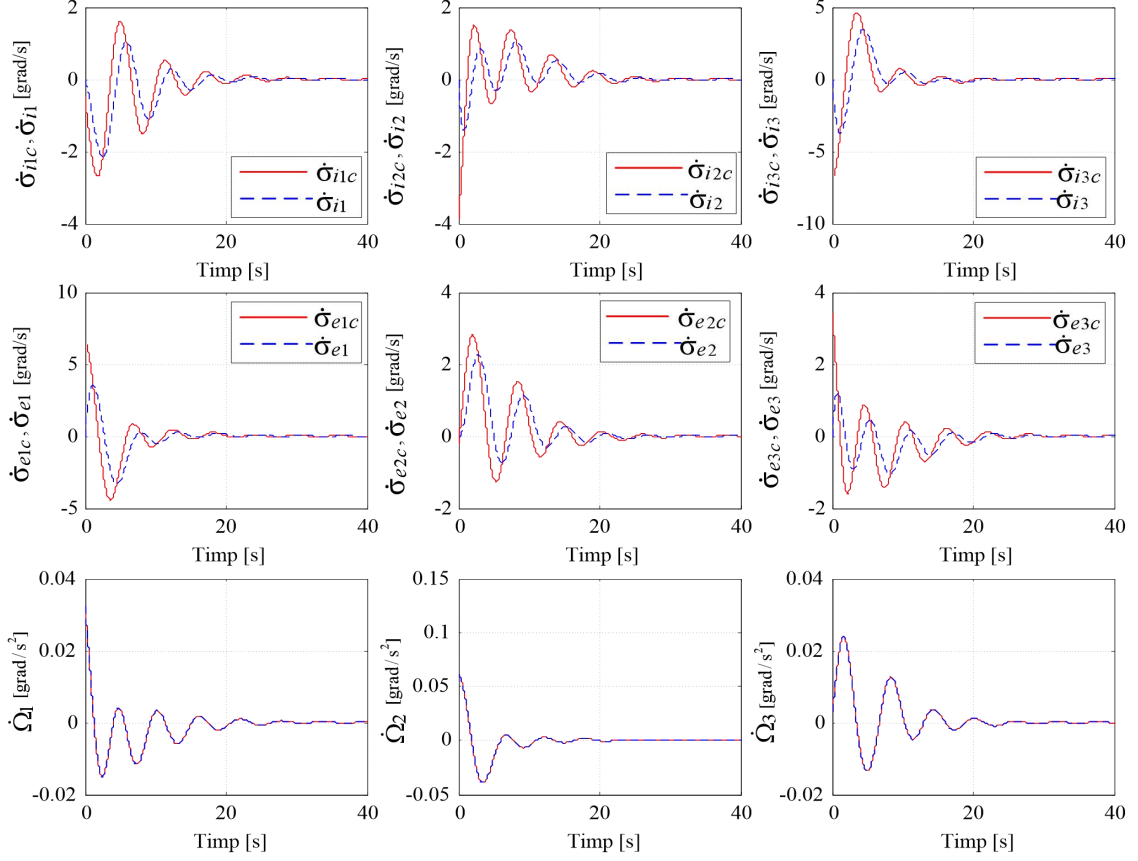
Fig.4.11. Dynamic characteristics for the actuator structure consisting of N=3 DGVSCMGs in orthogonal arrangement, without stored energy control

Satellite Attitude Control and Stored Energy (SCASES)

In this case the matrix Q will be modified. The kinetic energy stored and the power consumed by the N DGVSCMGs have the expressions respectively

$$E_c = \frac{1}{2}\boldsymbol{\Omega}^{\mathrm{T}}J_r'\boldsymbol{\Omega}, \tag{4.108}$$

$$P = \frac{\mathrm{d}E_c}{\mathrm{d}t} = \boldsymbol{\Omega}^{\mathrm{T}}J_r'\dot{\boldsymbol{\Omega}} = \begin{bmatrix} 0_{(1\times 2N)} & \boldsymbol{\Omega}^{\mathrm{T}}J_r' \end{bmatrix}\boldsymbol{u}_c, \tag{4.109}$$

with $\boldsymbol{u}_c = [\dot{\boldsymbol{\sigma}}_i^{\mathrm{T}} \quad \dot{\boldsymbol{\sigma}}_e^{\mathrm{T}} \quad \dot{\boldsymbol{\Omega}}^{\mathrm{T}}]^{\mathrm{T}}_{(3N\times 1)}$ and $J_r' = \mathrm{diag}[J_{r1} \quad \dots \quad J_{rN}], J_{rj}, j = \overline{1,N}$, moments of inertia of gyroscopic rotors relative to their own rotation axes.

Reuniting the relationship $\boldsymbol{M}_{kc} = -Q\boldsymbol{u}_c$ with (4.109), results the equation

$$\boldsymbol{M}_{kp} = [\boldsymbol{M}_{kc}^{\mathrm{T}} \quad P]^{\mathrm{T}}_{(4\times 1)} = -Q_{(4\times 3N)}\boldsymbol{u}_c = -\begin{bmatrix} Q_{i(3\times N)} & Q_{e(3\times N)} & Q_{r(3\times N)} \\ 0_{(1\times N)} & 0_{(1\times N)} & -\left(\boldsymbol{\Omega}^{\mathrm{T}}J_r'\right)_{(1\times N)} \end{bmatrix}\boldsymbol{u}_c. \tag{4.110}$$
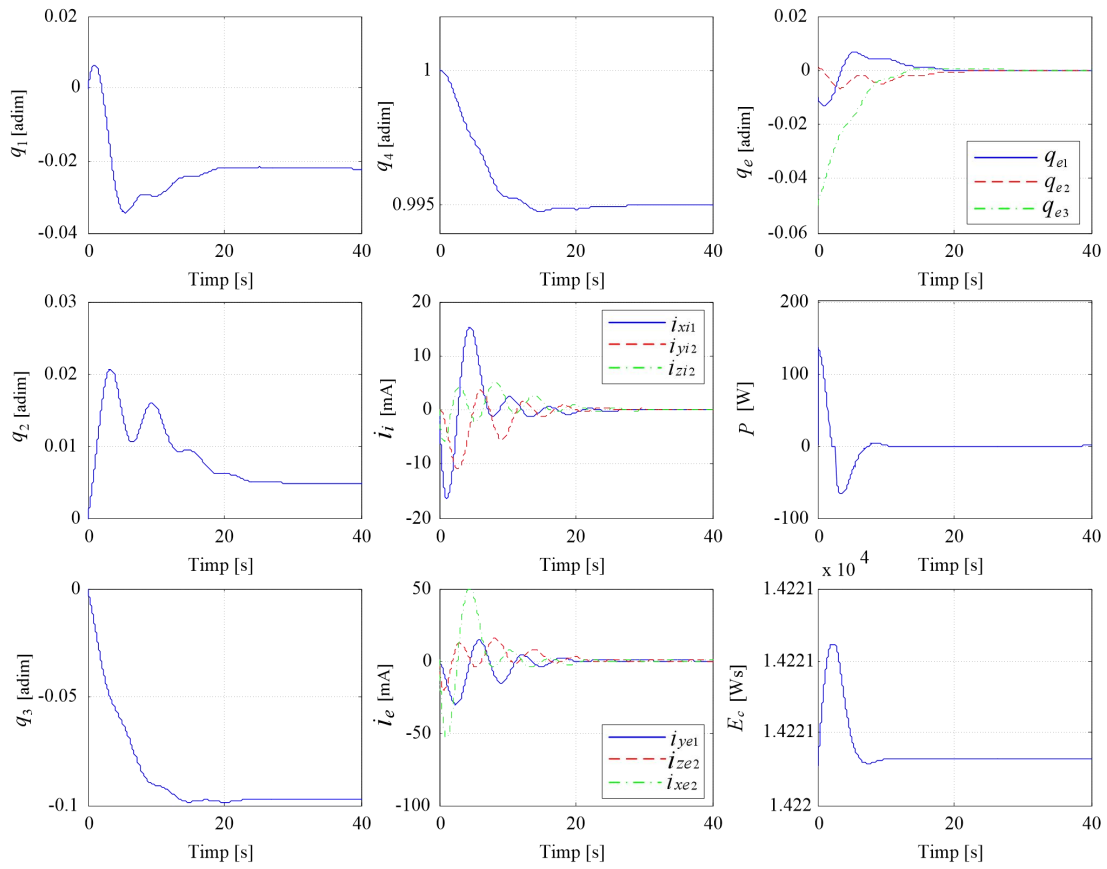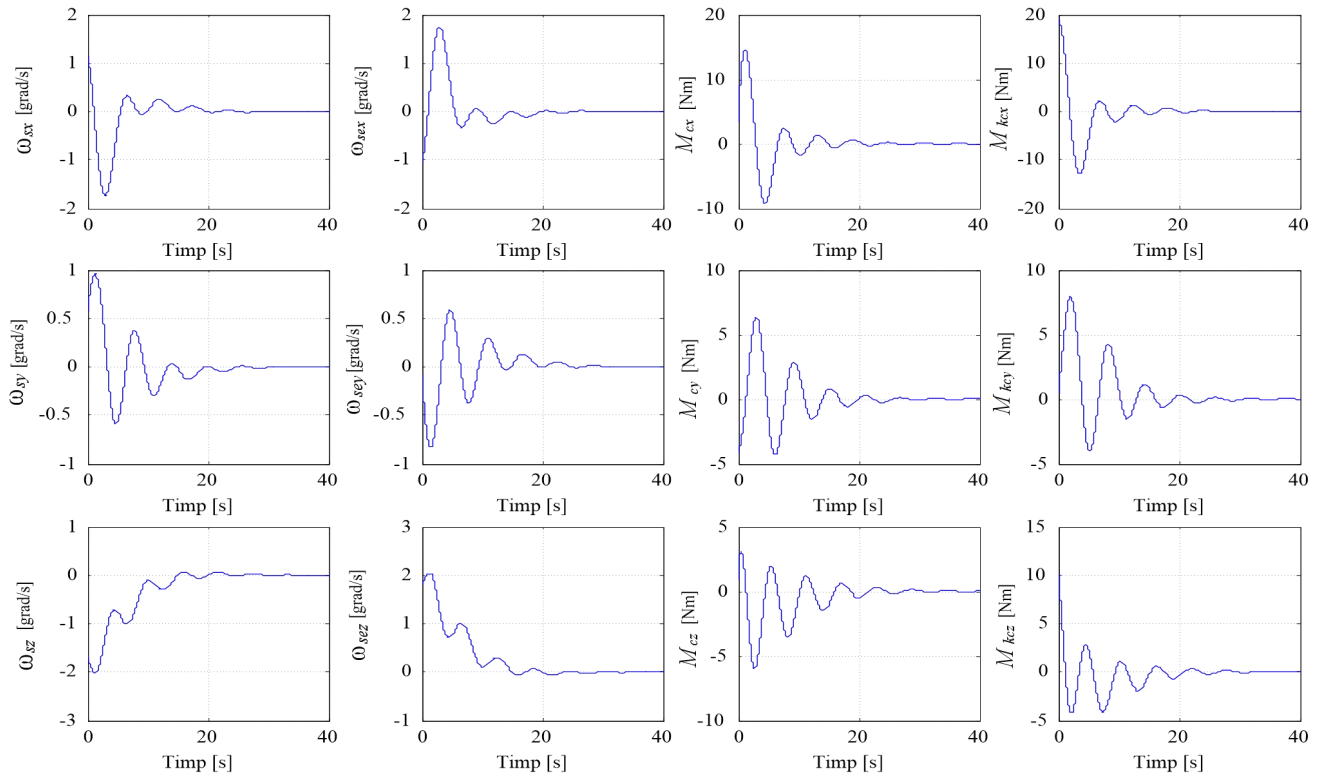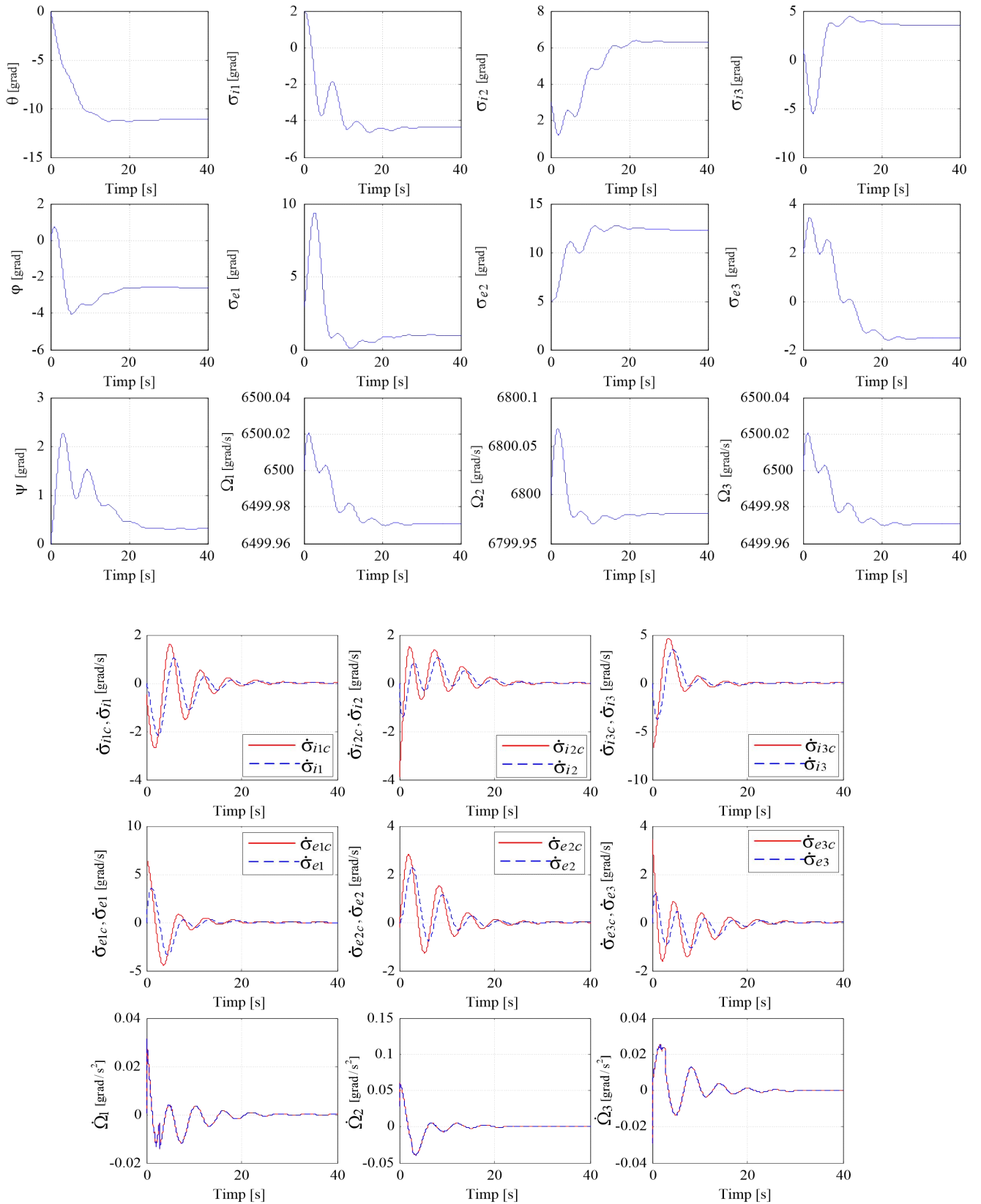
Fig.4.15. Dynamic characteristics of the satellite attitude and stored energy control structure with an actuator consisting of N=3 DGVSCMGs in an orthogonal arrangement

Automatic control of satellite attitude and stored energy with equalization of angular velocities of gyroscopic rotors (SCASESEVS)

In order to avoid the decrease of the angular velocity of a gyroscopic rotor, with implications on the quality of the satellite's attitude stabilization and on the energy storage, it is necessary to equalize the angular velocities of the gyroscopic rotors.

With $\Omega_j, j = \overline{1, N}$, the angular velocities of self-rotation of the gyroscopic rotors, with $\overline{\Omega}$ − their average value and with $\boldsymbol{\Omega}_e$ − the vector of deviations of the angular velocities from $\overline{\Omega}$, mean

$$\overline{\Omega} = \frac{1}{N} \sum_{j=1}^{N} \Omega_j , \boldsymbol{\Omega}_e = \boldsymbol{\Omega} - \overline{\Omega} \mathbf{1}_{N \times 1}, \tag{4.114}$$

$\boldsymbol{\Omega} = [\Omega_1 \quad \Omega_2 \quad ... \quad \Omega_N]^{\mathrm{T}}$ and $\mathbf{1}_{N \times 1}$ − the unit vector $(N \times 1)$, the indicator is expressed [101]

$$J_2(\boldsymbol{\Omega}) = J_2(\Omega_1, \Omega_2, ..., \Omega_N) = \frac{1}{2} \sum_{j=1}^{N} \left(\Omega_j - \overline{\Omega} \right)^2 = \frac{1}{2} \sum_{j=1}^{N} \Omega_{ej}^2 = \frac{1}{2} \boldsymbol{\Omega}_e^{\mathrm{T}} \boldsymbol{\Omega}_e, \tag{4.115}$$

having the derivative

$$\frac{\mathrm{d}J_2(\boldsymbol{\Omega})}{\mathrm{d}t} = \frac{\partial J_2}{\partial \boldsymbol{\Omega}} \dot{\boldsymbol{\Omega}} = \sum_{j=1}^{N} \frac{\partial J_2}{\partial \Omega_j} \dot{\Omega}_j = (\mathrm{grad} J_2) \dot{\boldsymbol{\Omega}} = \boldsymbol{\Omega}_e^{\mathrm{T}} \dot{\boldsymbol{\Omega}}. \tag{4.116}$$

Within SCASESEVS, the matrix Q from (4.110) becomes

$$Q_{(5 \times 3N)} = \begin{bmatrix} Q_{i(3 \times N)} & Q_{e(3 \times N)} & Q_{r(3 \times N)} \\ 0_{(1 \times N)} & 0_{(1 \times N)} & -\left(\boldsymbol{\Omega}^{\mathrm{T}} J_r'\right)_{(1 \times N)} \\ 0_{(1 \times N)} & 0_{(1 \times N)} & -\boldsymbol{\Omega}_e^{\mathrm{T}} \end{bmatrix}, \tag{4.120}$$

The control law is described by equation

$$\boldsymbol{u}_c = -Q^+ \boldsymbol{M}_{kp}, \boldsymbol{M}_{kp} = \left[\boldsymbol{M}_{kc}^{\mathrm{T}} \quad \frac{\mathrm{d}E_c}{\mathrm{d}t} \quad \frac{\mathrm{d}J_2}{\mathrm{d}t} \right]^{\mathrm{T}} = \left[\boldsymbol{M}_{kc}^{\mathrm{T}} \quad P \quad \frac{\mathrm{d}J_2}{\mathrm{d}t} \right]^{\mathrm{T}}. \tag{4.121}$$
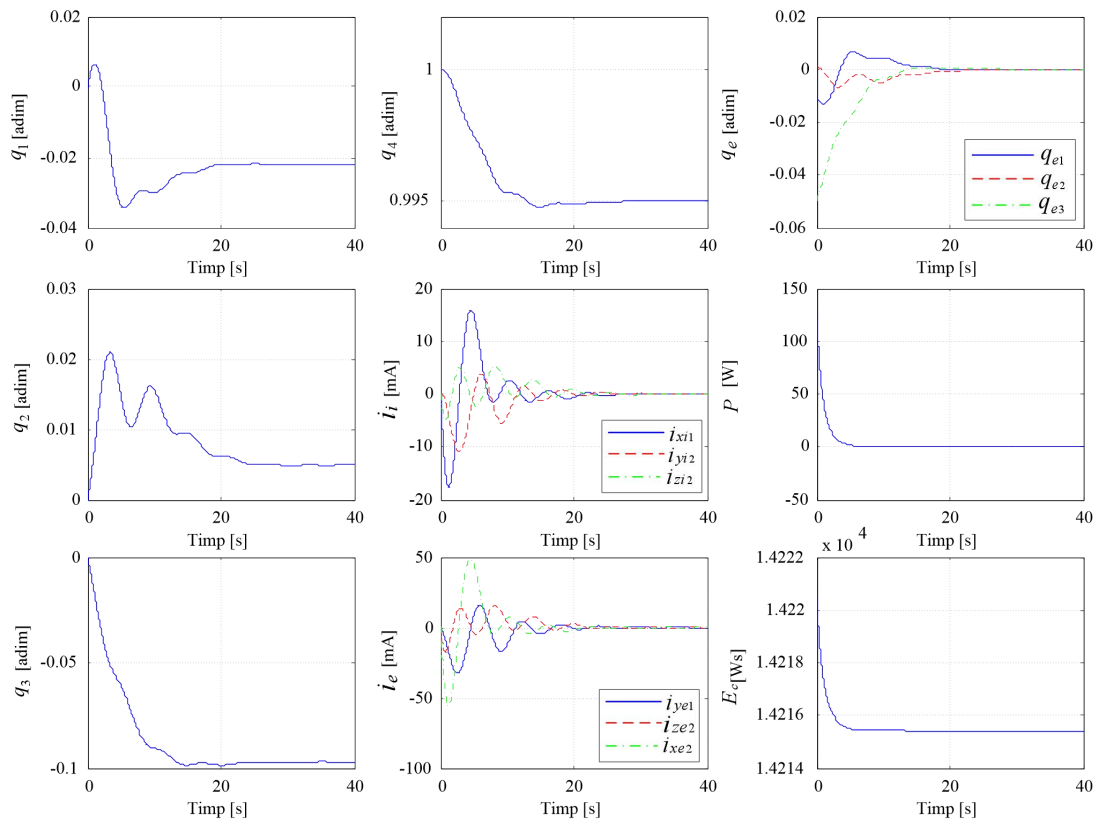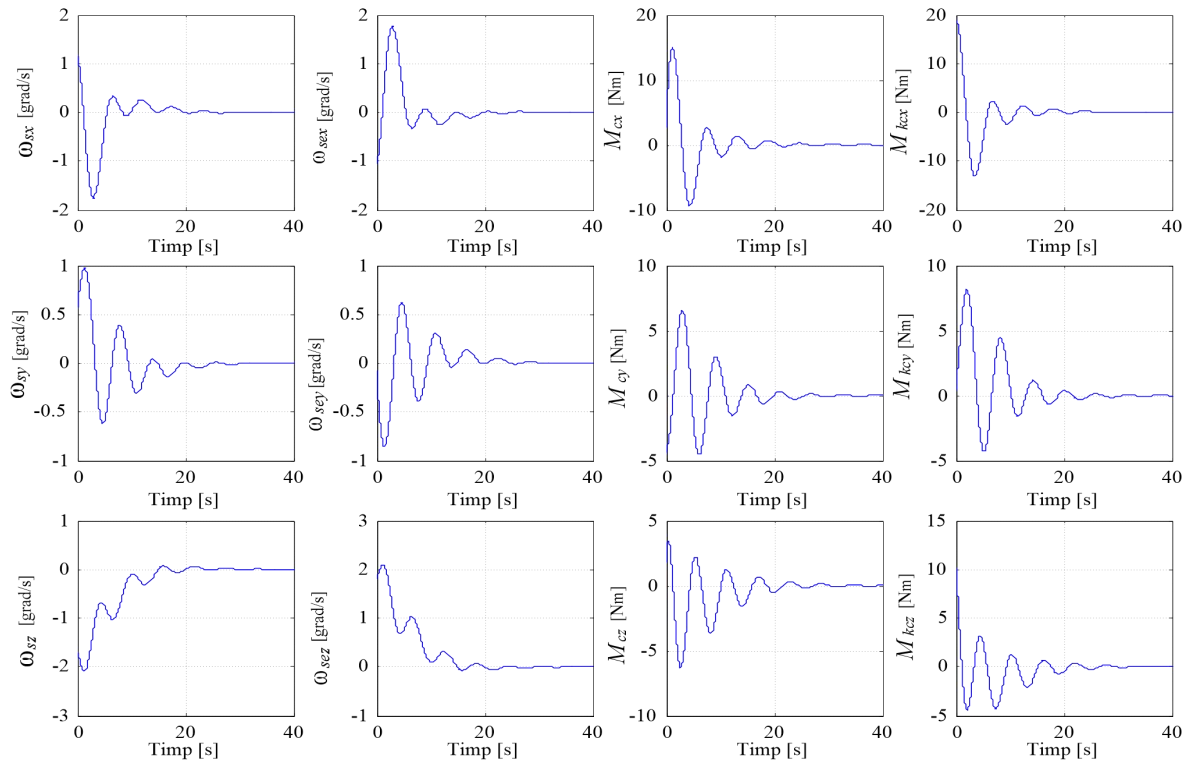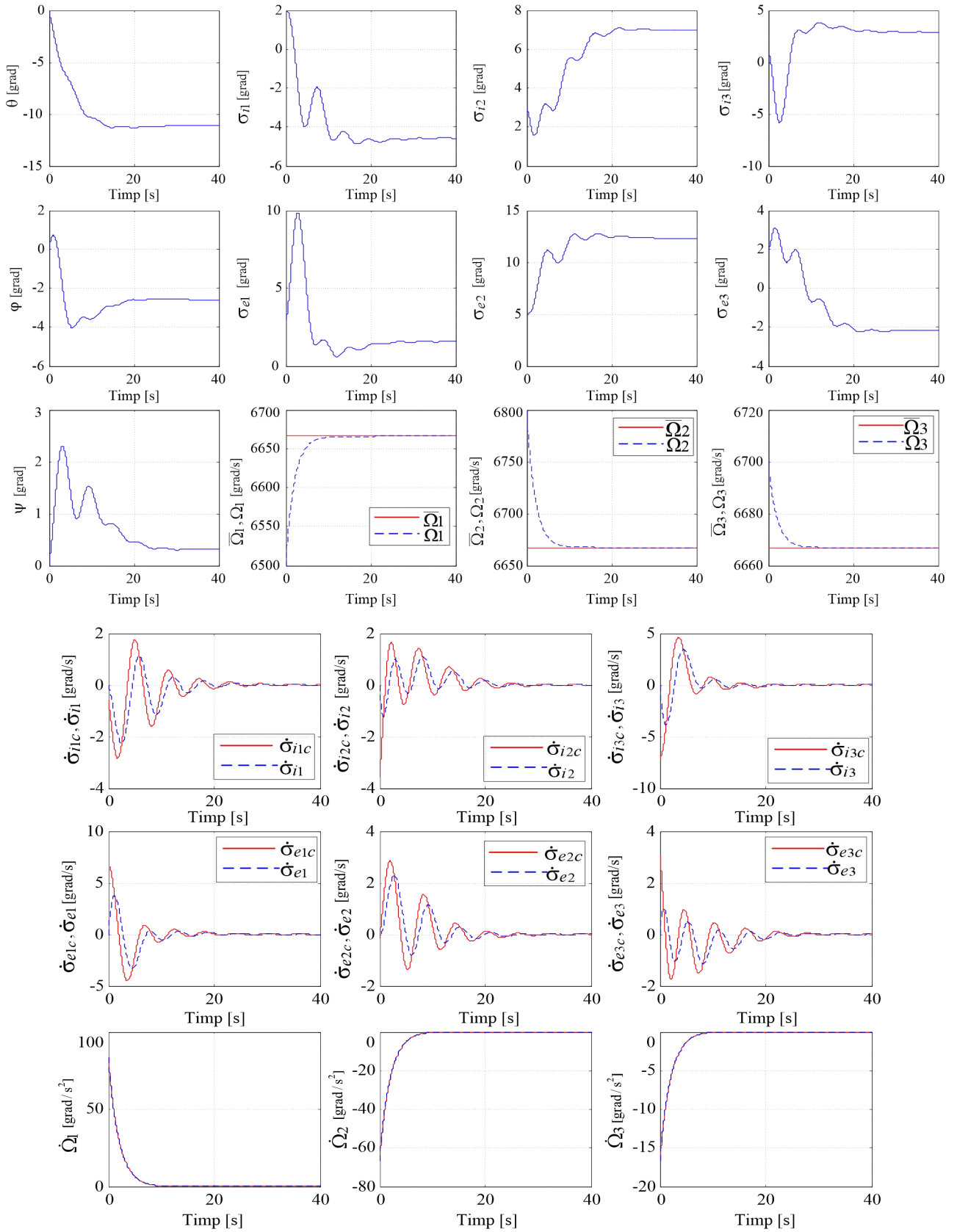
Fig.4.19. The dynamic characteristics of SCASESEVS, with actuator consisting of

N=3 DGVSCMGs in orthogonal arrangement

CHAPTER 5

CONCLUSIONS AND CONTRIBUTIONS

<u>CONCLUSIONS</u>

In chapter 1, the equations of motion (of translation and rotation) of the gyro rotor with magnetic bearings were derived, expressing the balance of forces (inertia and correction) and moments (of inertia, gyro and correction) acting on the gyro rotor , without considering the interactions of the rotor with the gyroscopic frames. **Then, nonlinear models of the rotational movements of the gyroscopic rotor (located in magnetic suspension on the inner frame), the inner frame and the outer frame of the gimbal suspension of the DGMSCMG** were built, taking into account rotor-gyroscopic frame interactions; the equations of kinetic moments (Euler's equations) were used for the three dynamic elements (rotor, inner frame and outer frame), in which the absolute angular velocities and the absolute kinetic moments are functions of the angular velocities of the base, the outer frame, the inner frame, the rotation matrices of the trihedrals related to the respective dynamic components, as well as the moments of the forces acting on the gyro rotor, inner frame and outer frame. **Finally, the non-linear dynamic model (1.64) of the DGMSCMG placed on a fixed base resulted and, after explaining the correction forces and moments as functions of the currents applied to the correction coils of the magnetic bearings and the servomotor currents for driving the inner and outer frames, respectively, the dynamic model expressed in the form of state equations (1.70) was obtained, respectively (1.72), with (1.71), (1.73)÷(1.76).** Then **the relative degrees for each of the output vector components of the nonlinear model of the DGMSCMG were determined, finally resulting in the second-order matrix-vector differential equation of the output vector (1.83), with the matrices $A(x)$ and $B(x)$ of the forms (1.84) and (1.85), using the theory of differential geometry; matrices were calculated $A(x)$ (1.88) and $B(x)$ (1.90). With these, by dynamic inversion, the function (1.95) was obtained, which describes the inverse nonlinear dynamics, that is, the control vector of the DGMSCMG model as a function of the state vector and the pseudo-control vector v.**

Considering the fact that **the nonlinear dynamic model of the rotor translational motion can be decoupled from the nonlinear dynamic model of the rotational motions of the rotor, inner frame, and outer frame, the relative degrees of the output vector components of the gyroscopic rotor translational motion model have been determined y_1 and , respectively, are the relative degrees of the output vector components of the rotational motion pattern y_2 of DGMSCMG, finally resulting in the second-order matrix-vector differential equations of the output vectors y_1**

and y_2 respectively the inverse dynamics equations (1.99) and (1.110); the decoupling of the dynamic models of the translational and rotational motions is based on the fact that the only coupling terms of the models are those containing the control variables represented as sums of the currents for creating the electromagnetic forces for the correction of the linear displacements of the gyroscopic rotor with, the currents for creating the torques of electromagnetic forces for the correction of angular displacements of the gyroscopic rotor; the summation of the currents is done by applying them to the same coils of the magnetic suspension bearings.

The structure of the automatic control system of the dynamics of the DGMSCMG subsystems from fig.1.7 was proposed and designed, for which the Matlab/Simulink model from fig.1.8 was built, with the numerical calculation annex A1.1 and, with it, the characteristics of time from fig.1.9.

Then, the problem of adaptive control of the translational and rotational dynamics of the gyroscopic rotor decoupled from the two frames was addressed, considering the rotational angular velocities of the frames to be calculated. **The adaptive control structures (based on the concept of dynamic inversion and neural networks) were proposed and designed for: the translational movement of the gyroscopic rotor (fig.1.11.a), the rotational movement of the gyroscopic rotor (fig.1.11.b) and the rotational movement of the gyroscopic frames (the block of servo systems for actuating the gyroscopic frames in fig.1.11.c). To reduce the number of sensors** (to the number of four linear displacement sensors for AMB-ROTOR and to the number of two rotation sensors for gyroscope frames) **the control laws modeled by the linear dynamic compensators in the composition of the two control subsystems of the linear displacements and the angular displacements of the AMB-ROTOR, respectively the control law modeled by the linear dynamic compensator in the composition of the control system of the angular velocities of the gyroscopic frames, are calculated as functions of the estimated error vectors of the three subsystems, provided by linear state observations.**

For the three adaptive control structures in fig.1.11, the Matlab/Simulink model in fig.1.12 was built, with the numerical calculation program in Appendix A2.1, and with it, the time characteristics in fig.1.13 were obtained. These characteristics are fast, have small overshoots and very small stationary errors, which highlights the fact that adaptive control structures based on the concept of dynamic inversion and neural networks provide superior quality indicators to control structures with conventional driving laws.

Chapter 2 presents the structure and equations of an automatic gyroscopic rotor control system with magnetic bearings, as well as dynamic models of the rotor, inner frame and outer frame of the DGMSCMG actuator located on a mobile base (satellite).

A servo system for actuating a gyroscopic frame was presented and designed. Then computational elements of satellite attitude using quaternions were presented.

The automatic attitude control system S from fig. 2.17 was designed, consisting of: P.D. type controller, DGMSCMG1 actuator and DGMSCMG2 sensor. Using a P-type control law of the gyroscopic rotor dynamics and linear servo systems for actuating the gyroscopic frames, for the structure in fig.2.17, the Matlab/Simulink models in fig.2.18 were built, with the numerical calculation program in Annex A2.1 and, with these, the dynamic characteristics of fig. 2.19 were drawn. Then, using the nonlinear models from fig.2.14 and fig.2.15 for the actuator and sensor, the Matlab/Simulink models from fig.2.20 were built, with the numerical calculation program from Appendix A2.2, and the dynamic characteristics were drawn from fig. 2.21. Compared to the dynamic characteristics in fig.2.19 (with large overshoots and very rapidly varying), those in fig.2.21 have small overshoots, are slowly variable and have small stationary errors.

In chapter 3, dynamic models were developed for the actuator-satellite interaction and for the actuator consisting of N=2 DGMSCMGs arranged in parallel, respectively orthogonal configuration, as well as for the related sensors. Also, dynamic models were developed for the actuator-satellite interaction and for the actuator consisting of N=3 DGMSCMGs arranged in an orthogonal configuration, as well as for the related sensor. The resulting systems are shown in fig.3.1, fig.3.2, fig.3.7 and fig.3.8. For these, the Matlab/Simulink models from fig.3.3, fig.3.5 and fig.3.9 were built.

An automatic attitude control system S (fig. 3.11) with P.D type controller was designed. and actuator consisting of N=2 and N=3 DGMSCMGs. For this system, the Matlab/Simulink models from fig.3.12, fig.3.13, fig.3.16, fig.3.17 were built, and with them, the dynamic characteristics from fig.3.14 were drawn (for actuator with N=2 DGMSCMGs in parallel configuration), from fig.3.15 (for actuator with N=2 DGMSCMGs in orthogonal configuration) and from fig.3.18 (for actuator with N=3 DGMSCMGs in orthogonal configuration).

In chapter 4, problems related to the dynamics and attitude control of satellites using actuators consisting of N DGVSCMGs were addressed. First, the dynamic model of the satellite was deduced with an actuator consisting of N=1 DGVSCMG located so that the plane of the outer frame is located in the plane of the undisturbed satellite's elliptical orbit. **The equation of the actuator-satellite system of the form (4.22) and (4.32), respectively, was obtained, in which the control gyroscopic moment has the form (4.26). The applied command vector DGVSCMG is of the form (4.31), with the matrix having components of the form (4.35).** Then the same problem was addressed for actuators consisting of N=2 DGVSCMGs. **For the actuator consisting of N=2 DGVSCMGs in parallel arrangement, the control moment has the form (4.43), respectively (4.45), the control**

law being of the form (4.41) and the matrix Q having the components (4.46.). Proceeding similarly, **for an actuator consisting of N=2 DGVSCMGs having the axes of the outer frames perpendicular to each other (one of them having the outer frame located in the plane of the elliptical orbit of the undisturbed satellite) similar results were obtained, with the matrix Q having the components (4.60).**

For a **satellite equipped with an actuator consisting of N=3 DGVSCMGs in an orthogonal arrangement, a model was obtained in which the command moment has the form (4.73), the command law is of the form (4.41) and the matrix Q having the components (4.75) and (4.78), respectively.**

Designed automatic attitude control system S using N DGVSCMGs with reference model and P.D type controller. from fig.4.5., using the Lyapunov function (4.79). If the energy stored in the N DGVSCMGs is not controlled, the pseudo-inverse of the matrix is Q calculated with the formula (4.88) or (4.90), so that the possibility of the appearance of singularities is eliminated; in the case of attitude control S and stored energy, as well as equalization of angular velocities of gyroscopic rotors, relations (4.112) and (4.113) were used. **The Matlab/Simulink model from fig.4.7 of the system from fig.4.5 was built, with the numerical calculation program from Appendix A4.1 and, with it, the time characteristics from fig.4.8 ÷ 4.11 were plotted for actuators with N= 1 DGVSCMG, with N=2 DGVSCMGs in parallel arrangement, with N=2 DGVSCMGs in orthogonal arrangement and with N=3 DGVSCMGs in orthogonal arrangement.** Similarly, **in the case of attitude control and stored energy, with and without the equalization of the angular velocities of the gyroscopic rotors, the time characteristics were obtained in fig.4.12 ÷ 4.15 and those of fig.4.16÷4.19,** for the four actuator variants.

CONTRIBUTIONS

The main contributions made in the paper are the following:

1. Deduction of nonlinear dynamic models of DGMSCMG from the forms (1.64) și (1.70), with (1,73) ÷ (1.76).

2. Using the theory of differential geometry, the model was constructed (1.83), with matrices $A(x)$ and $B(x)$ of the forms (1.84) and (1.85), resulting matrices (1.88) and (1.90). Also, using the same method, decoupled dynamics models of gyro rotor translations (1.97), rotor rotations, and gyro frames were deduced (1.109), with (1.102) ÷ (1.104) și (1.108).

3. The structure of the automatic control system of the dynamics of the DGMSCMG subsystems from fig.1.7 was proposed and designed, for which the Matlab/Simulink model from

fig.1.8 was built, with the numerical calculation program from Annex A1.1, and with these, the the dynamic characteristics from fig.1.9.

4. The adaptive control structures based on the concept of dynamic inversion and neural networks from fig.1.11.a, fig.1.11.b and fig.1.11.c were proposed and designed for the three decoupled dynamics: dynamics of gyroscopic rotor translations; dynamics of gyroscopic rotor rotations; dynamics of rotations of gyroscopic frames. For the three adaptive control structures in fig.1.11, the Matlab/Simulink model in fig.1.12 was built, with the numerical calculation model in Appendix A2.1, and with them, the dynamic characteristics in fig.1.13 were drawn.

5. To increase the accuracy of the automatic attitude control system of the satellite (S) equipped with DGMSCMG type actuator, a second DGMSCMG (DGMSCMG2) was introduced, identical in structure to the actuator, DGMSCMG2 having the role of sensor for measuring the absolute angular velocity of the base (of the satellite) $\boldsymbol{\omega}_b$, thus resulting in an actuator-sensor-satellite subsystem, which provides, in a stabilized regime, a control torque applied to the satellite depending only on the absolute angular velocity of the satellite.

6. The design of the automatic attitude control system S from fig. 2.17 with P.D type controller. by the error quaternion vector $\boldsymbol{q}_e$, respectively of type P.I. by relative angular velocity $\boldsymbol{\omega}_s$ of S (relative to the local orbital trihedral) using the Lyapunov function (2.150), with (2.151) and (2.152), as well as a P-type control law of the gyro rotor dynamics and linear servo systems for actuation of the actuator and sensor gyro frames. The Matlab/Simulink model from fig.2.18 was built, with the numerical calculation program from appendix A2.1, and the dynamic characteristics from fig.2.19 were plotted.

7. 7.Using the same attitude controller in the system from fig.2.17, but with the nonlinear models from fig.2.14 (for the actuator) and from fig.2.15 (for the sensor), the Matlab/Simulink models from fig.2.20 were built, with the numerical calculation program from annex A2.2 and, with them, the dynamic characteristics from fig.2.21 were drawn; these dynamic characteristics are superior to those in fig.2.19 from the point of view of quality indicators (they have smaller overshoots, are slowly variable and with smaller stationary errors).

8. 8. Elaboration of the dynamic models of the actuator-satellite, satellite-sensor subsystems and of the actuator subsystems consisting of N=2 DGMSCMGs arranged in a parallel configuration and, respectively, in a rectangular configuration (shown in fig. 3.1 and fig. 3.2), as well as and Maltab/Simulink models (together with their subsystems) from fig.3.3 and fig.3.5.

9. Development of the dynamic models of the actuator-satellite, satellite-sensor subsystems and of the actuator subsystems consisting of N=3 DGMSCMGs arranged in an orthogonal

configuration (shown in fig.3.7 and fig.3.8), as well as the Maltab/Simulink model (together with its subsystems) from fig.3.9.

10. The design of the automatic attitude control system S from fig. 3.11, with a P.D. type controller. (based on the use of the Lyapunov function (3.50), with (3.51)(3.53) and (3.62)) and with the actuator-sensor-satellite subsystem from fig.3.10 (the actuator being constituted by N=2, respectively N=3 DGMSCMGs arranged in parallel and orthogonal configuration), for which the Matlab/Simulink models from fig.3.12, fig.3.13, fig.3.16 and fig.3.17 and the numerical calculation programs from annexes A3.1, A3.2 and A3.3 were developed and, with them, the dynamic characteristics of fig.3.14, fig.3.15 and fig.3.18 were drawn.

11. Calculation of the control moments of S produced by actuators consisting of N DGVSCMGs (N=1,2,3), in parallel or orthogonal arrangement, of the forms (4.32), (4.45), (4.73), respectively of the control vectors apply to servo systems for controlling the angular velocities of gyro frames and the vector of angular accelerations of gyro rotors as functions of the matrices Q, with their components Q_i, Q_e, Q_r of the forms (4.35), (4.46), (4.60) și (4.78).

12. Design of the servo system in fig.4.6 for controlling angular velocities of gyro frames and angular accelerations of gyro rotors using the concept of dynamic inversion, reference models, linear dynamic compensators and state observations.

13. 13. The design of the automatic attitude control system S from fig. 4.5, with actuators consisting of N DGVSCMGs (N=1,2,3), in parallel or orthogonal arrangement, without the control of the stored energy (with the matrix components of the forms (4.35), (4.46), (4.60) and (4.78)), with the control of the energy stored in the N DGVSCMGs (with the matrices of the form (4.110)), respectively with the control of the energy stored in the N DGVSCMGs and the equalization of the speeds angular values of gyroscopic rotors (with matrices Q of the form (4.120)).

14. The Maltab/Simulink models from fig.4.7 of the attitude control system S from fig.4.5 were elaborated, with the numerical calculation program from Appendix A4.1, and with them the dynamic characteristics from fig.4.8 ÷ fig.4.11 for actuators with N=1 DGVSCMG, with N=2 DGVSCMGs in parallel arrangement, with N=2 DGVSCMGs in orthogonal arrangement and with N=3 DGVSCMGs in orthogonal arrangement. Also, for the S attitude control and the energy stored in the N DGVSCMGs, without and with the equalization of the angular velocities of the gyroscopic rotors, the dynamic characteristics of fig.4.12 ÷ fig.4.15and those of fig.4.16 ÷ fig.4.19, for the four actuator variants.

SELECTIVE BIBLIOGRAPHY

[1].Ahmed, J., Bernstein, D.S. *Adaptive Control of Double-Gimbal Control Moment Gyro with Unbalansed Rotor.* Journal of Guidance, Control an Dynamics, Vol. 25, Nr.1, 2002

[3].Bai, J.G., Zhang, X.Z., Wang, L, M *A Flywheel Energ. Storage System with Active Magnetic Bearings.* In Proc. Of 2012 International Conference on Future Energy, Environment and Material, 2012, pag. 1124-1128

[7]. Chen, M., Knospe, C.R. *Feedback Liniearization of Active Magnetic Bearings Current-Mode Implementation.* IEEE/ASME Transactions Mechatronics, Vol. 10, Nr. 6, 2005, pag. 632-639

[10]. Cui, P., Cui, J., Yang, Q., Zheng, S. *The Coupling Characteristic Investigation of Double-Gimbal Magnetically Suspended Control Moment Gyro Used on Agile Maneuver Spacecraft.* In Mathematical Problems in Engineering, Vol. 2015, 11 pag

[22]. Han, B., Ma, Chen, Y., J., Li, Ha., Yang, Li. *Discrete Model Reference Adaptive Control for Gimbal Servosystem of Control Moment Gyro with Harmmonic Drive,* Publishing Corporation Mathematical Problems Engineering Volume, 2013, 10 pag

[23]. Han, B., Ma, J., Li, Ha. *Research on Nonlinear Friction Compensation of Harmonic Drive in Gimbal Servo-system of DGCMG.* Journal of Control, Automation and Systems, 14(3), 2016, pag. 779-786

[26]. Ioan, M., Lungu, M., Lungu, R. *Control of the Satellites' Attitude using a Pyramidal Configuration of Four Variable Speed Control Moment Gyros.* Scientific Bulletin – University Politehnica Bucharest, Series D: Mechanical Engineering, vol. 79, nr. 2, 2017, pag. 59-70

[28]. Jikuya, I., Fujii, K., Yamada, K. *Attitude Maneuver of Spacecraft with a Variable-Speed Double-Gimbal Control Moment Gyro.* Advances in Space Research, Vol. 58, nr. 7, 2016, pag.1303-1317

[39]. Kurokawa, H. *A Geometry Study of Single Gimbal Control Moment Gyros-Singularity Problem and Steering Law.* Tech. Rep. Report No.175, Mechanical Engineering Laboratory, Japan, January 1998.

[40]. Kurokawa, H. *Constrained Steering Law of Pyramid-Type Control Moment Gyros and Ground Tests.* Journal of Guidance, Control, and Dynamics, vol. 20, nr. 3, 1997, pag. 445-449

[46]. Lungu, M. *Backstepping Control Method in Aerospace Engineering.* Academica Greifswald, 2022

[47]. Lungu, M. *Control of Double-Gimbal Control Moment Gyro Systems using the Backstepping Control Method and Nonlinear Disturbance Observer*. Acta Astronautica, Vol. 180, 2021, pag. 639-649

[48]. Lungu, M. *Neuro-Observer based Control of Double Gimbal Control Moment Gyro Systems*. Aerospace Science and Technology, Vol. 110, 2021

[49]. Lungu, M., Lungu, R. *Adaptive Neural Network-based Satellite Attitude Control by using the Dynamic Inversion Technique and a VSCMG Pyramidal Cluster*. Complexity, 2019, pag. 1-16

[50]. Lungu, M., Lungu, R. *Estimarea stării aparatelor de zbor*. Editura Sitech, Craiova, 2014

[53]. Lungu, M., Lungu, R., **Efrim, C**., Bombaker, O. *Backstepping Control of Magnetically Suspended Double-Gimbal Control Moment Gyroscope*. 24 IEEE International Conference on System Teory, Control and Computing, Sinaia, Românîa, 2020, pag. 154-159,

[55]. Lungu, R. *Echipamente şi sisteme giroscopice,* Editura Universitaria, Craiova, 1997

[57]. Lungu, R., **Efrim, C**., Zheng, Z., Lungu, M. *Dynamic Inversion based of Control of DGMSCMGs. Part 1: Obtaining Nonlinear Dynamic Model*. IEEE International Conference on Applied and Theroretical Electricity (ICATE), 2021, pag. 1-6

[58]. Lungu, R., **Efrim, C**., Zheng, Z., Lungu, M. *Dynamic Inversion based of Control of DGMSCMGs. Part 2: Control Arhitecture Design and Validation*. IEEE International Conference on Applied and Theroretical Electricity (ICATE), 2021, pag. 7-12

[59]. Lungu, R., Ioan, M., Lungu, M. *Controlul giroscopic al atitudinii sateliţilor*. Editura Sitech, Craiova, 2017.

[61]. Lungu, R., Lungu, M., **Efrim, C**. *Adaptive Control of DGMSCMG Using Dynamic Inversion and Neural Networks*. Advances and Space Research, vol. 68, nr.8, 2021, pag. 3478-3494

[62]. Lungu, R., Lungu, M., **Efrim, C**. *Attitude Adaptive Control of Satellites using Double-Gimbal Magnetically Suspended Control Moment Gyros*. Aerospace Science and Technology, Vol. 126, 2022

[70]. Peng, C., Fang, J., Xu, S. *Composite Anti-Disturbance Controller for Magnetically Suspended Control Moment Gyro Subject to Mismatched Disturbances Nonlinear Dyn,* 2015*, pag. 1563-1573.*

[75]. Sasaki, T., Shimomura, T. *Convex Optimization for Power Tracking of Double-Gimbal Variable-Speed Control Moment Gyroscopes*. Journal of Spacecraft and Rockets, Vol. 55, nr. 3, 2018, pag. 541-551

[78]. Sasaki, T., Shimomura, T., Kanata, S. *LPV Control and Singularity Avoidance of a Spacecraft with DGCMGs*. IFAC-Papers On Line 49-17, 2016, pag.152-157

［79］. Sasaki, T., Shimomura, T., Pullem, S., Schaub, H. *Attitude and Vibration Control with Double-Gimbal Variable-Speed Control Moment Gyros.* Journal Acta Astronautica, 152, 2018, pag.740-751

［81］. Sasaki, T., Shimomura, T., Schaub, H. *Robust Attitude Control Using a Double-Gimbal Variable-Speed Control Moment Gyroscope.* Journal of Spacecraft and Rockets, Vol. 55, 2018, pag.1235-1247

［89］. Su, D., Xu, S. *The Precise Control of a Double Gimbal MSCMG Based on Modal Separation and Feedback Linearization.* In Proceedings of 2013 International Conference on Electrical Machines and Sytems, Oct. 26-29, Korea, pag. 1355-1360

［92］. Tsiotras, P. *Stabilization and Optimality Results for the Attitude Control Problem.* Journal of Guidance, Control and Dynamics, vol. 19, nr. 4, 1996, pag 772 – 779

［94］. Walker, J.M., Culbertson, H., Raitor, M., Okamura, A. *Haptic Orientation Guidance Using Two Parallel Double-Gimbal Control Moment Gyroscopes.* IEEE Transactions on Haptics, Vol. 11, nr. 2, 2018, pag.267-278

［96］. Wie, B., Bailey, D., Heiberg, C. *Acquisition and Pointing Control of Single-Gimbal Control Moment Gyros.* Journal of Guidance, Control and Dynamics, Vol. 25, nr. 1, 2002, pag.96-104

［99］. Xiaocen, Ch., Maoyin, Ch. *Precise Control of Magnetically Suspended Doble-Gimbal Control Moment Gyroscope Using Differential Geometric Decopling Method.* In Chinese Journal of Aeronautics, 26(4), 2013, pag. 1017-1028

［101］. Yoon, H., Tsiostras, P. *Spacecraft Adaptive Attitude and Power Tracking with Variable Speed Control Moment Giroscopes.* Journal of Guidance, Control and Dynamics, vol. 25, nr. 6, 2002, pag. 1081 – 1090

［107］. Zhou, J., Zhou, D. *Spacecraft Attitude Control with Double-Gimbaled Control Moment Gyroscopes.* In Proceedings of the 2007 IEEE International Conference and Biomimetics, December, 15-18, China, 2007, pag. 1557-1562